2007:40

DOCTORAL THESIS

Microwave Treatment of Wood

Lars Hansson

Luleå University of Technology
LTU Skellefteå
Division of Wood Physics

2007:40 | ISSN: 1402-1544 | ISRN: LTU-DT -- 07/40 -- SE

LULEÅ
UNIVERSITY
OF TECHNOLOGY

Microwave Treatment of Wood

Lars Hansson

Luleå University of Technology
Division of Wood Physics
Skellefteå Campus
Skeria 3, SE-931 87 Skellefteå, Sweden

ABSTRACT

Drying wood using microwave energy is not very common, but could be a complement to conventional air-circulation drying due to the possibility to dry wood faster than the conventional drying methods with preserved quality. Furthermore, this technique could be used to condition boards with too high moisture content gradient. In this study, an industrial-scale, online microwave drier for wood components has been used and adapted to wood treatment. The aim of the present work was to investigate if the microwave drying method itself affects such wood properties as bending strength, hardness and colour change. Another aim was to explain, with finite element model simulations, the interaction between microwaves and wood during heating and drying and to a lesser extent also during microwave scanning of wood. Tests of the mechanical properties of wood showed no difference in bending strength in comparison with the conventional air circulation method. Nor was there any significant difference in wood hardness (Janka) perpendicular to the grain between the drying methods or between different temperature levels during the microwave drying. However, the results showed that there is a significant difference in wood hardness parallel to the grain between the methods when drying progressed to relatively lower levels of moisture content; i.e. wood hardness becomes higher during microwave drying. The developed multiphysics finite element model is a powerful evaluation tool for understanding the interaction between wood and microwaves during heating and drying as well as scanning. The model can be used for simulation of different microwave treatments of wood.

Keywords: Wood; FEM; Bending strength; Hardness; Matched samples; CT scanning; Microwave; Heating; Phase transition; Drying.

PREFACE

This thesis was carried out at Luleå University of Technology, the Division of Wood Physics, Skellefteå Campus, under supervision of Dr. Lena Antti and Prof. Tom Morén.

Freely translated, the Swedish poet Karin Boye says:

”Yes, there is goal and meaning in our path
- but it's the way that is the labour's worth.”

The road to completing this thesis has been quite long and maybe a little bit winding. But I would surely say that my knowledge is greater now than if the road had been straight. It has given me the opportunity to penetrate microwave treatment of wood from different directions. Besides, I have had the privilege to collaborate with competent people. First of all, Lena Antti, who deserves my warmest thanks for her patient and excellent supervising. Many thanks also to Nils Lundgren for the inspired collaboration and to Tom Morén for supervising and for being a good adversary in our tennis games. I would also thank my other colleagues at the Division of Wood Physics, especially Margot Sehlstedt-Persson, who has helped me to get an artistic touch to the figures and illustrations. In fact, I owe many thanks to so many other employees at the Department in Skellefteå for uplifting discussions, conversations or just a good laugh. A special thanks to Brian Reedy for the language reviewing of this thesis.

Finally, I would like to express my sincere gratitude to my Elisabeth, who has been a tremendous support all through this work.

Skellefteå, 2007-10-31

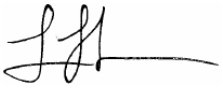

Lars Hansson

LIST OF PAPERS

This thesis is based on the work reported in following papers, referred to by Roman numerals:

I Hansson, L. & Antti, A.L. 2003. The effect of microwave drying on Norway spruce woods strength: a comparison with conventional drying. Journal of Materials Processing Technology, 141, pp 41-50.

II Hansson, L. & Antti, A.L. 2003. Design and performance of an industrial microwave drier for on-line drying of wood components. The 8th International IUFRO Wood Drying Conference. 24-29 August, Brasov, Romania, pp 156-158.

III Hansson, L. & Antti, A.L. 2005. The effect of drying method and temperature level on the hardness of wood. Journal of Materials Processing Technology, 171, pp 467-470.

IV Hansson, L., Lundgren, N., Antti A.L. & Hagman O. 2005. Microwave penetration in wood using imaging sensor. Journal of International Measurement Confederation, 38(1), 15-20.

V Hansson, L., Lundgren, N., Antti A.L. & Hagman O. 2005. FEM simulation of interactions between wood and microwaves. Journal of Wood Science, 52(5), 406-410.

VI Lundgren, N., Hansson, L., Hagman O. & Antti A.L. 2006. FEM simulation of interactions between microwaves and wood during tawing. 2nd Conference on Mathematical Modelling of Wave Phenomena. 14-19 August 2005, Växjö, Sweden. In: AIP Conference Proceedings, 834, 260-267.

VII Hansson, L., Lundgren, N., Antti A.L. & Hagman O. 2005. FEM simulation of heating wood in an industrial microwave applicator. 10th International Conference on Microwave and High Frequency Heating. 12-15 September, Modena, Italy.

VIII Hansson, L. & Antti A.L. 2007. Modelling Heating and Drying of Wood. Submitted to Drying Technology, 31 May.

CONTRIBUTION TO THE INCLUDED PAPERS

I – III and **VIII**: These works were written by the author with supervision and comments by Lena Antti.

IV – VII: These works were written by the author in collaboration with Nils Lundgren and with supervision and comments by Lena Antti and Olle Hagman. In papers IV–VI the main part of collection and analysis of the microwave scanner data was done by Nils Lundgren.

CONTENTS

1 INTRODUCTION

Freshly sawn wood needs to be dried before making furniture, buildings, etc., since a living tree has a dry-weight moisture content (mc) often exceeding 0.8, which means that the cell walls in this complex material are fully saturated and the voids contain considerable amounts of free liquid water. Besides water, wood is composed of cellulose, lignin, hemicelluloses and a minor amount of extractives. As long as human beings have used wood, man has attempted to dry it. In the beginning wood was probably only dried with the help of air and sun; during the last century there has been a constant development in artificial drying. The most common drying method nowadays is air-circulation drying. This drying is based on heat conduction from the surface of the wood towards the interior for evaporation of moisture. Furthermore, the moisture moves to the surface by mass flow in liquid and vapour phases. This mass flow is divided into three different phases: capillary, transition and diffusion phase [1]. If the wood has an mc higher than the fibre saturation point (fsp), the internal moisture reduction is a form of free water loss. The fsp is an imaginary point where all the free water is removed from the voids or vessels in the wood. Generally, the fsp is about 0.3. However, it varies a little within each piece and with the wood temperature. During the drying process, there are no significant dimensional changes as long as the mc exceeds the fsp, but when bound water releases from the cell walls, dimensional changes start to take place. These dimensional changes are not the same in all directions.

Less common drying methods for industrial processing based on high-frequency (HF) electromagnetic fields are microwaves (MW), a combination of vacuum and MW [2] or radio frequency (RF) and vacuum [3, 4]. An RF drying system creates an alternating electric field between two electrodes. In order to avoid interfering with radio communications, the Federal Communications Commission has reserved radio frequencies at 13.56, 27.12 and 40.68 MHz for industrial use, with corresponding wavelengths of about 22.1, 11.1 and 7.4 metres. With shorter wavelengths, the power penetration depth will decrease.

Combining RF and vacuum for heating enables a lower boiling point with decreasing pressure, which in turn means that the required drying temperature in order to vaporize the water from the wood will decrease. Microwave and RF drying techniques, in contrast to conventional drying, are based on the principle that heat is instantly absorbed throughout the wet load. The microwave frequency spectrum is approximately 0.3 GHz to 30 GHz with corresponding wavelengths from one metre to one millimetre. The microwave spectrum is mainly used for transmission and reception of information for communication purposes. However, certain regions called Industrial, Scientific and Medical (ISM) bands have been allocated for microwave heating processes. The most commonly used frequencies for heating are 915 MHz and 2.45 GHz with wavelengths of approximately 33 and 12 centimetres. A typical microwave heating system has two main components, the microwave source and the cavity. The most commonly used microwave generators are magnetrons. These microwave generators began to be used in industrial microwave heating and drying equipment in the 1940s, and they were very expensive. Nowadays magnetrons at 915 MHz and 2.45 GHz are relatively cheap, because they are used in domestic microwave ovens and are therefore mass-produced. The cavity is a metal box into which the microwaves are guided and effectively reflected by the metallic walls. Furthermore, the waves resonate and will form standing waves. The position of the nodes and antinodes of the standing waves in the cavity depends on the design of the cavity, i.e., its dimensions. Also, the dielectric properties and the position of the load have some influence on the field distribution. The nodes and antinodes make the heating uneven; i.e., hotter and colder spots will be developed in the material. If microwave heating technology is used for drying, then a consequence of this uneven heating will be uneven drying, which in turn could cause drying stresses.

The technology of microwave heating and drying in the field of forest products started to be used in the early 1960s. At a frequency of 2.4 GHz, a drying rate of 0.4 fractional mc per hour could be reached for boards of spruce and beech [5].

With a frequency of 915 MHz and a manipulated microwave input power and hot air, a 25-mm-thick pine plank could be dried in less than three hours [6] without drying defects. A prototype continuous microwave dryer for softwood structural lumber could dry 50-mm-thick hemlock and Douglas fir in 5–10 hours with small drying defects [7]. Antti [8] has shown that it is possible to dry pine and spruce 20–30 times faster than with conventional methods. For hardwoods such as beech, birch and ash, the drying time is approximately half the time required for softwood.

The main problem in using this technique in wood drying is the uniform field. In order to reduce the problems of uneven field distribution and power intensity, an industrial-scale online microwave drier for wood components has been adapted for wood at Luleå University of Technology, Division of Wood Physics [9, 10], to achieve a fairly uniform heating of the load in order to prevent stress development. Too high energy absorption may cause steam expansion checks. Oloyede and Groombridge [11] state that microwave heating could reduce the strength of dried wood by as much as 60%. Furthermore, Machado [12] has obtained a clear loss of compression strength parallel to the grain in microwave-exposed clear oak pieces. Torgovnikov and Vinden [13] use the steam expansion caused by microwaves of high intensity to modify selected hardwoods by increasing their permeability. After the modification, environmentally friendly resin is infused throughout the wood, whereupon the wood is compressed, resulting in a wood-resin composite material.

Microwave technology can also be applied to the scanning of wood, making it possible to detect such wood properties as density and mc [14, 15]. The frequency used in this microwave scanning project is 9.375 GHz.

One way to understand and explain the physical processes in the interaction between wood and microwaves, which could be the basis for controlling and scheduling the heating, with or without drying, or for microwave scanning, is to make simulation models [8, 16, 17, 18].

1.1 The objectives of this thesis

There is a necessity to demonstrate the fact that microwave drying is a complement and an adequate alternative to conventional drying methods as well as to demonstrate its advantage in quality gains with the rapid heating and drying. The objectives of this thesis are to study whether the drying method itself affects such mechanical properties as bending strength and hardness. Raised temperature in conventional drying gives rise to some changes in the wood characteristics, such as changes in colour. A brief study of colour response in microwave-dried wood is included in the thesis. Some of the results have been taken from studies made on a specially designed microwave drier for wood components. Hence, a description of the specially designed microwave drier for wood components is included in this thesis. The objective of the thesis is also to develop an FEM model capable of explaining the interaction between microwaves and wood during heating and drying and, to a lesser extent, also scanning.

1.2 Outline of the thesis

This thesis contains, apart from a summary of the papers, a chapter describing relevant features of wood as well as some theoretical explanations of microwaves and the interaction between microwaves and wood. Some further clarifications and new information about the models and some of the studies that are not included in the papers are also included in this thesis. Almost all results are based on the papers outlined in the schematic diagram, figure 1. In addition, figure 1 depicts the relationships between the papers included in the thesis.

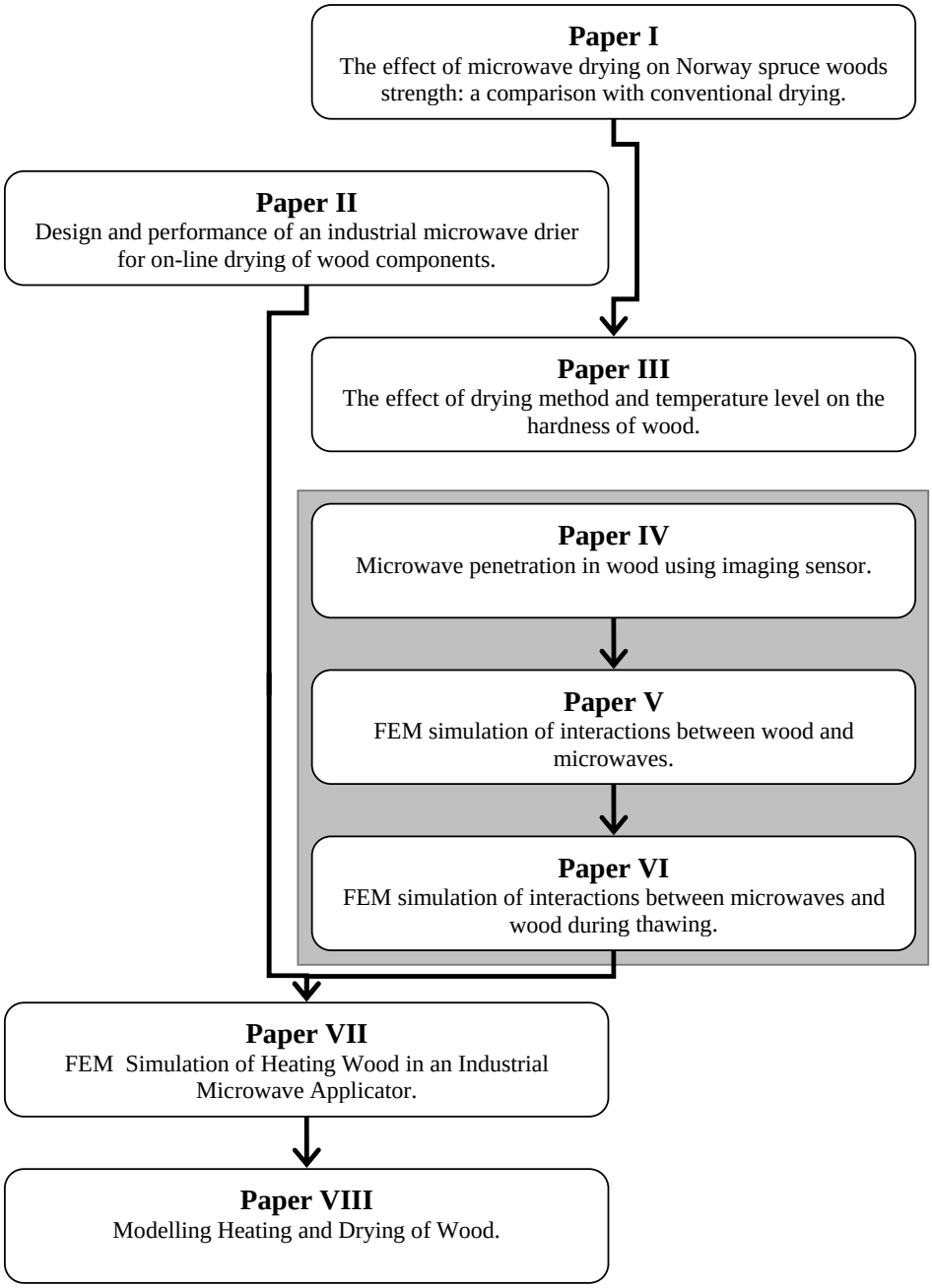

Figure 1. Disposition of the papers included in the thesis.

2 THEORY

2.1 Wood

Wood is a complex material composed of cellulose, lignin, hemicellulose and minor amounts of extractives. The wood structure consists of a tissue of cells of various shapes and sizes (figures 2 and 3) in which the elements are more or less linked together. These cells are arranged in radial files, and their longitudinal extension is oriented in the vertical direction or in the direction of the stem axis.

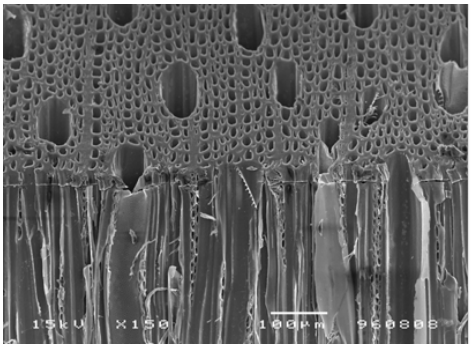

Figure 2. Scanning Electron Microscope (SEM) photography of the cell structure of birch. Reprinted by permission of Margot Sehlstedt-Persson.

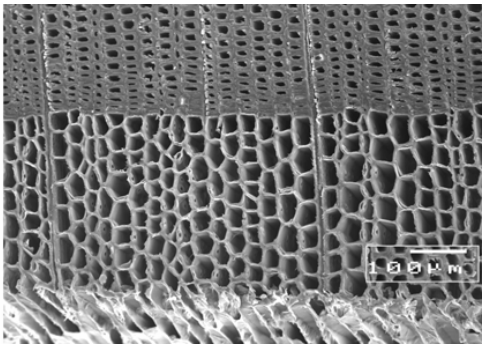

Figure 3. SEM photography of the cell structure of Scots pine. Reprinted by permission of Margot Sehlstedt-Persson.

Most cells are aligned in the vertical axis, in softwood about 90% of the cells and in hardwood 80%-95%. These cells are known as tracheids in softwood, in hardwoods as tracheids, fibres and vessels [19]. A taper tube with close ends is the approximate form of a tracheid, and the connections between them in the wood structure are small holes or pits. The vessels, on the other hand, have the form of continuous pipelines in an end-to-end arrangement. During the growing season, the wood structure develops differently at different times.

In the early period the tracheid walls become thin, and in the late period the walls grow thicker (figure 3). The remaining cells in the wood structure are rays, which consist of parenchyma cells. They are aligned perpendicular to the vertical axis. The functions of these various cell types are support and conduction for the vertically aligned cells and storage function for the cells situated perpendicularly to the vertical axis.

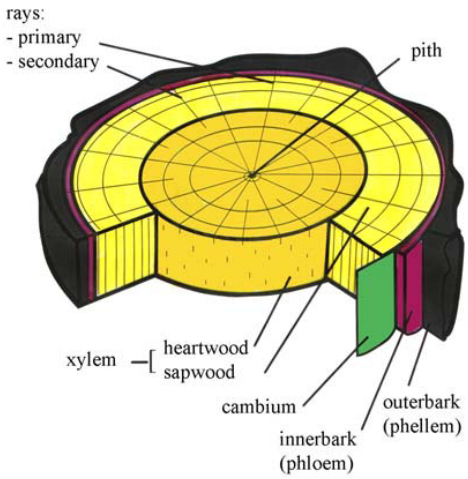

Figure 4. A cross-section of a stem. Reprinted by permission of Margot Sehlstedt-Persson.

The layer (cambium) between the bark and pith can be divided into two different kinds of functions for the wood (figure 4). The sapwood is located adjacent to the cambium and handles the transport of sap and water. Furthermore, heartwood consists, in contrast to sapwood, of inactive cells without functions in either water conduction or sustenance storage. Many wood species form heartwood. In the region where the sapwood makes the transition to heartwood, the extractive content is increased. Increased extractive content reduces permeability and makes this part of wood more difficult to dry. However, the permeability of the wood, i.e., how large the wood voids are and how they are connected, has the main influence and sets a limit to the drying rate when microwave drying technology is used.

2.2 Electromagnetic waves

An electromagnetic wave has two components: an electric (*E*) and a magnetic (*H*) field. They oscillate perpendicular to each other (figure 5), and they are perpendicular to the direction of propagation.

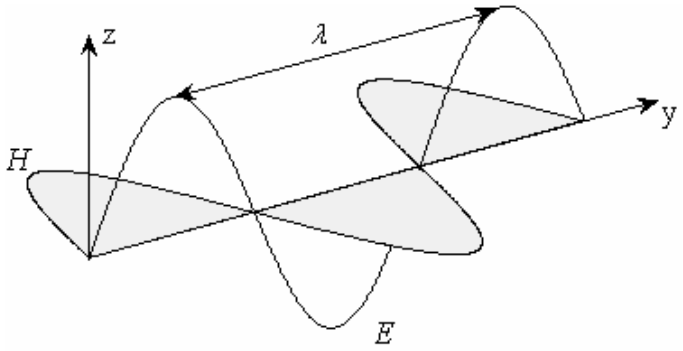

Figure 5. A monochromatic electromagnetic wave polarized in the y-z plane.

A monochromatic electromagnetic wave is a sinusoidal wave of one single frequency and thus one single wave length (λ). The direction of the electric field is described by the polarization. When the wave is horizontally polarized, the electric field is horizontal, for example. The wave, which is moving in the y direction, can be described mathematically [20] as a harmonic wave:

$$\mathbf{E}(x, y, z, t) = \mathbf{E}_0 e^{j\omega - \gamma y} \tag{1}$$

$$\mathbf{H}(x, y, z, t) = \mathbf{H}_0 e^{j\omega - \gamma y} \tag{2}$$

where $\mathbf{E}_0$ and $\mathbf{H}_0$ are the amplitudes, or strengths, of the electric and magnetic fields and oriented transverse to the *y* direction.

Furthermore, ω is the angular frequency and γ the complex distribution factor defined as:

$$\gamma = j\omega\sqrt{\varepsilon\mu} = \alpha + j\beta\,, \tag{3}$$

where μ is the complex permeability. For wood, which is not a magnetic material, the complex permeability μ is equal to the permeability of free space, μ_0. Furthermore, α is the attenuation factor, and β is the phase factor of the wave. ε is the relative complex permittivity defined as:

$$\varepsilon = \varepsilon_0\left(\varepsilon' - j\varepsilon''\right), \tag{4}$$

where ε_0 is the absolute permittivity for vacuum, ε' is the relative permittivity and ε'' is the relative dielectric loss factor. Relative permittivity indicates how much slower the electromagnetic wave propagates in the material compared to propagation in vacuum. The relative dielectric loss factor includes all loss mechanisms that can arise in a dielectric material when an electromagnetic wave penetrates or propagates through it. The loss is caused by frictional, inertial and elastic forces when the internal field in the material induces translational motion of bound or free charges, such as ions or electrons, and rotation of charge complexes, such as dipoles, e.g., water molecules. The relative dielectric loss factor and the relative permittivity in wood have been thoroughly investigated [21]. These investigations have shown that the dielectric properties of wood depend on mc, density, material temperature, frequency and the direction of the electric field relative to the fibre direction.

Figures 6 and 7 depict these dependencies in wood at a stated dry density. If the density increases or decreases, the value of relative permittivity and the dielectric loss factor will also increase or decrease. Figure 7 shows that at high mc the dielectric loss factor decreases as the temperature increases. This means that the energy absorption decreases as the temperature increases.

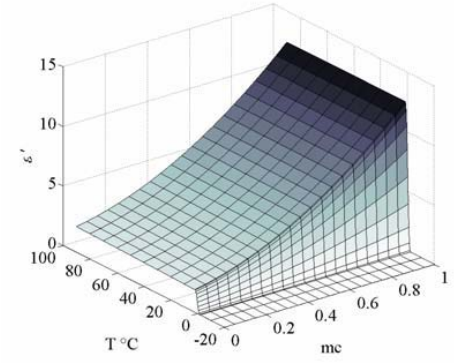

Figure 6. Relative permittivity as a function of mc and temperature for a dry density of 490 kg/m^3.

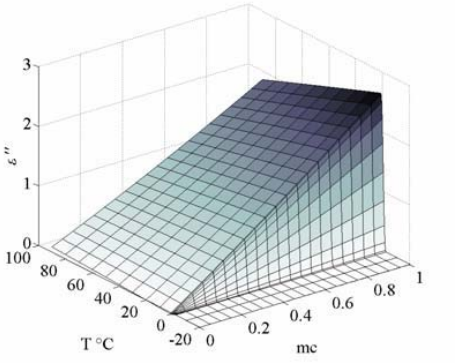

Figure 7. Dielectric loss factor as a function of mc and temperature for a dry density of 490 kg/m^3.

The relative permittivity and dielectric loss factor values used to form the diagrams in figures 6 and 7 are interpolated and collected from Torgovnikov's measurements [21], assumed to have a step transition as the water changes phase around zero degrees Celsius.

Combining equations 3 and 4 enables separation of the real and imaginary parts, and the expressions for the attenuation factor and phase factor will be:

$$\alpha = \omega\sqrt{\varepsilon_0\mu_0}\left(\frac{\varepsilon'}{2}\left(\sqrt{1+\left(\frac{\varepsilon''}{\varepsilon'}\right)^2}-1\right)\right)^{\frac{1}{2}}, \qquad (5)$$

and

$$\beta = \omega\sqrt{\varepsilon_0\mu_0}\left(\frac{\varepsilon'}{2}\left(\sqrt{1+\left(\frac{\varepsilon''}{\varepsilon'}\right)^2}+1\right)\right)^{\frac{1}{2}}. \qquad (6)$$

Combining equation 3 with wave equation 1 shows that the wave amplitude attenuates exponentially with the factor $e^{-\alpha y}$ and shifts phase with a factor $\phi = \beta y$, as the wave penetrates the wood material.

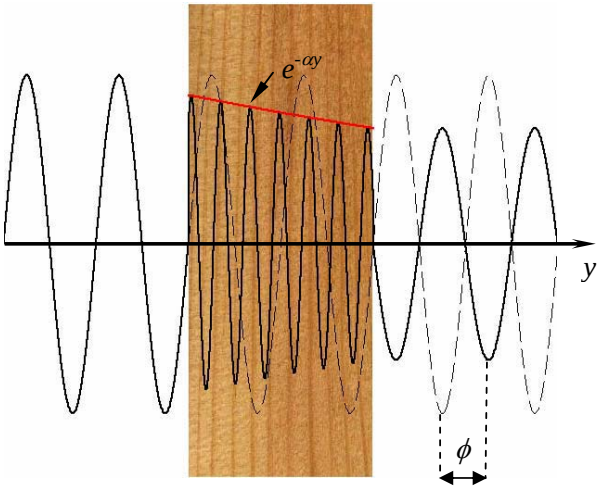

Figure 8. An electromagnetic wave transmitted into wood (solid line) compared to a wave transported in vacuum (dashed line).

Figure 8 shows two electromagnetic waves, one in the form of a dashed line that perceives wood as a transparent material and the other in the form of a solid line that is influenced by the wood material properties. The disturbed wave is attenuated and makes a phase change relative to the undisturbed wave as it is transmitted through the wood material. A phase change is the displacement between reference points on each wave and is usually expressed in an angular displacement ϕ (figure 8). The size of the phase shift and the attenuation depend on the mc and the dry density.

These parameters, attenuation and phase shift, are experimentally determined in the wood scanning equipment in Papers IV, V and VI. These works give a better understanding of how the microwaves are scattered and reflected by variations in the wood. In addition, the wood scanning FEMs provide a good foundation for the microwave heating models in Papers VII and VIII.

When the electromagnetic field oscillates, the polarity will change according to the frequency. Furthermore, the polar molecules in the wood try to oscillate in phase with these changes. However, as described earlier, these induced motions will be slowed down by frictional, inertial and elastic forces, causing the production of heat in the material. The heating, which occurs by microwaves, is a conversion of the electromagnetic energy into heat. The law of conservation of energy states that the total amount of energy in an isolated system remains constant. However, it may change form. For example, friction turns kinetic energy into thermal energy. Conservation of the electromagnetic field's energy is stated by the Poynting theorem [22]. From this theorem, the average total absorbed power can be expressed as:

$$P_{av} = \omega \varepsilon_0 \varepsilon'' E_{rms}^2 V \,, \tag{7}$$

where E^2_{rms} is the root mean square of the effective electric field and V is the volume.

When the transmitted power decays to *1/e* of its original value from the surface of the material, the power penetration depth [22] is defined as:

$$D_p = \frac{1}{2\alpha} \,. \tag{8}$$

The penetration depth is affected by the dielectric properties of wood. Higher densities and moisture contents result in decreased power penetration depth, as shown in figure 9. The temperature has a minor effect on the power penetration depth, apart from the step transition at zero degrees (figure 10). Microwave energy penetrates far deeper into frozen wood than into wood at room temperature.

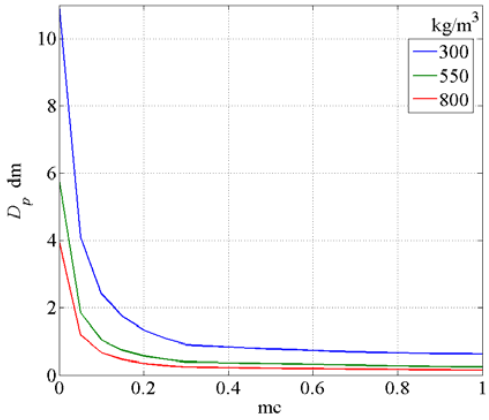

Figure 9. Power penetration depth as a function of mc for different dry wood densities at room temperature at a frequency of 2.45 GHz.

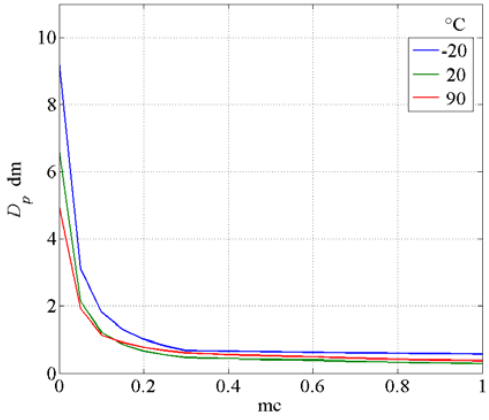

Figure 10. Power penetration depth as a function of mc in wood at different temperatures, dry density 490 kg/m^3 and frequency 2.45 GHz.

2.3 Electromagnetic heating of wood

There are various methods that can be applied for heating a material. In convective heating, heat is transferred to the material surface by a circulating fluid. In radiation, heat is transferred to the material surface by radiation. In conductive heating, heat is transferred to the material surface through connection to another material surface with higher temperature. In internal heating, only the material will be heated, compared to conventional heating where the surrounding area takes part in the transfer of energy or heat. The material heats instantly in the interior regions, making heating faster than with convectional heating.

Wood with a high mc, above the fibre saturation point, is capable of absorbing a great amount of electromagnetic energy. The amount of energy required to raise the temperature is determined by the specific heat capacity value of the material. Low values require less electromagnetic energy to increase the temperature. The specific heat capacity for wood is influenced by the mc, dry density and the temperature [23, 24, 25, 26]. The higher the mc, dry density and temperature, the higher becomes the specific heat. Furthermore, the specific heat for wood has a phase transition at zero degrees C, since it contains water. The higher the mc is, the higher is this change, which is obvious, since water has this quality at zero degrees Celsius. When the water changes phase, from solid (ice) to liquid or from liquid to gas (vapour), the energy alters the water structure and a certain amount of heat is transmitted to the water instead of increasing the temperature. This required amount of energy to change phase from solid to liquid is called heat of fusion; from liquid to vapour it is called heat of vaporization.

To implement this quality of behaviour in a physical model, a normalized pulse around the temperature transitions can be used (figure 11). This will avoid the convergence problem in the simulation caused by the sharp change in the thermal properties when the temperature varies.

A normalized pulse is equal to unity in a specified interval, in this case at the temperature intervals where the phase transitions from ice to water and from water to vapour occur.

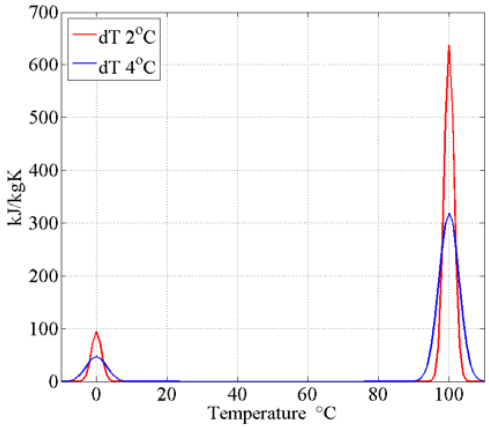

Figure 11. Normalized pulses around the temperature transitions.

The narrower this pulse is, the more it resembles a phase shift. However, it requires considerable computational power to integrate this phase transition into physical models.

When wood absorbs microwave energy, the total volume will be instantly heated if the wood volume and the MW frequency are adjusted to each other. However, the heating will not be uniform throughout the volume due to the nature of MW and the varying material properties. Heat conduction will serve to level out the uneven temperature distribution. The thermal conductivity of wood is dependent on mc, dry density, temperature and fibre direction [23, 25, 26]. The higher the mc, dry-weight density and temperature, the higher the thermal conductivity. Furthermore, the conductivity in the direction of the grain is higher than across the grain. The temperature variation in a given region in the wood over time can be described physically in a transient energy-balance equation. This heat equation describes the heat transfer by conduction and convection.

In the 2-D models that were developed, internal heat transfer by convection is omitted because of the small influence on the solution and because the omission makes the model less complex to solve. The energy-balance heating equation has the form:

$$\rho C \frac{\partial T}{\partial t} - \nabla(k \nabla T) - Q = 0, \tag{9}$$

where T is the temperature, ρ is wet wood density, t is time, C is the specific heat capacity, k is the thermal conductivity of wood and Q is the external heat source. The specific heat capacity is a function of the specific heat capacity of water and wood. In Paper VI, in which microwave scanning is described, the heat term, i.e., the microwave energy, is zero, since the electric field is very low during microwave scanning. However, in Paper VII and VIII, in which wood heating is modelled, the external heat source is the resistive heat generated by the electromagnetic field and is defined as:

$$Q = \frac{1}{2} \mathrm{Re}\left[\left(\sigma |E|^2 - j\omega\left(ED^*\right)\right)\right], \tag{10}$$

where σ is the conductivity, E is the electric field and D^* is the conjugate of the electric displacement.

2.4 Physical parameters used in the models

To determine physical parameters as dielectric properties, heat conduction, heat capacity, void volume, mc and wet and dry wood densities need to be known. By using a computed tomography (CT) scanner (Siemens Somatom AR.T.), wet and dry wood densities can be experimentally measured. A CT scanner works, in simple terms, such that several beams of X rays are sent from different angles through the scanning object, and after transmission, they are detected and their strength measured. Beams that have passed through less dense parts, such as for example dry sapwood, will be stronger, whereas beams that have passed through denser parts, such as for example wet sapwood, will be weaker. This information will be computer processed, resulting in a cross-section image of 512 x 512 pixels in which the densities of the object are shown in the form of grey-scales. If the shape of the area profile is the same for the wet and dry density images, it would be possible to calculate the mc from the CT images directly by subtracting the images. Since wood starts to shrink as it dries below the fibre saturation point towards zero mc, it changes its geometrical shape. This means that more thorough transforming calculations are needed in order to determine the mc. Hence a transformation must be done on the CT image of the dry wood to the shape of the wet wood prior to the calculation of the dry-weight moisture content (figure 12). This transformation is done by an elastic registration [27] in which a source image is unwarped, in this case the dry-density CT image, to resemble a target image, the wet-density CT image.

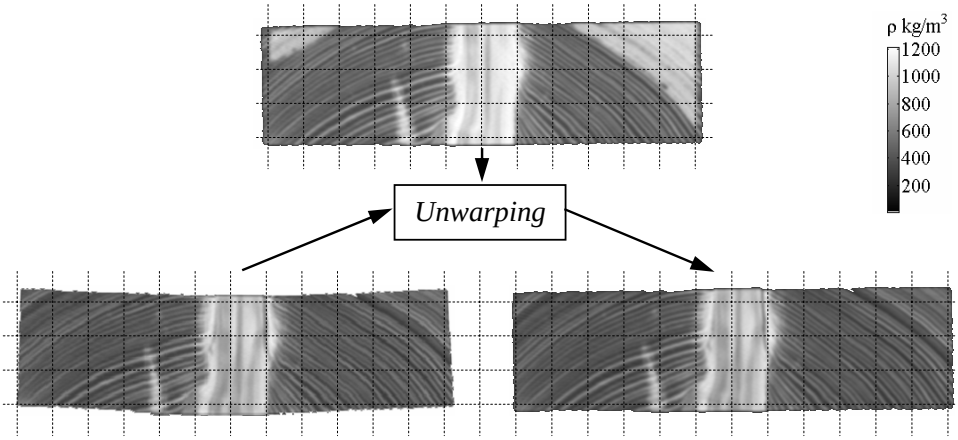

Figure 12. CT images of a completely dried Scots pine (Pinus sylvestris) wood piece (mc=0) (left), a wet wood piece (top) and the completely dried wood piece after elastic registration (right).

Dimensional changes in wood during drying make the heat and mass transfer model complex. Moisture-related definitions will be explained for that reason. When the mc exceeds the fibre saturation point, the green volume is determined by:

$$V_{green} = \frac{V_0}{(1-\beta_{\max})}, \tag{11}$$

where V_0 is the dry volume of wood and $\beta_{\max}$ is the maximum shrinkage coefficient [28]. The maximum shrinkage coefficient for different species has been determined previously [28]. It is necessary to distinguish between wet and dry volume, mass and density expressions. Combining the definitions of mc, density for wet wood ($\rho_{u,u}$) and dry wood ($\rho_{0,0}$) and equation (11) gives an expression for mc based on wet and dry density values:

$$u = \frac{\rho_{u,u} - \rho_{0,0}(1-\beta_{\max})}{\rho_{0,0}(1-\beta_{\max})}, \quad u \geq u_{fsp}. \tag{12}$$

However, if the mc is below the fibre saturation point, the total wet volume will be written as:

$$V_u = V_{green}(1-\beta_u) = \frac{V_0}{(1-\beta_{\max})}(1-\beta_u), \tag{13}$$

where β_u is the shrinkage coefficient at mc below the fibre saturation point and V_u is the total volume at mc below the fibre saturation point.

The shrinkage coefficient has an approximately linear behaviour below the fibre saturation point:

$$\beta_u = \frac{\beta_{\max}}{u_{fsp}}(u_{fsp} - u) \tag{14}$$

where u_{fsp} is the mc at the fibre saturation point, which is dependent on species and temperature. However, it has an approximately maximal value of 0.3 at of 20˚C. If the temperature increases, the fibre saturation point will decrease [28].

The corresponding expression for mc below fibre saturation, combining the definitions of mc, density for wet wood and dry wood and equations (13) and (14) is:

$$u = \frac{(1-\beta_{\max})u_{fsp}(\rho_{u,u} - \rho_{0,0})}{(\rho_{0,0}(1-\beta_{\max})u_{fsp} - \rho_{u,u}\beta_{\max})} \qquad u < u_{fsp}. \tag{15}$$

The algorithm for the mc calculation in the model works as follows. If the result of equation (15) is higher than the mc at the fibre saturation point, the moisture content is recalculated by equation (12).

This recalculation is possible since the wood volume doesn't change when the mc is higher than the fibre saturation point. Figure 13 shows the error that appears if the shrinkage below the fibre saturation point is not considered. The density values for Scots pine below the fibre saturation point, which are used to make the estimation in figure 13, are given by Esping [29].

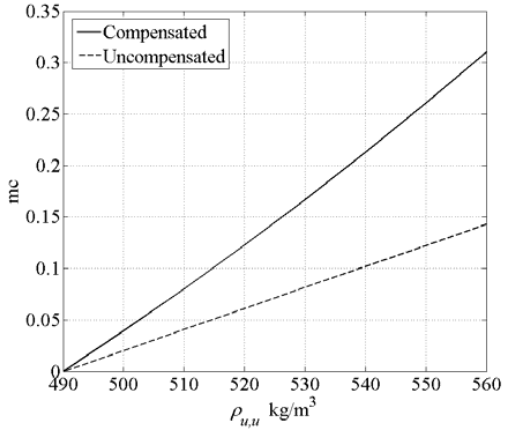

Figure 13. Calculated moisture content as a function of wood density: the effect on mc if considering volume shrinkage (compensated) or not (uncompensated) in the calculations.

The calculation of mc in the model sometimes gives unrealistic values, such as negative mc, for which reason the calculation results need to be filtered. These unrealistic values arise in the transformation process of the CT-scanned images. The images deviate in position relative to each other, in most cases at the wood area border. The filtering is done when an unreal value is found, replacing it with an average of surrounding values. Figure 14 shows the mc distribution calculated by the algorithm described. The figure also shows the large difference in mc level between heartwood and sapwood.

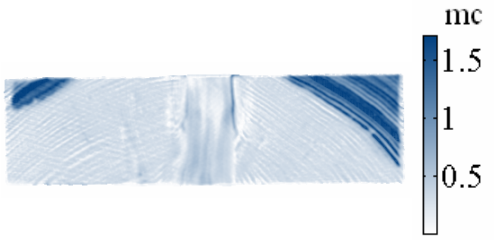

Figure 14. Calculated dry weight mc.

From the dry density and mc it is possible to estimate physical parameters, such as the dielectric properties, heat conduction, heat capacity and void volume. A schematic description of the procedure for generating an FEM model is shown in figure 15.

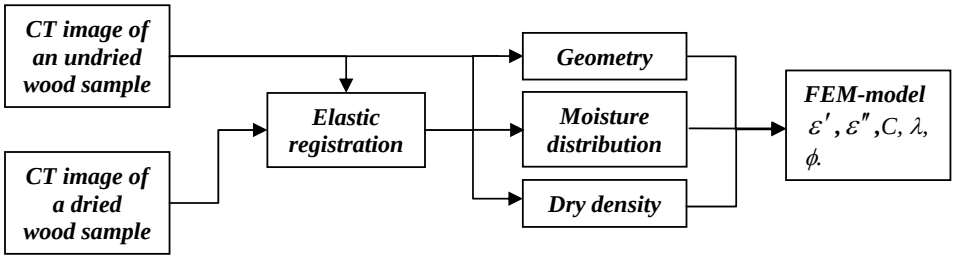

Figure 15. Description of working procedure for generating the FEM models. The physical wood properties, such as the dielectric properties (ε' , ε''), heat conduction (λ), heat capacity (C) and void volume (ϕ), are calculated as functions of temperature, dry density and moisture content in the model.

2.5 Finite Element Method (FEM)

To describe the physical system involving the microwaves' interaction with the wood during scanning or heating and drying, integral equations or partial differential equations (PDE) are used. Usually it is very difficult to obtain solutions to these mathematical equations that explain the behaviour of the given physical system. FEM divides a physical system into numbers of discrete elements or cells, since the complete system may be complex and irregularly shaped. However, the individual elements or cells could be easy to analyse. The multiphysics software that is used for generating the FEM models in Papers V, VI, VII and VIII is a modelling package for the simulation of any physical process that could be described with PDEs [30]. As there were limitations in the available computational power, a third dimension was ignored. However, the two dimensions were chosen along and across the fibres to keep the information of the internal structure as high as possible in order to solve the present multiphysics challenge.

2.6 Heat energy transfer between wood and the surrounding environment

When there is a significant fluid motion around wood, the convection heat transfer cannot be ignored. In general, the geometry and the ambient flow condition are used to determine the value of the heat transfer coefficient. In Papers VI and VII, simplified equations [31] are used for estimation of the free and forced convection heat transfer and the radiation heat transfer with the surrounding environment. The heat flux due to the evaporation from the wood surface is ignored in the models presented in Papers VI and VII, which show that it has a significant influence on the modelled surface temperature. The model in Paper VIII is further complemented with the heat flux due to evaporation.

Wood is a hygroscopic and porous dielectric medium, which means that fresh, undried wood has both free and bound water within the solid matrix. Free water can appear as vapour or liquid in the pores. Wood with mc below the fibre saturation point contains mainly bound water captured in the cell matrix structure. If the mc is above the fibre saturation point during the absorption of electromagnetic energy, the temperature of the wet wood piece will reach the boiling point of water. As the temperature increases, the internal pressure will also increase, causing moisture evaporation that will be forced from the interior towards the surfaces of the wood piece. How fast the vapour will be transported from the wood piece depends on the wood structure, i.e., how large the wood voids are, how they are connected and how much energy is needed to release the bound water in the wood cell structure.

2.7 The media flow in wood during heating and drying

In porous media such as wood, the mass transport is caused by several mechanisms. These mechanisms are molecular diffusion, capillary movement and convection or Darcy flow. The molecular diffusion is movement of molecules from a region where their concentration is high to a region that has low concentration. Capillary movement occurs when the adhesive intermolecular forces between the water and wood substance are stronger than the cohesive intermolecular forces inside the water. The Darcy flow is stated as a proportional relationship between movement of fluids through permeable or porous media, such as wood, and the pressure gradient. Permeability is defined as the ability of a material to transmit fluids.

If the initial mc is greater than the fibre saturation point, the Darcy flow could undergo a complex multiphase flow during microwave drying. Since the water in the wood could change form in a phase shift from liquid to gas, the Darcy flow for each phase can be approximated [32].

Apart from the different permeabilities for liquid and gas flow, wood permeability varies depending on species. Softwoods are often less permeable than hardwoods. Furthermore, the age of the wood affects permeability, the heartwood thus being less permeable than sapwood. Permeability depends as well on the direction of flow. The flow along the fibres is greater than the flow transverse to the fibres [28]. In short, wood permeability is very complex.

The results in Paper VII show that the finite element modelling gives a good estimation of heat distribution when microwave heating is applied to a well-described porous material such as wood. In this paper, no mass flow in the wood piece during the heating process was included. The mobile media in wood, apart from air, can be water in liquid phase, in vapour phase or a combination of both. Furthermore, extractives in soft wood can also be included as one of the mobile media.

During the thawing and heating process (Paper VII), the weight of the specimens decreases about 0.1 kilogram, which approximately corresponds to a reduction in mc from 0.84 to 0.76. Figure 16 shows the difference between the mc before and after thawing and heating. The mc estimations are based on the previously mentioned algorithm using CT images (chapter 2.4).

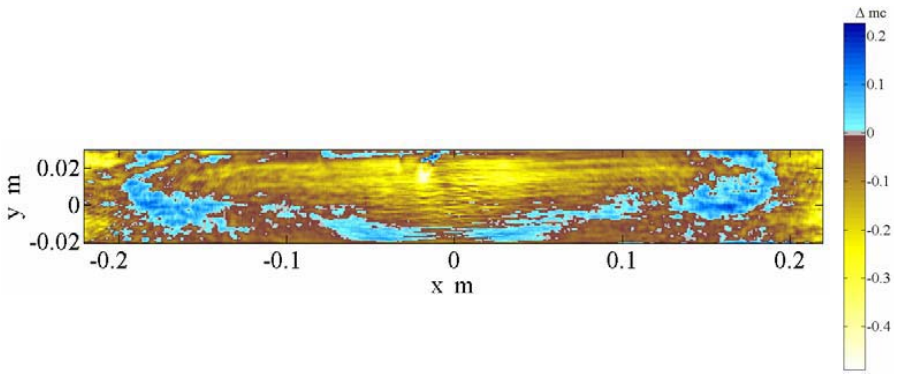

Figure 16. A subtraction image from CT-scanning that shows the difference in mc before and after the heating process.

The brown and yellow areas in figure 16 show a negative difference between before and after the heating process. The blue area is where the difference is positive or zero. The interpretation of this is that the water has been forced out through the butt ends and also down towards the lower surface. A comparison of this pattern with the simulated internal temperature profile, figure 17, shows that mc decreases where the hotter spots appear. This is physically correct, since the water and water vapour pressure in the wood increase as the temperature increases.

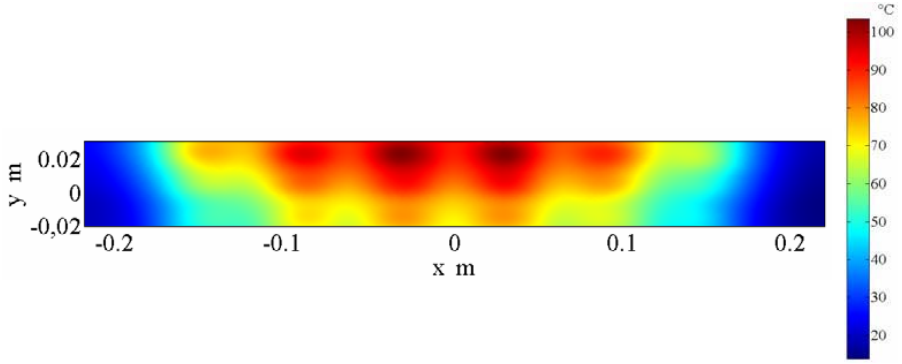

Figure 17. Simulated internal wood temperature after about 30 minutes of 1 kW microwave heating. The mean mc value was 0.84.

The uneven internal wood temperature is caused by the electromagnetic field distribution and the power penetration depth; i.e., the higher the mc is, the less is the power penetration.

The results from process simulation using the developed 2-D FEM heat and mass transfer model, Paper VIII, give a convincing correspondence between the theoretical approaches used in the model and the experiment. The simulated core temperature values as well as the mc values agree well with the measured ones. In the experiments, the maximum input power was chosen to keep the wood temperature below 110°C. This temperature limit is based on earlier experiences in which fast heating above this limit often causes too high internal vapour pressure, which gives rise to internal cracks. These cracks seem to arise where the ray cells are situated in the wood structure. Figure 18 shows an exaggerated result of uncontrolled microwave drying.

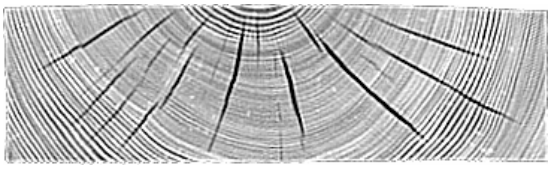

Figure 18. A CT image showing internal checks within a Scots pine wood cross-section caused by uncontrolled drying.

2.8 The microwave heating and drying equipment

As a prelude to the design work of the online microwave wood drier, simulations were performed by Risman [33] using the QW3D software in order to optimize the field distribution in the cavity, i.e., to determine the cavity dimensions to achieve as even heat distribution as possible. The field distribution, and consequently the heat distribution, depends on the design of the cavity [34]. The electromagnetic waves interfere with each other in the cavities and thereby give rise to a specified electric field within the space. The cavity or applicator that was developed for wood drying is not quite a single-mode cavity. Actually, there is a supplemental mode that allows the heat distribution to extend further in the longitudinal direction (figure 3 in Paper II). This will decrease the crosstalk between the cavities. Crosstalk means that the fields in the different cavities affect each other disadvantageously and out of control. It is for that reason of great importance to minimize this effect. The heat distribution in the cavities gives rise to longitudinally directed hotter spots in the wood load (figure 19). The balance between these spots is affected or caused by two vertical and two horizontal strip plates (figure 3 in paper II) that also reduce the crosstalk. The heat distribution shown in figure 19 was captured by an IR camera (AGEMA 550).

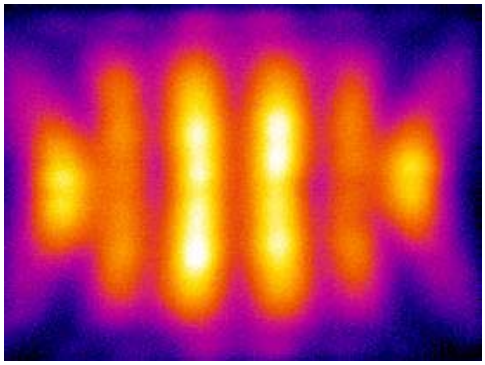

Figure 19. IR image showing the heat distribution at the wood surface beneath one applicator.

The microwave online drier is constructed as a tunnel containing modules consisting of 5 applicators (cavity, waveguide and magnetron) placed side by side. Each such cavity has a length of approximately 0.44 metres and a width of 0.31 metres. The number of cavities determines the possible length of the wood components, in this case 2.2 metres. The magnetrons, or microwave generators, have a nominal maximum output power of 1 kW, and the power for each magnetron can be regulated continuously [35]. The possible wood load thickness can be chosen from 15 to 55 mm. Since the tunnel is open at both ends, chokes are placed in the end openings to eliminate microwave radiation leakage. The modules in this design are manufactured to have a parallel displacement of 35 mm between each other (figure 20) to prevent the hotter regions formed in the material (figure 19) from appearing at the same positions in the wood load as they are conveyed through the tunnel during the drying process. The size of the displacement depends on the wavelength. The hotter regions are formed with a distance of a half wavelength, and for that reason the displacement is a quarter wavelength.

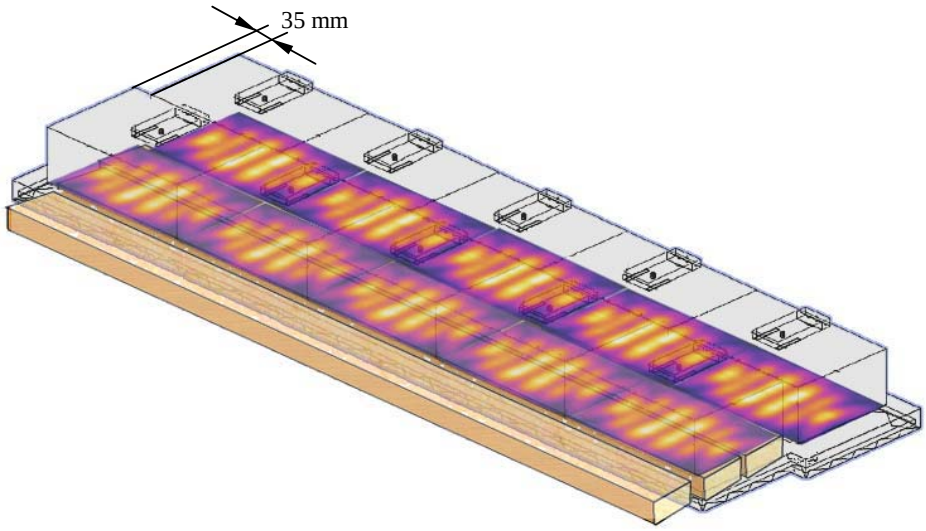

Figure 20. The microwave drier consists of modules that have a parallel displacement of 35 mm between each other.

2.9 Change in wood material properties

When the drying process begins, the temperature increases, and then the internal vapour pressure and volume change arise. If the mc exceeds the fibre saturation point, the water in the cells will be forced out from the wood because of the increasing interior water and vapour pressure during the heating process. Furthermore, as the temperature rises, the water in the cells, bounded or free, starts to vaporize, and the mixture of water and gas will be forced out from the wood. Hence, when the mc decreases below the fibre saturation point, the remaining water consists of bound water in the wood cell walls and will be forced out of the wood in the form of vapour. If the internal pressure exceeds the strength value in the wood tissue, it causes internal checks in the wood structure, which in turn affect the wood properties. Another phenomenon that might appear if the process is uncontrolled is thermal runway.

Figure 21. An internal char spot in birch wood caused by thermal runaway.

Localized thermal runaway can occur if the thermal conductivity is low and if the dielectric properties, such as the loss factor, increase, resulting in uncontrolled rate of temperature rise. This thermal effect may occur towards the end of the drying process, as the mc in some positions becomes almost zero. Then a rapid pyrolysis in the wood interior appears (figure 21) and results in changed material

properties. A pyrolysis is a process wherein the material is heated without the presence of oxygen, but where char production occurs. This destructive result that affects the properties of wood needs to be avoided during microwave drying.

Oloyede and Groombridge [11] stated that the strength reduction in wood was 60% compared to air-circulation drying when microwave energy was used for drying. In a later article [36] they have also mentioned that if the microwave drying of wood is controlled, the process can be much more reliably performed in terms of quality of the final products. Machado [12] also obtained a clear loss in compression strength parallel to the grain in clear oak wood when it was exposed to microwaves. However, it needs to be pointed out that the microwave exposure was not controlled and this lack of control surely affected the result [37].

The drying method, regardless of whether it is microwave drying or air-circulation drying, has shown to have no impact on wood strength, at least in Norway spruce, during controlled drying conditions (Paper I). Further, in Paper III the effect of temperature level on wood hardness during microwave drying is investigated, as well as whether the response is different from that of conventionally dried wood. The results show that drying wood to an mc of 0.12 at drying temperatures of 60°C and 100°C does not affect wood hardness parallel or perpendicular to the grain differently, regardless of drying method. The same can be concluded for wood hardness perpendicular to the grain when drying proceeds to mc 0.08 at drying temperatures of 60°C and 100°C. Nor is wood hardness parallel and perpendicular to the grain differently affected by the drying temperature, at least at 60°C, 100°C and 110°C, when the wood is dried by microwave heating to an mc of 0.08 or 0.12. However, the results show that the there is a significant difference in wood hardness parallel to the grain between the two drying methods when the samples are dried at temperature levels of 60°C and 100°C to mc 0.08. One possible explanation of these results is the drying technique, since the microwave drying method moves the moisture and the extractive substance by an internal pressure to the surface. This substance, which accumulates at the ends, could cause the differences in the measured values. Why this difference does not

appear when the wood pieces are dried to mc 0.12 could depend on the drying time. The wood pieces dried to mc 0.08 are microwave treated much longer, and therefore more extractives could accumulate in the ends.

2.10 Colour response

There are advantages with this online microwave drier due to the possibility of heating and drying wood faster than conventional methods and with preserved quality. Colour changes are normally unavoidable in conventional drying, and the reason is believed to be a combination of drying time and temperature levels during the different drying phases. In fact, drying wood with microwave energy causes almost no colour change, which is positive, as there is a demand for pale products in some countries. In the furniture and flooring industries, where products made of hardwoods are common, the colour of wood is important. Higher temperatures during drying make the colour of the products darker [38]. Therefore, conventional air circulation drying of hardwoods needs to be maintained at relatively low drying temperatures in order to produce pale-coloured products.

An investigation in which conventional drying was compared to microwave drying with respect to the colour changes of birch wood before and after drying [8] shows that microwave-dried wood undergoes less change in colour than does conventionally dried wood. Colours can be classified in terms of their hue angle (h), lightness (L^*), and saturation (C^*). These coordinates make a three-dimensional colour space (figure 22). The hue angle is expressed in degrees. The colour red defines the start at 0 degrees. Yellow is found at 90 degrees, green at 180 degrees and blue at 270 degrees. The lightness of an area is judged relative to the brightness of a similarly illuminated area that appears to be white or highly transmitted [39]. Chroma is the colourfulness of an area judged in proportion to the brightness of a similarly illuminated area that appears to be white or highly transmitting [39].

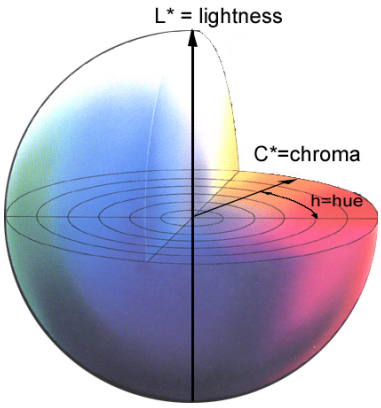

Figure 22. Colour space in terms of h, L^* and C^* coordinates ([40] modified).

Table 1 shows results from an earlier test with conventional drying [41] and results from the microwave online drier. Colour measurement was done with a portable photoelectric colorimeter, Minolta chromameter CR 310. In the conventional drying test, the maximum dry-bulb drying temperature during the drying process was 69°C [41], and the interior temperature maximum was 105°C in the microwave drying test. In both cases, the colour measurement was done at the pith side of a board newly planed 1 mm. Both of the results in table 1 are average values at a 95% confidence interval, and the values are based on measurements of 20–30 boards for the conventionally dried pieces and 10 boards for the microwave-dried pieces.

Table 1. Colour measurement values for conventional and microwave-dried birch.

Drying method	L^*	C^*	h
Microwave	78.0 ± 0.6	20.6 ± 0.6	73.0 ± 0.2
Conventional	74.5 ± 0.4	21.0 ± 0.2	73.2 ± 0.2

As the tests were not done on the same occasion, the investigation does not include matched samples. The results show that there is a tendency towards greater lightness when using microwave heating compared to the conventional

method. The C^* and h results show no or small differences between the drying methods. The ΔE^*_{ab} value indicates the degree of colour difference and is defined as [39]:

$$\Delta E^*_{ab} = \sqrt{\left(\Delta L^*\right)^2 + \left(\Delta a^*\right)^2 + \left(\Delta b^*\right)^2}\,, \tag{16}$$

where the a^* and b^* coordinates can be calculated by these relations

$$C^* = \sqrt{\left(a^*\right)^2 + \left(b^*\right)^2}\,, \tag{17}$$

$$h = \tan^{-1}\left(\frac{b^*}{a^*}\right). \tag{18}$$

If the colour difference value exceeds 2–3 units, it is possible for the human eye to see the colour difference [42]. For this test, the value exceeded approximately 3.5 units, and this result verifies the previously mentioned result [8] that showed that the microwave process produces lighter-coloured wood products than does the conventionally drying process.

3 CONCLUSIONS

- The drying method has no impact on wood's bending strength under controlled drying conditions.

- There is no significant difference in hardness perpendicular to the grain between wood dried by microwaves or air circulation under controlled drying conditions.

- The investigation of wood colour response from different drying methods verifies that microwave drying causes less colour change than does the air-circulation drying method.

- The developed simulation model is a very good tool to use to demonstrate and explain the interaction between wood and microwaves during scanning.

- The simulations using the developed microwave heating model correspond very well to experimental temperature measurements.

- The correspondence between the 2-D FEM heat and gas mass transfer model and the experiment is convincing.

4 FUTURE WORK

Since modelling is a good tool to use for explaining and understanding the microwave heating and drying process, it would be a challenge to make a microwave drying model that involves a multiphase flow, i.e., water flow in liquid and gas form. Another possibility would be to develop the model by including thermal runaway. Such a complete model should also be basis for future scheduling of the microwave drying process.

Furthermore, it would be interesting to investigate the effects of microwave heating and drying on foreign wood species, apart from the Nordic kinds of wood, i.e., how the properties such as mechanical and colour properties would be affected. The development of a heating and drying model for foreign species with varying liquid permeability would also be a useful step.

Lastly, an important step would be to develop a sensor system for measuring mc without interrupting the drying process, i.e., a system for controlling the drying process adaptively.

5 REFERENCES

1. Wiberg, P. 2001. *X-ray CT-scanning of Wood During Drying*. Ph.D. Thesis. Vol. 10. Luleå University of Technology, Division of Wood Physics.

2. Leiker, M., and Adamska, M. 2004. Energy efficiency and drying rates during vacuum microwave drying of Wood. Holtz als Roh- und Werkstoff 62:203–208.

3. Avramidis, S., Zwick, R. L., and Neilson, B. J. 1994. Commercial scale RF/V drying of softwoods. Part I. Basic kiln design considerations. Forest Prod. J., 46(5):44–51.

4. Avramidis, S., and Zwick, R. L. 1994. Commercial scale RF/V drying of softwoods. Part II. Drying characteristics and degrade. Forest Prod. J. 46(6):27–36.

5. Egner, K., and Jagfeld, P. 1964. Versuche zur künstlichen Trocknung von Holtz durch Mikrowellen. Holtz-Zentralblatt 129:297–300.

6. McAlister, W. R., and Resch, H. 1971. Drying 1-inch ponderosa pine lumber with a combination of microwave power and hot air. Forest Prod. J. 21(3):26–34.

7. Barnes, D., Admiraal, L., Pike, R. L., and Mathur, V. N. P. 1976. Continuous system for the drying of lumber with microwave energy. Forest Prod. J. 26(5):31–42.

8. Antti, A. L. 1999. *Heating and drying wood using microwave power*. Ph.D. Thesis. Vol. 35. Luleå University of Technology, Division of Wood Physics.

9. Antti, A. L., Zhao, H., and Turner, T. 1999. Investigation of the heating of wood in an industrial microwave applicator: theory and practice. Drying Technology 18(8) (Sept. 2000):1665–1676.

10. Antti, A. L., and Perré, P. 1999. A microwave applicator for on-line wood drying: Temperature and moisture distribution in wood. Wood Science and Technology 33:123–138.

11. Oloyede, A., and Groombridge, P. 2000. The influence of microwave heating on mechanical properties of wood. *Journal of Material Processing Technology* 100:67–73.

12. Machado, J. S. 2006. Effect of Microwave Treatment on Oak Compression Strengh. Silva Lus. 14(1):51–58.

13. Torgovnikov G., and Vinden, P. 2000. New Wood Based Materials Torgvin and Vintorg. 5th Pacific Rim Bio-Based Composite Symposium, 10–13 December 2000, Canberra, Australia. Proceedings:756–764.

14. Johansson, J. 2001. *Property Predictions of Wood Using Microwaves*. Licentiate Thesis. Vol. 35. Luleå University of Technology, Division of Wood Technology.

15. Lundgren, N. 2007. *Microwave Sensor for Scanning Sawn Timber*. Doctoral Thesis. Vol. 9. Luleå University of Technology, Division of Wood Technology.

16. Perré, P, and Turner, I. W. 1999. The use of numerical simulation as a cognitive tool for studying the microwave drying of softwood in an over-sized waveguide. Wood Science and Technology 33(6):445–464.

17. Zhao H., and Turner, I. W. 2000. The use of a coupled computational model for studying the microwave heating of wood. Applied Mathematical Modelling 24:183–197.

18. Perré, P., and Turner, I. W. 2004. Environmental and Energy Engineering Microwave drying of softwood in an oversized waveguide: Theory and experiment. AIChE Journal 43(10):2579–2595.

19. Dinwoodie, J. M. 2000. *Timber: Its nature and behaviour*. 2nd ed. London: Spon Press.

20. Hippel, A. von, 1954. *Dielectric and waves*. New York: John Wiley & Sons.

21. Torgovnikov, G. I. 1993. *Dielectric Properties of Wood and Wood-Based Materials*. New York: Springer-Verlag.

22 Metaxas, A. C. 1996. *Foundations of electroheat*. New York: John Wiley & Sons.

23. Kollman F. F. P. and Côté, W. A. 1984. *Principle of Wood Science and Technology* (Vol. 1. *Solid wood*). New York: Springer.

24. Kanter, K. R. 1957. The Thermal Properties of Wood. *Derev Prom*. 6(7):17–18.

25. Steinhagen, H. P. 1977. *Thermal Conductive Properties of Wood, Green or dry, from -40 to 100 ˚C: A literature review*. USDA Forest Service General Technical Report FPL-9, Forest Products Laboratory, Madison, WI.

26. MacLean, J. D. 1941. Thermal Conductivity of Wood. *Heating, Piping and Air Conditioning* 13(6):380–391.

27. Sorzano, C. O. S., Thévenaz, P., and Unser, M. *Elastic Registration of Biological Images Using Vector-Spline Regularization*, IEEE Transactions on Biomedical Engineering: 2005. Vol. 52:652–663.

28. Siau, J. F. 1995. Wood: Influence of moisture on physical properties. Virginia Polytechnic Inst. and State Univ., Blacksburg.

29. Esping, B. 1992. *Trätorkning 1a: grunder i torkning*. Göteborg: Graphic Systems AB.

30. Comsol AB. Tegnérgatan 23 SE-11140 Stockholm. Home page: www.comsol.se.

31. Holman, J. P. 1997. *Heat Transfer.* 8th edition. New York: McGraw-Hill.

32. Ni, H., Datta, A. K., and Torrance, K. E. 1999. Moisture transport in intensive microwave heating of biomaterials: a multiphase porous media model. Int. J. of Heat and Mass transfer 42:1501–1512.

33. Microtrans AB. Sandsjön 800, SE-43892 Härryda, Sweden. Home page: www.por.se.

34. Risman, Per. O. 2005. *Microwave heating applicator*. Patent WO 2005/022956 A1.

35. Dipolar AB. Gymnasievägen 16 SE-931 57 Skellefteå. Home page: www.dipolar.se

36. Oloyede, A., and Groombridge, P. 2000. A Control System for Microwave Processing of Materials. Journal of Manufacturing Science and Engineering 122: 253–261.

37. Antti, A. L., Jönsson, A. and Nilsson, M. 2001. The effect of drying method on mechanical properties of wood: comparisons between conventional kiln and microwave-dried Scots pine. *Third European Cost E15 Workshop on Wood Drying, Helsinki, Finland*. Proccedings pp. 1–9.

38. Stenudd, S. 2003. Colour Response Of Silver Birch To Press Drying. *8-th International IUFRO Wood Drying Conference, Brasov, Romania, 24-29 August*. Proceedings pp. 449–454.

39. Hunt, R. W. G. 1995. *Measuring colour*. 2nd ed. Hertfordshire: Ellis Horwood Limited.

40. Minolta, 1993. Precice Color Communication, color control from feeling to inspiration. Minolta Camera Co., Ltd. J307(E)-A2.

41. Sundqvist, B. 2000. *Wood Colour Related to Kiln Drying*, Licentiate. Thesis. vol. 38. Luleå University of Technology, Division of Wood Physics.

42. Hon, D. N.-S. and Minemura, N. 1991. Color and Discoloration. In. D. N.-S. Hon and N. Shiraishi (Eds.). *Wood and Cellulosic Chemistry*, New York: Marcel Dekker, Inc. pp. 395–454.

APPENDIX

Errata

Paper VI: On page 3 in the result chapter, there is an error in the average moisture content. The correct value is 0.84, rather than 0.43.

Paper VII: On page 266 in the results and discussion chapter, the measured and the simulated surface temperatures, figure 8 and figure 9, were inadvertently switched.

I

ELSEVIER

Journal of Materials Processing Technology 141 (2003) 41–50

Journal of Materials Processing Technology

www.elsevier.com/locate/jmatprotec

The effect of microwave drying on Norway spruce woods strength: a comparison with conventional drying

L. Hansson*, A.L. Antti

Luleå University of Technology, Division of Wood Physics, Skellefteå Campus, SE-931 87 Skellefteå, Sweden

Received 17 June 2002; accepted 22 November 2002

Abstract

The purpose of the present work was to investigate whether the drying method itself affects strength of wood apart from fibre direction, density, temperature in the wood, moisture content and with which angle the microfibril is placed in the middle layer at the secondary cell wall S_2. The drying methods compared were microwave drying and conventional air-circulation drying, and the species tested was Norway spruce. The result shows that it is not possible to demonstrate any difference between the two drying methods with respect to the strength of the wood. What affects wood strength are such variables as moisture content, number of annual rings and the density properties weight, width and thickness.

Keywords: Microwave drying; Wood; Strength

1. Introduction

There are different methods of drying wood, and the most common is conventional air-drying. One of the methods that have been investigated in recent years is drying wood by microwave heating [1]. If wood is exposed to an electromagnetic field with such high frequency as is characteristic for microwaves, the water molecules, which are dipoles, begin to turn at the same frequency as the electromagnetic field. However, wood consists not only of water but also of polymers as cellulose, hemicellulose and lignin. These polymers are also polar molecules, and therefore even they are likely to be affected by the electromagnetic field. According to Oloyede and Groombridge [2] the strength reduction in wood was 60% when microwave energy was used for drying as opposed to air-circulation drying. However, that result may be dependent on the method used to carry out the drying process, which according to Antti et al. [3] was entirely out of control and only a way to remove moisture from wood.

The strength in wood varies a lot between specimens of the same species, but also within one and the same specimen. That is because wood is a biological material that consists of different structures for different purposes for its life. In conifers the dominant wood types are sapwood and heartwood. Juvenile wood is a structure of wood that is not as dominant; it usually includes the first 10–20 annual rings closest to the pith, and it can affect wood strength to a relatively large extent [4]. The strength can also vary within one and same wood construction as a result of reaction wood. That can depend on interference in the wood recession, for instance as a consequence of the tree having grown on a sloping ground surface, which causes the tree to produce compression wood to counteract the tendency to lean and to maintain upright growth.

In order to examine the strength of wood, the three-point bending test was used. That gives a bending stress that is a combination of tensile strains, compressive strains and shear strains. In investigations of the mechanical properties of wood, the modulus of elasticity (MOE) and the modulus of rupture (MOR) are determined. As the wood material properties vary, it is necessary to perform a quantity of tests and analyse them statistically to obtain values for the wood's MOE and MOR. The MOR expresses the ultimate bending strength, and this modulus is actually the equivalent stress in the extreme fibre of the specimen at the point of failure. For the wood type Norway spruce (*Picea abies*) with 12% moisture content, MOE lies between 8.3 and 13 GPa and for MOR 66–84 N/mm^2 [5,6].

With Oloyede and Groombridge [2] as a point of departure, the aim of the present work was to investigate whether

* Corresponding author.
E-mail address: lars.hansson@tt.luth.se (L. Hansson).

0924-0136/$ – see front matter © 2002 Elsevier Science B.V. All rights reserved.
doi:10.1016/S0924-0136(02)01102-0

the drying method additionally affects the strength of the wood, apart from fibre direction, density, temperature at the sample, moisture content and with which fibre angle the microfibril is placed in the middle layer at the secondary cell wall S_2. The fibre angle in particular has an important effect on strength [5,7]. The parameters that were investigated were variables that affect density, such as moisture content, number of annual rings, weight, width and thickness, drying temperature and drying method. The drying methods that were compared were conventional air-circulation drying and microwave drying.

2. Materials and methods

The wood species that was investigated in this study was Norway spruce (*P. abies*) and it was received in green sawn condition with a dimension of 50 mm × 100 mm (in dried condition), from a sawmill in the north of Sweden in the period of December 2001. The selected specimens were pith sawn and as clear of knots as possible and if possible not taken from the same tree of origin. From these, 500 mm pieces were then cut into 40 samples in total, which thereafter were divided into four equal main groups containing specimens from different places of origin. Then the pieces in the main groups were divided longitudinally into two equal groups (Fig. 1) from which one part went to conventional drying. The second group was additionally divided up longitudinally into four pieces for microwave drying. From each sample, small pieces were picked out for determination of the moisture content, for which the oven-dried weight basis was used. This was in order to estimate weight for the sample when it had reached the correct end moisture content. The design that was selected by the sample division enabled a good statistical analysis of the difference between the drying methods. This is because the samples for the two drying methods were picked out from specimens from the same tree of origin. Therefore, the samples are very nearly mirror images of each other; i.e. matched samples were obtained.

2.1. Drying methods

Of the four main groups, two groups were dried at a temperature of 60 °C to an end moisture content of 8 and 12%, respectively. The drying temperature for the two other groups was 100 °C and the end moisture content was 8 and 12%, respectively. The lower drying temperature is typical for low-temperature drying, and the higher is at the limit for high-temperature drying. That the level for the higher drying temperature was set to 100 °C was due to limitations of the air-circulation laboratory kiln that was used. The following

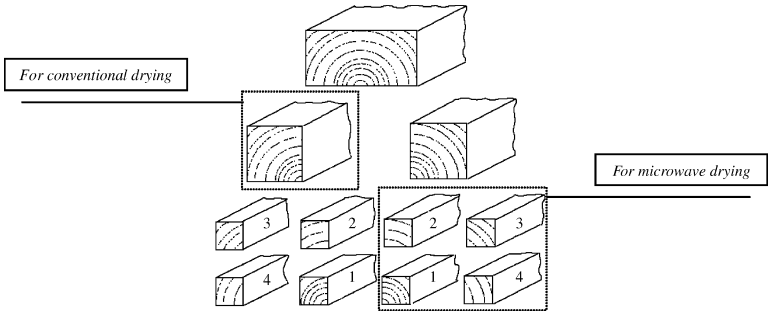

Fig. 1. Sample dividing.

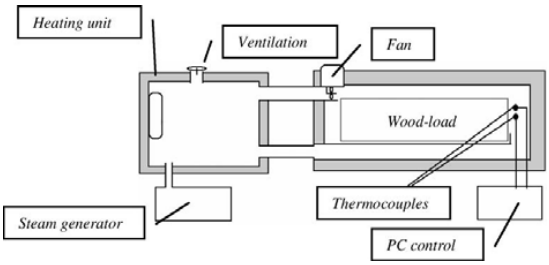

Fig. 2. Schematic schedule of the conventional drying kiln.

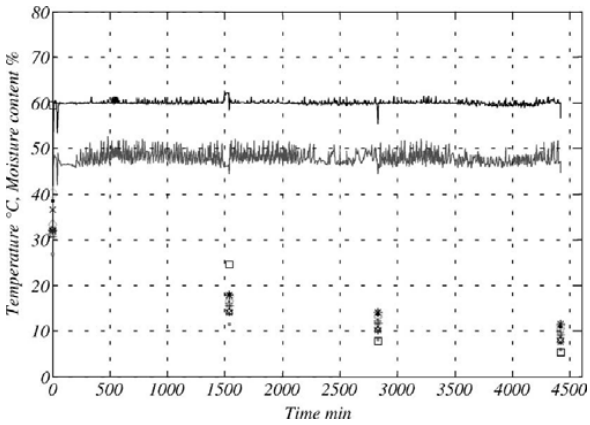

Fig. 3. Conventional drying: 60 °C to a moisture content at 8%.

sections describe how the two different drying methods were performed.

2.1.1. Conventional drying

The conventional drying was performed in a laboratory kiln built of aluminium with a height of about 0.3 m and a length of about 0.8 m (Fig. 2) in which the air circulates around the load with a speed of approximately 2 m/s. DOS laboratory software controls the air climate conditions with the help of thermocouples which measures the dry and wet temperature in the kiln. Climate control is done using an air heater and a steam boiler that have a maximum effect of 6 kW each.

The two groups which were dried to a final moisture content of 12% at drying temperatures of 60 and 100 °C were dried in a constant climate with a wet bulb temperature of approximately 49 and 91 °C, respectively until the equilibrium moisture content in the wood was reached at 8%. During the drying course, a moisture content gradient was formed between the wood surface and its interior since the surface dries faster. The difference in moisture content between these two areas causes strains in the material. In order to equalise the moisture content, and thereby do stress compensation, the samples were conditioned for approximately 8 h in a climate with a wet temperature of about 57 and 98 °C, respectively, which gave final moisture content of approximately 15%. During the drying and conditioning processes, the weight of each specimen was also measured in order to determine when the correct end moisture content was reached. The groups with a final moisture content of 8% were dried in the same way as the above mentioned groups, but now in a climate with a wet temperature of approximately 41 and 82 °C, respectively, so that the wood achieved an equilibrium moisture content of 5%. Also these groups were conditioned for approximately 8 h, but in a climate with a wet temperature of approximately 55 and 96 °C, respectively, which gave an end moisture content of the wood of approximately 12%.

Fig. 3 shows the wet- and dry-bulb temperature, as well as the reduction of moisture content, for the samples during the process. Thereafter, the test samples were conditioned for a further 8 h. The total drying time for this experiment is displayed in Table 1. Since the other drying cycles were performed in the same way as has been described, drying times for these cycles are also displayed in Table 1. Each load had a volume of approximately 12.5 dm^3.

2.1.2. Microwave drying

Microwave drying was performed in a domestic microwave oven (Fig. 4). In order to measure the temperature in the middle of a sample, a drill hole was made into which a fibre-optic sensor (ASEA 1110) was placed. The approximately 6.25 dm^3 wood load was exposed to the oven's maximum power emission (1.4 kW) during the time when the temperature in the middle of the sample was lower than the current drying temperature. The control of this process was done with laboratory software. During the drying process, the weight of the pieces was continuously measured in order to pick them out from the microwave oven when they had reached the correct end moisture content. Fig. 5

Table 1
Drying times: conventional drying

Drying temperature (°C)	End moisture content (%)	Drying times (min)
60	8	4420
100	8	1835
60	12	4035
100	12	1715

Fig. 4. Domestic microwave oven (Philips 8100).

Table 2
Drying times: microwave drying

Drying temperature (°C)	End moisture content (%)	Drying time (min)	Total microwave time (min)
60	8	1128	52
100	8	299	58
60	12	497	35
100	12	154	36

shows the temperature measured in the middle of a sample, and also the reduction of moisture content for the samples during drying. Where the temperature decreases in the figure, the test samples have been taken out of the microwave oven to be weighed. The total drying time for this experiment is shown in Table 2. Since the other drying cycles were performed in the same way as has been described, drying times are displayed for these drying cycles in Table 2, also.

2.1.3. Test samples and bending test

A width and thickness of 10 mm and a length of 250 mm were the dimensions selected for the samples for the bending test. Before the samples were cut into lengths after the drying, they were kept for about a week in a climate that retained the equilibrium moisture content that was determined for the samples. This was in order to ensure the equilibrium moisture content. Also after the crosscut, before the bending test, the pieces were kept in an air-conditioned chamber. At crosscutting, the specimens that contained knots, compression wood or other properties that could affect the bending test were rejected. The important thing with this sorting was that if, for instance, a microwave-dried sample had any property that could affect the bending test, then both that sample and its air-dried mate were rejected, since the experiment was based upon using matched specimens.

The bending test was performed in a Hounsfields (H2SK-S) test apparatus with a three-point bending test tool. The software of the test equipment produced the rates for the test pieces' MOE and MOR. The test was performed with a bending rate of 2 mm/min until the pieces were broken. In total, 132 pieces were tested, which means 66 matched samples divided among the four main groups.

2.2. Data processing

In order to interpret the large quantity of information that was received from the trial, two different methods of analysis were used: multivariate principal component analysis (PCA) and a classical statistical test. The following sections describe how these analyses were performed.

2.2.1. Multivariate PCA

SIMCA-P 8.0 software, developed by UMETRICS AB [8], was used for the multivariate PCA. Multivariate PCA is based on the transformation of a smaller number of variables or components of variables that have been received from, for instance, a measurement. These components are a linear combination of the original variables, which in present work

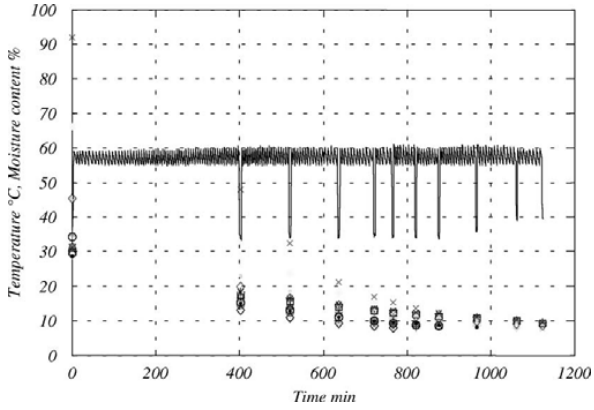

Fig. 5. Microwave drying: 60 °C to a moisture content at 8%.

are MOE, MOR, drying temperature, drying method and variables that effect density, and perpendicular to each other. They are also transformed so that the fluctuation in the observations is explained as simple as possible. The transformation is based on the first principal component being adjusted so as to explain most of the variation in the observations. Furthermore, the next principal component is adjusted to explain the second greatest part of the variation in observations, and so on. It is then possible that only two or three principal components offer a satisfactory description of all original variables. That makes it simpler to interpret the observations. PCA can be described in brief as a method of simplifying the interpretation of the observations by reducing the number of variables. The observation coordinates in the new system, i.e. their coordinates related to the principal components, are called scores, and the corresponding relations between the original variables and the new principal components are called loadings. In the score figure it is possible to find statistical outliers and groups of observations.

The SIMCA software describes the explained variation in the PC model, with the parameter R^2, which was received from the observations. A value close to 1 for parameter R^2 explains most of the variation in the observations, whereas if the value is close to 0 almost none of the variation is explained. The predicted variation in the model is stated with the parameter Q^2 in the software and is calculated by cross-validation [9]. Values close to 1 for Q^2 mean that a reliable model with a good level of prediction has been obtained, and a value close to 0 means an unreliable model.

2.2.2. Classical statistical test

In the classical statistical test, the difference between the samples' average values for each coefficient of elasticity and the maximum bending strength at maximum load was calculated.

The zero hypothesis was written as

$$H_0: \quad \mu_1 - \mu_2 = D_0, \tag{1}$$

where μ_1 and μ_2 are the mean values for the different groups, and D_0 the difference between the average values of the groups. In the analysis, it was assumed that there was no difference under present conditions between the average values, which means that $D_0 = 0$. The opposite hypothesis is

$$H_1: \quad \mu_1 - \mu_2 \neq D_0. \tag{2}$$

Since the number of observations was small, fewer than 30 pieces, the test function was written as

$$t = \frac{\bar{d} - D_0}{\text{S.D.}\sqrt{n}}, \tag{3}$$

where the t-distribution is based on $n - 1$ degrees of freedom, $\bar{d}$ represents the difference between the average values of the samples and S.D. the standard deviation for these. When the zero hypothesis is valid, the test functions' values should not deviate significantly from zero. For large values of the test function it is, therefore, a matter of course to reject the zero hypothesis.

3. Results

3.1. Principal component analysis

In the following section, score and loading figures obtained from the analysis software SIMCA are illustrated, as well as how the most important main features can be interpreted from these figures. Table 3 shows an explanation of the observation points in the score figures. Furthermore, Table 4 shows an explanation of variable shortening in the loading figures.

3.1.1. Modulus of elasticity

A result with four principal components with $R^2 = 0.857$ and $Q^2 = 0.743$ was obtained from the PCA. The score figure in Fig. 6 shows the down-projected observations in the plane defined by the axes that represent the components $t[1]$ and $t[2]$. The distribution of the observations in relation to each other is portrayed. The matched samples from both drying methods lie relatively neatly collected in the plane. Observations on samples that were dried at a temperature of 100 °C to a moisture content of 12% are situated in the upper

Table 3
Marking explanation

Marking	Drying method		Drying temperature		Moisture content	
	MW	K	High	Low	High	Low
○	×		×		×	
●		×	×		×	
□	×			×	×	
■		×		×	×	
+	×		×			×
*		×	×			×
◆	×			×		×
I		×		×		×

Table 4
Variable shortening

Shortening	Explanation
MW	Microwave drying
K	Conventional drying
T_LOW	Drying temperature, 60 °C
T_HIGH	Drying temperature, 100 °C
MC_LOW	Moisture content, 8%
MC_HIGH	Moisture content, 12%
WEIGHT	Weight of the sample
M_TH	Mean thickness
M_BR	Mean breadth
N_O_A_R	Number of annual rings
MOE	Modulus of elasticity
MOR	Modulus of rupture

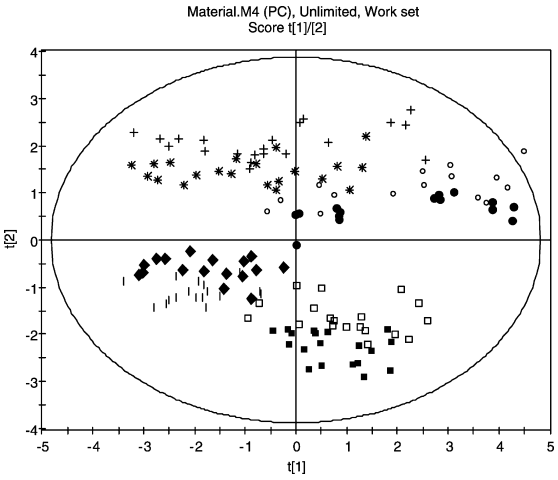

Fig. 6. Score figure MOE: $t[1]$ against $t[2]$.

right quadrant. In the upper left quadrant are the observations on samples dried at 100 °C to a moisture content of 8%. In the lower left quadrant are the observations on samples dried at 60 °C to a moisture content of 8%. Finally, the lower right quadrant contains the observations on samples that were dried at 60 °C to a moisture content of 12%. The fact that the observations are situated together so well indicates that they have similar properties.

The loadings figure in Fig. 7 shows the projected variables in the plane defined by the axes that represent the principal components $p[1]$ and $p[2]$ and shows information about the relations between the original variables and the principal components. That means how much each variable contributes to each principal component. The figure shows that the variables WEIGHT, MC_LOW, MC_HIGH, N_O_A_R, M_TH and M_BR contribute most to principal component

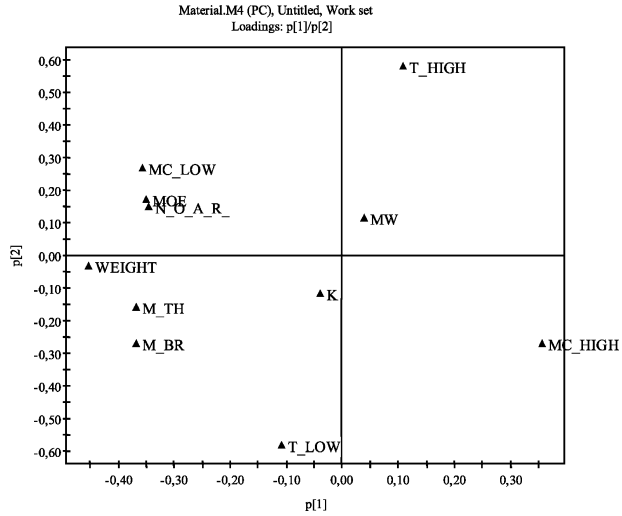

Fig. 7. Loading figure MOE: $p[1]$ against $p[2]$.

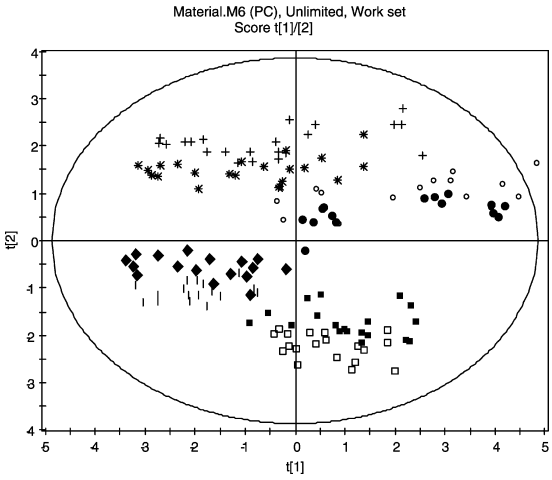

Fig. 8. Score figure MOR: $t[1]$ against $t[2]$.

$p[1]$ and almost nothing to $p[2]$, while T_HIGH and T_LOW have the greatest influence on principal component $p[2]$. The distance of the variables to origin also provides a satisfactory image of what influence they have in the model. The variables situated near origin, such as K and MW, have insignificant influence on the principal components $p[1]$ and $p[2]$ and thus little influence in the PCA model. The variables that correlate most positively to the variable MOE according to Fig. 7 are WEIGHT, MC_LOW, N_O_A_R, M_TH and M_BR. This means that if they increase or decrease their value, the variable

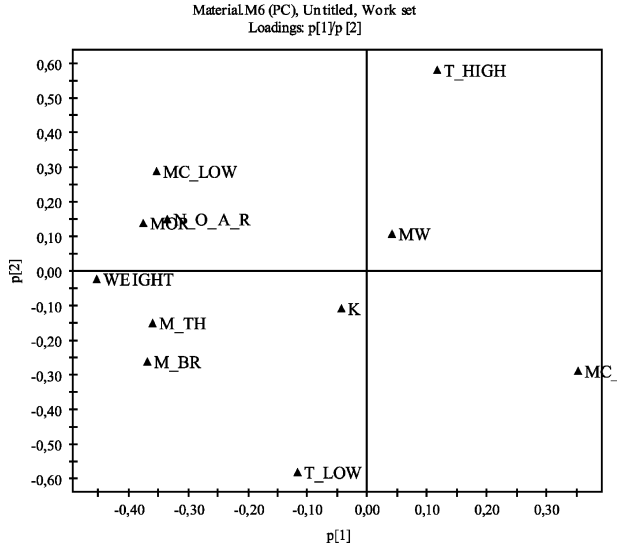

Fig. 9. Loading figure MOR: $p[1]$ against $p[2]$.

MOE has a tendency to be influenced in the same direction. On the other hand, according to the loading figure, MC_HIGH is negatively correlated to the variable MOE, which means that if MC_HIGH increases its value, the variable MOE tends to decrease.

3.1.2. Modulus of rupture

A result with four principal components with $R^2 = 0.903$ and $Q^2 = 0.674$ was obtained by PCA. Also here, as for the variable MOE, the variables that correlate most positively to the variable MOR are WEIGHT, MC_LOW, N_O_A_R, M_TH and M_BR, whereas the variable MC_HIGH is most negatively correlated to the variable MOR (Fig. 8). The score plot also shows that the matched samples from both drying methods are collected in the plane.

3.2. Statistical test

The following section discusses the classical statistical test. Dots aligned vertically to each other are matched samples in Figs. 11–18. Other explanations of the figures are shown in Fig. 9.

3.2.1. Modulus of elasticity

From the difference between the average values and their standard deviations, the test function, Eq. (3), was calculated to 0.062 for the samples that were dried to a moisture content of 8% at a temperature of 60 °C. For the samples that were dried at 100 °C, the result for the test function was 0.009. The result of the calculations for the samples that were dried to a moisture content of 12% at 60 °C was 0.032. For the samples that were dried at 100 °C, the result was 0.038. The low test-statistic values mean that the zero hypothesis is valid with a high probability.

3.2.2. Modulus of rupture

From the difference between the average values and their S.D.'s, the test function, Eq. (3), was calculated to 0.062 for the samples that were dried to a moisture content of 8% at a temperature of 60 °C. For the samples that were dried at 100 °C the test function result was 0.009. For the samples that were dried to a moisture content of 12% at 60 °C, the calculations gave a result of 0.009. Finally, for samples that were dried at 100 °C, the result was 0.034. The low test-statistic values mean that the zero hypothesis is valid with a high probability.

4. Discussion

Spruce with a moisture content of 12% has MOE values between 8.3 and 13 GPa and MOR values of 66–84 N/mm^2 [5,6]. Compared with the values obtained from the bending tests in this investigation, the results harmonise well with each other.

+ *Microwave dried mw.*
O *Conventional dried k.*
Average value MW.
Average value K.
95 % confidence interval mw.
95 % confidence interval k.

Fig. 10. Explanation of the symbols used in the figures.

The results from the PCA model, with the variable MOE for the matched and samples, indicate that the variables that affect MOE most are moisture content, number of annual rings, weight and the dimension parameters width and thickness (Fig. 7). This means that if the moisture content decreases, the MOE value increases, and if the number of annual rings, the weight, or any of the dimension parameters increases, the value of MOE also increases. That indicates that the density of the samples has a very important effect on the result. The variables that have least influence on the MOE are the drying methods and the drying temperature. Antti et al. [3] have also shown with multivariate data analysis that material parameters such as fraction of heartwood and distance between annual rings have greater influence on mechanical properties than to the drying method and drying temperature for Scots pine. That a drying temperature up to 110 °C has no effect on the result has also been shown

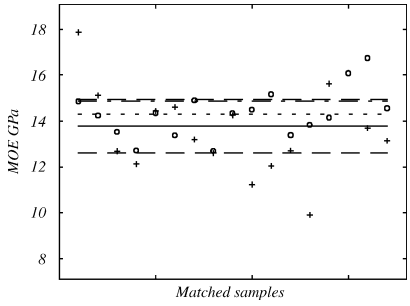

Fig. 11. Drying temperature 60 °C, moisture content 8%.

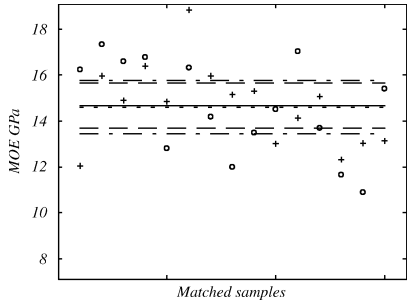

Fig. 12. Drying temperature 100 °C, moisture content 8%.

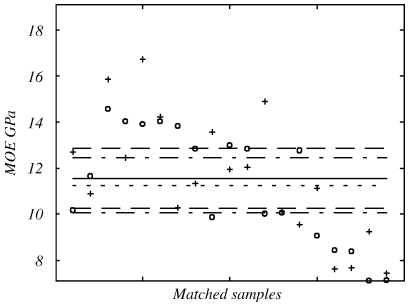

Fig. 13. Drying temperature 60 °C, moisture content 12%.

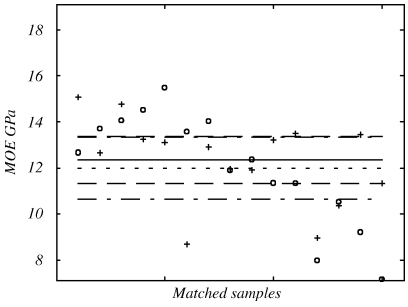

Fig. 14. Drying temperature 100 °C, moisture content 12%.

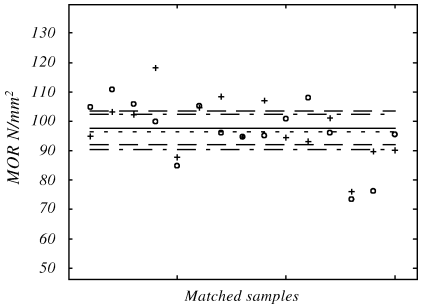

Fig. 16. Drying temperature 100 °C, moisture content 8%.

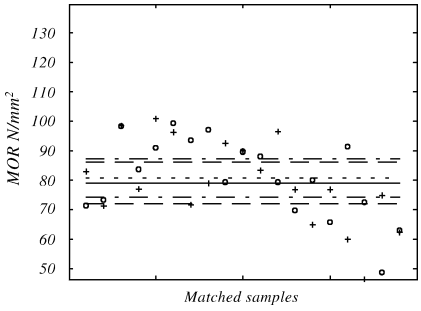

Fig. 17. Drying temperature 60 °C, moisture content 12%.

by Teischinger [10]. All results mentioned for MOE are also valid for the variable MOR (Fig. 10). The fact that the drying method has no important impact on the result either for the variable MOE or for MOR is also shown by the classical statistical test for the matched samples. Figs. 11–18 show that no significant difference exists between the results for both the drying methods. Antti et al. [3] have also shown that there is no difference in MOE, MOR and tensile stress at 5% significance level between the two drying methods for Scots pine.

The present work shows that, contrary to Oloyede and Groombridge [2], the drying method, regardless of whether it is microwave drying or air-circulation drying, has no impact on the strength of the wood under the conditions presented here. The fact that wood can vary in strength in part between different items, but also within the one and

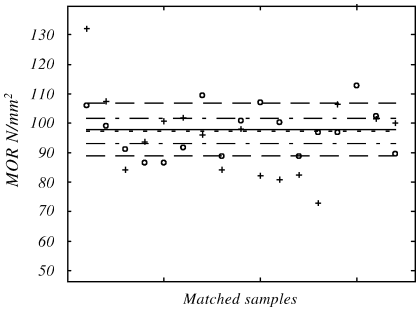

Fig. 15. Drying temperature 60 °C, moisture content 8%.

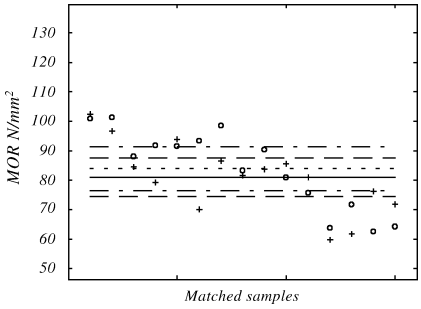

Fig. 18. Drying temperature 100 °C, moisture content 12%.

same individual, makes it important, not to say necessary, that comparative investigations such as the present one use matched samples in order to decrease the risk that large differences will be found in the results. In point of fact, the differences arise from variations in the wood and not from the parameters that were tested.

References

[1] A.L. Antti, Heating and drying wood using microwave power, Ph.D. Thesis, vol. 35, Luleå University of Technology, Division of Wood Physics, Skellefteå, 1999.
[2] A. Oloyede, P. Groombridge, The influence of microwave heating on the mechanical properties of wood, J. Mater. Process. Technol. 100 (2000) 67–73.
[3] A.L. Antti, A. Jönsson, M. Nilsson, The effect of drying method on the mechanical properties of wood: comparisons between conventional kiln and microwave-dried Scots pine, in: Paper Presented to the Third European Cost E15 Workshop on Wood Drying, Helsinki, Finland, 2001.
[4] T. Thörnqvist, Juvenile wood in coniferous trees, Document No. D13:1993, Swedish Council for Building Research, Stockholm, 1993.
[5] J.M. Dinwoodie, Timber: Its Nature and Behaviour, 2nd ed., E&FN Spon, London, 2000.
[6] J.B. Boutelje, Träfakta, 2nd ed., Trätek, Stockholm, 1989.
[7] F.F.P. Kollman, W.A. Côté, Principle of Wood Science and Technology, Solid Wood, vol. 1, Springer, New York, 1984.
[8] L. Eriksson, E. Johansson, N. Kettaneh-Wold, S. Wold, Introduction to Multi- and Megavariate Data Analysis Using Projection Methods (PCA and PLS), UMETRICS AB, Umeå, 1999.
[9] S. Wold, K. Esbensen, P. Geladi, Principal component analysis, Chemometrics Intell. Lab. Syst. 2 (1987) 37–52.
[10] A. Teischinger, Effect of different drying temperatures on selected physical wood properties, in: Proceedings of the Third IUFRO Conference on Wood Drying, Vienna, Austria, 1992.

II

Design and performance of an industrial microwave drier for on-line drying of wood components

L. Hansson *Luleå University of Technology, Department of Wood physics*
Campus in Skellefteå,
Skeria 3, S-931 87 Skellefteå, Sweden
E-mail: Lars.Hansson@tt.luth.se

A.L. Antti *Luleå University of Technology, Department of Wood physics*
Campus in Skellefteå,
Skeria 3, S-931 87 Skellefteå, Sweden
E-mail: Lena.Antti@tt.luth.se

ABSTRACT

The most common industrial method for drying wood is by air circulation. However, an alternative method—microwave drying—has been investigated at the Division of Wood Physics, Luleå University of Technology in Skellefteå, Sweden. The use of microwave energy to dry wood is not very common, but it could be advantageous due to the possibility of heating and drying wood much faster than conventional methods and with preserved quality. The objective of the investigation is to install an on-line microwave drier for wood components and, furthermore, to integrate this drying process into the total production. The purpose of this paper is to briefly describe the design and performance of this on-line microwave drier, its advantages and its limitations.

INTRODUCTION

Microwave energy can be used to heat dielectric materials. Wood is a dielectric material in which all charges are bound rather strongly to constituent molecules. If the wood is exposed to an electric field, which the microwave creates, the electrostatic charges in the wood begin to oscillate. These oscillations give rise to heating due to friction heat from the oscillating charges. This method is used in many processes within industry in order to heat and dry different products. Drying wood by microwave energy is not so common, but has been investigated in recent years by several scientists: Antti (1999) has investigated the heating and drying of wood using microwave power; Perré and Turner (1997) have investigated microwave drying of softwoods in an oversized waveguide; Torgovnikov (1993) has investigated dielectric properties of wood and wood-based materials. Furthermore, comparisons with conventional air circulation drying have shown that it is possible to dry wood much faster with microwave energy without deteriorating the quality of the dried products. Using microwave power, it takes less than five hours to dry green wood to a moisture content (MC) of about 7%. However, this depends on the kind of wood and the thickness and length of the products. Another result of microwave drying of wood is that colour change is almost nonexistent.

At Luleå University of Technology (LTU), research into microwave drying of wood continues with focus on an on-line dryer. An industrial-scale, on-line microwave construction for wood components is under development. The drier will be mainly used for demonstration, product testing and for students' laboratory work. The purpose of this report is to briefly describe the design, advantages and limitations of this on-line construction.

MICROWAVES IN WOOD

Dielectric materials are nonconductive or are poor conductors of electric current. When dielectric materials are placed in an electromagnetic field, there is practically no electric current, and compared with metal they have no loosely sitting or free electrons that can drift through the material. Instead, an electrical polarization occurs, which means that the positive charges move into the same directional orientation as the electric field and the negative charges in the opposite direction. This small separation of the charges, or polarization, reduces the electric field inside the dielectric material. When a material is exposed to an electrical field, three possibilities can arise: the energy can be reflected, transmitted or absorbed, which entirely depends on the material properties. Because of this, the material will not be heated at all, or it will be heated up slowly or just certain parts of material will be heated up. A dielectric material is characterised by a complex, frequency-dependent dielectric constant:

$$\varepsilon(\omega) = \varepsilon_0 \cdot (\varepsilon'(\omega) - j \cdot \varepsilon''(\omega)), \quad (1)$$

where the real part ε' measures how many times greater the electrostatic charge arising in the material is than that in a vacuum. The complex part ε'' is the relative loss factor, which measures how well the material absorbs energy from the electrical field and how much energy will be converted to heat.

Wood is a biological dielectric material with a complex structure. If wood is placed in an electric field, both the field and the wood influence each other, which creates electric current in the material. Interaction between electromagnetic fields and wood has been thoroughly investigated by Torgovnikov (1993). These investigations have shown that the dielectric properties of wood depend on the MC, density, material temperature and direction of electric field relatively to fibre direction. As a result, the dielectric property of wood will change during heating and drying.

GENERATIONS OF MICROWAVES

A magnetron is usually used to generate microwaves. The magnetron is a vacuum tube containing a cylindrical cathode and a coaxial anode. Between these, the electrons move in curved paths influenced by an electric field and a magnetic field. When the electrons move toward the anode, energy is emitted into the microwave field, which is transported out to a wave-guide. In this on-line drier, several standard magnetrons working with a frequency of 2.45 GHz generate the energy. The power of the magnetrons is 1 kW, and the wave-guides that are used are simple rectangular pipes, which are dimensioned for the current frequency.

THE APPLICATOR

In many industrial microwave installations, as well as in domestic microwave ovens, multimode applicators are used. A multimode applicator is a metal box (cavity, see figure 1) into which the microwaves are guided. Inside the cavity, the waves reflect against the walls. Furthermore, the waves interfere with each other and thereby distribute the electric field intensity in the cavity space. The field distribution depends on the design of the cavity, i.e., its dimensions, the dielectric property of the load, its position in the cavity and its size.

The modes that will develop in a cavity with a certain dimension can be determined by calculations. Also, simulations of developed field distribution with a specific load in the cavity can be performed. As a prelude to the design work, modelling was been done by *Microtrans AB* in order to optimize field distribution, i.e., to achieve as even heat distribution as possible. Figure 2 shows an infrared (IR) image of the heat distribution across the load surface for the first-generation multimode applicator that was used in this development process. Now, the third-generation multimode applicator is in use (see figure 3). Figure 4 shows a simulated field distribution for this third-generation multimode applicator. A comparison of figures 2 and 4 shows that a distribution with distinct strips is achieved with the new applicator. This indicates more uniform heating in these areas.

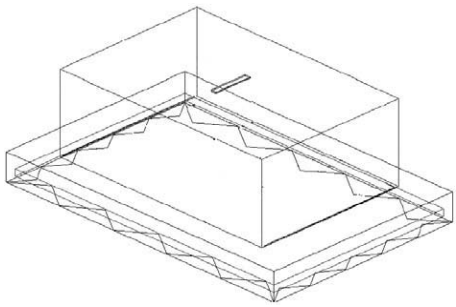

FIGURE 1. First generation applicator.

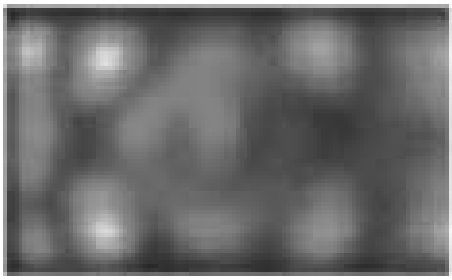

FIGURE 2. IR-image, first generation applicator.

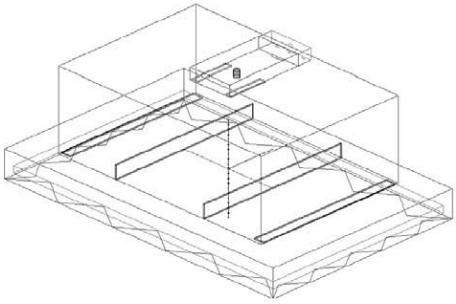

FIGURE 3. Third generation applicator.

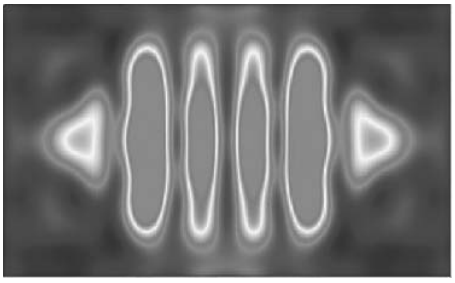

FIGURE 4. Simulated field distribution, third generation applicator.

THE DESIGN OF THE MICROWAVE CONSTRUCTION

The microwave tunnel construction contains modules with applicators. Such a module consists of five applicators in series, as shown in figure 5. Furthermore, two such modules are placed together with a parallel displacement of 35 mm**.** This means that heat distribution will be more uniform when the wood components pass under the cavities. Rates of speed vary between 5 and 500 mm per min., and the wood components pass edge by edge crosswise through the tunnel space, which includes a number of the modules described above. The purpose is to dry wood components with thickness varying from 15-55 mm from green condition to a MC of 8%. In order to avoid deformation during drying, the internal height of the tunnel is regulated to adjust eventual twist. The applied compressing force is in the range of 0-5 MPa.

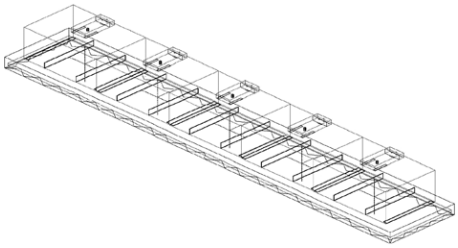

FIGURE 5. Microwave module.

THE CONTROL SYSTEM

The control system is PC-based and has feedback; i.e., control is based on signals from the drying process. These signals display both the wood's position in the tunnel and its dielectric property. On the basis of these signals, the system controls each separate magnetron, or microwave module; i.e., the entire drying process is adaptively controlled so that the microwave power is adjusted to the load properties. The power for each magnetron can be regulated continuously from about 30% to 100% of its nominal maximum output power.

OTHER ASPECTS

Wood can contain much water, and when the drying process starts the water will resign as water or water steam. The water that is in liquid form drain out from the tunnel and the water, which is in vapour form, convey away by circulating air. This is a very important part in the process, because if condense has been formed in the cavity it doesn't work optimally and that brings on a poor drying process.

FURTHER WORK

In order to achieve an optimum drying process, further investigation is needed. Below are some of these investigations, which have been done or are planned:

During drying above fibre saturation point (FSP), the temperature rises to evaporation and remains at that level. However, when MC drops below FSP, the temperature increases further. If the drying temperature becomes too high, quality can be affected. Measuring surface temperature by IR pyrometer may make it possible to detect when the wood reaches fibre saturation point. Ceramic sensors indicate energy absorption and may be useable for MC detection; i.e., they could give a signal when fibre FSP is reached during the drying process.

When wood dries, it shrinks, and for some species twist easily occurs. Keeping the components constricted can prevent this. This fixing point could be adjusted during the drying process to account for shrinkage.

REFERENCE

Antti, A.L. (1999). Heating and drying wood using microwave power (Doctoral thesis, 1999:35). Skellefteå: Luleå University of Technology, Division of wood physics.

Perré, P and Turner, I. (1997). Microwave drying of softwood in an oversized waveguide: Theory and Experiment. AIChE Journal 43(10) pp 2579-2578.

Torgovnikov, G. I. (1993). Dielectric properties of wood and wood–based materials. Springer-Verlag. ISBN 3-540-55394-0.

III

Journal of Materials Processing Technology 171 (2006) 467–470

Journal of Materials Processing Technology

www.elsevier.com/locate/jmatprotec

The effect of drying method and temperature level on the hardness of wood

Lars Hansson *, A.L. Antti

Luleå University of Technology, Division of Wood Physics, Skellefteå Campus, SE-931 87 Skellefteå, Sweden

Received 16 June 2004; accepted 17 August 2005

Abstract

The purpose of the present work was to investigate whether wood hardness is affected by temperature level during microwave (MW) drying and whether the response is different from that of conventionally dried wood. Matched samples of Norway spruce (*Picea abies*) were therefore dried from green state to different moisture content (mc) at different temperature levels, both conventionally by air circulation and by MW. The results show that specimens dried by any of the two methods at a temperature level of 100 or 60 °C there is a significant difference in wood hardness parallel to the grain between the methods when drying progresses to relatively lower level of moisture content, i.e. wood hardness becomes higher during MW drying. Temperature level in the range 60–110 °C during MW drying has no significant influence on wood hardness. Variables such as density and mc have a greater influence on wood hardness than does the drying method or the drying temperature. Since wood is a biological material, its strength varies within the specimens as well as between different samples. For this reason it is important to use matched samples when performing this type of comparative investigation.

Keywords: Microwave drying; Air circulation drying; Janka; Matched sample

1. Introduction

Wood hardness is an important property, especially in the flooring and furniture industries. In order to determine the hardness of wood material, usually methods such as Brinell and Janka are used. These tests are performed in such a way that a steel hemisphere is forced into the surface under test. The difference between these methods is found in what is measured: the Brinell method measures the diameter of the mark caused by the steel ball in the specimen, while the Janka method measures the power needed to force a steel hemisphere of diameter 11.28 mm into the wood to a depth of half of its diameter. A problem that might occur using the Brinell method is connected to the relaxation of the dent mark—the accuracy of the measurement becomes doubtful [1].

Investigations have shown that wood hardness is influenced by its density and moisture content (mc) [2]. Selhlstedt-Persson [3] has investigated the effect different drying temperatures during air-circulation drying have on wood hardness. The maximum drying temperature in those studies was 115 °C. The result indicates no significant influence of temperature on hardness; still, the specimens dried at higher temperatures gave a hard and brittle impression.

When measuring wood hardness, the direction of indentation vis-à-vis the orientation of the wood grain affects the result. The reason is, according to [4], that the amount of and stiffness of fibres carrying the load are lower when the load direction is angled to the grain direction than if it is parallel with the grain. For the wood species Norway spruce (*Picea abies*) with mc 0.12 and a density between 390 and 480 kg/m^3, the Janka hardness is in the range of 2650–2840 N when applied longitudinally and 1570–2260 N when applied tangentially [5].

Wood is most commonly dried by air circulation at different temperatures and humidity levels. A less customary method that has been investigated in recent years is the use of microwave power to heat and dry wood [6]. If wood is exposed to an electromagnetic field with the high frequency that is characteristic of microwaves, the water molecules, which are dipoles, begin to oscillate at almost the same frequency as the electromagnetic field. This causes an increase of temperature and pressure in the test samples. However, wood consists not only of water but

* Corresponding author. Tel.: +46 910 585396; fax: +46 910 585399.
E-mail address: lars.hansson@tt.luth.se (L. Hansson).
URL: http://www.tt.luth.se.

0924-0136/$ – see front matter © 2005 Elsevier B.V. All rights reserved.
doi:10.1016/j.jmatprotec.2005.08.007

also of polymers such as cellulose, hemicelluloses and lignin. These polymers are also polar molecules, and therefore even they might be affected by the electromagnetic field. This could possibly cause degradation in terms wood hardness.

Do temperature levels and drying method affect wood hardness? The aim of the present work was to investigate this hypothesis by comparing wood hardness in specimens dried by microwaves and by conventional air circulation at different temperature levels. Parameters to control during the tests were wood density and mc.

2. Materials and methods

The wood species investigated in this study originated from fresh sawn Norway spruce (*Picea abies*) grown in the north of Sweden. The dimensions of the specimens were approximately 55 mm thick and 105 mm wide. The selected specimens were taken from planks from different logs that were pith sawn at a sawmill. Some logs were sawn in December, the rest in September. Samples including knots were avoided.

The specimens cut in December were used to investigate the effect of drying method on the hardness of wood. A total of 40 pieces 300 mm long were selected from different planks. These were distributed into four main groups that included pieces from the different original planks. Further, the pieces in the main groups were cut in two lengthwise, with one of the resulting pieces reserved for conventional drying and the other for microwave drying. Of the four main groups, two were dried at a temperature of 60 °C to an end moisture content (mc) of 0.08 and 0.12, respectively. The two other groups reached the same mc levels but were dried at 100 °C. The lower drying temperature is a typical level for low-temperature drying, while the higher is at the limit for high-temperature drying and in fact was limited by the efficiency of the air-circulation laboratory kiln.

The specimens cut in September were used for further study of the effect of drying temperature on the hardness of wood. A total of 60 pieces 150 mm long were selected from different planks and distributed into two main groups that included pieces from the different original planks. In other respects, the procedure was the same as in the previous test, except that three levels of drying temperature were selected: 60, 100 and 110 °C. One combination group was dried at a temperature of 60 °C, and its mirror at 100 °C. The next combination was dried at 60 °C, and its mirror at 110 °C. The last combination was dried at 100 °C, and its mirror at 110 °C.

From each sample taken from the two sawing periods, small pieces were cut out to determine the initial mc. Here, the oven-dried method, based on dry weight, was used. In this way the final weight of the sample after drying could be determined and translated to desired mc.

The sample design used enables a good statistical analysis to determine whether the drying methods or drying temperatures affect the hardness of the wood. This method of matching samples from the same tree of origin makes it possible to perform a reliable comparison of responses arising from different drying methods and temperature levels.

2.1. Drying methods

2.1.1. Conventional drying

Conventional drying was performed in a laboratory kiln built of aluminium with a height of 0.3 m and a length of 0.8 m, in which the air circulates around the load with a speed of about 2 m/s. Climate conditions were controlled by computer software. Sensors, Pt 100 type, were used to measure the dry- and wet-bulb temperature in the kiln. For climate control, an air heater and a steam boiler were used, each with a maximum effect of 6 kW.

The two groups which were dried to a final mc of 0.12 at the drying temperatures 60 and 100 °C were exposed to a constant climate with a wet-bulb temperature of 49 and 91 °C, respectively. Drying proceeded until the equilibrium mc of 0.08 was reached. An mc gradient developed between the wood surface and its interior as the surface dried faster. The difference in mc between these two areas causes strains in the material. In order to equalise the mc and thereby compensate for stresses, the samples were conditioned for about 8 h in a climate with a wet-bulb temperature of 57 and 98 °C, respectively. The final mc then reached about 0.15. During the drying process and conditioning, the weight of each specimen was measured in order to control when the desired final mc was reached.

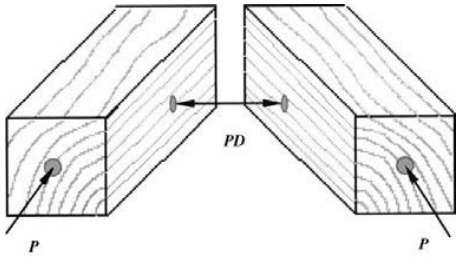

Fig. 1. Matched samples.

The same line of action was followed with the specimens dried to the final mc 0.08. The wet-bulb temperatures, however, were 41 and 82 °C, which correspond to the equilibrium mc 0.05. These groups were also conditioned for about 8 h to reach a higher final mc of 0.12. In this case, the wet-bulb temperatures were 55 and 96 °C, respectively.

2.1.2. Microwave drying

Microwave drying was performed in a domestic microwave oven. In order to measure the temperature in the centre of a sample, a hole was drilled into which a fibre-optic sensor (ASEA 1110) was placed. The wood load was exposed to the maximum power emitted by the oven (1.4 kW) as long as the temperature in the sample was below the current drying temperature. The process was computer controlled.

2.1.3. Test samples and the hardness test

The dimensions selected for the specimens subjected to hardness tests were 40 mm × 40 mm × 120 mm. After drying, and before cutting the samples for hardness tests, they were kept for a week in a climate chamber that retained the equilibrium mc. Prepared specimens were also stored there until it was time for the test. The hardness test was performed in a Hounsfields (H2SK-S) test apparatus. The software of the test equipment produced the Janka rating in Newtons; i.e., a steel hemisphere 11.28 mm in diameter was pushed into the material to a depth equal to half of its diameter at a speed of 6.35 mm/min. These impacts were made perpendicular to the grain (PD) and parallel to the grain (P) (see Fig. 1).

3. Results and discussion

The results obtained from the surface hardness measurements are presented in Figs. 2–5. Table 1 explains the nomenclature used in the figures.

The results show no significant difference in hardness perpendicular and parallel to the grain between the two drying methods when the samples were dried at temperature levels of 100 and 60 °C to mc of 0.12. The hardness perpendicular to the grain was the same for samples dried at temperature level of 100 and 60 °C to mc of 0.08. On the other hand, a significant difference in hardness parallel to the grain is shown between the drying methods for samples dried at temperature level of 100 and 60 °C to mc 0.08.

The results show that specimens dried by any of the two methods to mc 0.12 at a temperature level of 100 or 60 °C do

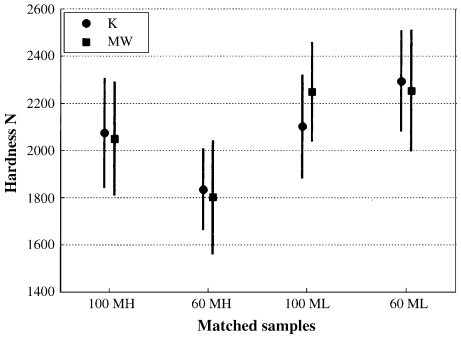

Fig. 2. The average values in hardness for the matched pairs measured perpendicular to the grain and the 95% confidence interval at different temperature levels and moisture contents.

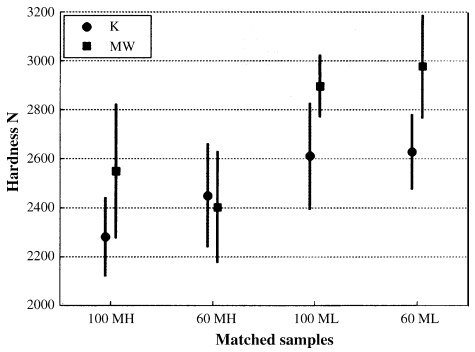

Fig. 3. The average values in hardness for the matched pairs measured parallel to the grain and the 95% confidence interval at different temperature levels and moisture contents.

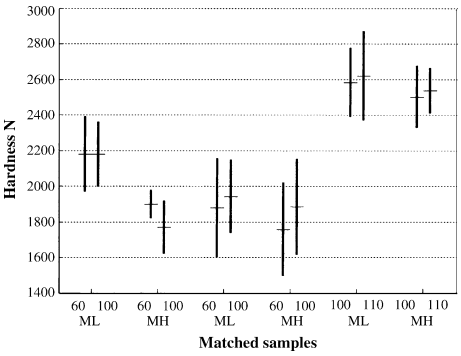

Fig. 4. The average values in hardness for microwave dried samples of the matched pairs that were measured perpendicular to the grain and the 95% confidence interval at different moisture contents and temperature levels.

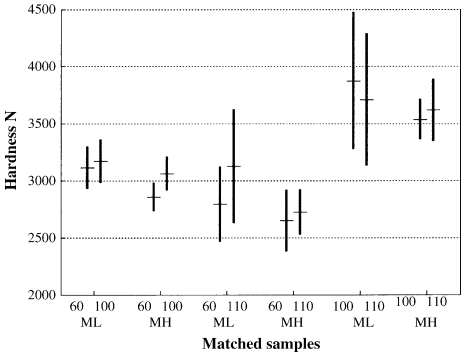

Fig. 5. The average values in hardness for microwave dried samples of the matched pairs that were measured parallel to the grain and the 95% confidence interval at different moisture contents and temperature levels.

Table 1
Variable shortening

Shortening	Explanation
MW	Microwave drying
K	Conventional drying
60	Drying temperature, 60 °C
100	Drying temperature, 100 °C
110	Drying temperature, 110 °C
MH	Moisture content, 12%
ML	Moisture content, 8%
P	Parallel to the grain
PD	Perpendicular to the grain

not indicate any significant difference in wood hardness either parallel or perpendicular to fibre direction. However, there is a significant difference in wood hardness parallel to the grain between the methods when drying progresses to mc 0.08 at a temperature level of 100 or 60 °C; i.e., wood hardness becomes higher during MW drying.

One factor that affects the hardness is the mc. The samples that were dried to mc 0.08 tend to be harder. However, this result is obvious as the mc influences the wood's strength [7]. Norway Spruce with densities from 390 to 480 kg/m^3 and with mc 0.12 has hardness values between 1570 and 2260 N perpendicular to the grain [5]. These results harmonise well with the values obtained in this investigation.

Hardness values parallel to the grain for Norway spruce with densities from 390 to 480 kg/m^3 and with mc 0.12 are in the interval 2650–2840 N [5]. These values are somewhat higher

Table 2
Density average values (kg m^{-3}) and the 95% confidence interval for microwave and conventional dried test samples

	Microwave dried		Conventional dried	
	MC 8%	MC 12%	MC 8%	MC 12%
60 °C	497 ± 19	466 ± 23	483 ± 17	461 ± 26
100 °C	473 ± 16	474 ± 26	473 ± 19	457 ± 23

Table 3
Density average values (kg m^{-3}) and the 95% confidence interval for microwave dried test samples at different temperature levels

	Moisture content 8%			Moisture content 12%		
	60 °C	100 °C	110 °C	60 °C	100 °C	110 °C
60 °C	–	466 ± 24	426 ± 23	–	435 ± 12	530 ± 18
100 °C	464 ± 23	–	516 ± 31	488 ± 10	–	443 ± 35
110 °C	392 ± 36	500 ± 28	–	448 ± 31	522 ± 22	–

than those obtained in the present investigation. This variance cannot be due to low density (Table 2), which is an important factor that influences hardness [2,7]. One factor that can affect the values measured is the direction of grain in relation to the direction of load. When the load is applied at an angle to the grain, the amount of and stiffness of fibres carrying the load are lower than when the load is applied in the direction of the grain [4].

The results show no significant difference in hardness between the different drying temperatures for the matched samples. The results for the matched samples from this investigation, 60 °C with 100 °C and 60 °C with 110 °C, harmonise well with table values [5]. For the matched samples 100 °C with 110 °C, the measured values are higher than the values reported by Boutelje and [5]. This difference is explained by the high density value (Table 3). Higher density values increase the hardness value, and as the mc increases, hardness decreases.

4. Conclusion

Drying by microwaves or by air circulation to mc 0.12 at drying temperatures 60 and 100 °C does not affect wood hardness parallel or perpendicular to the grain. The same can be concluded for the wood hardness perpendicular to the grain when drying to mc 0.08 at a drying temperatures 60 and 100 °C.

The results show that there is a significant difference in wood hardness parallel to the grain between the two drying methods when the samples are dried at temperature levels of 100 and 60 °C to mc 0.08.

Wood hardness parallel and perpendicular to the grain is not affected by the drying temperature, at least at the levels 60, 100 and 110 °C, when the wood is dried by microwave heating to mc 0.08 or 0.12.

References

[1] J. Doyle, J.C.F. Walker, Indentation hardness of wood, Wood Fibre Sci. 17 (3) (1984) 369–376.
[2] F.F.P. Kollman, W.A. Côté, Principles of Wood Science and Technology. Vol. 1: Solid Wood, Springer, New York, 1984, pp. 406–412.
[3] S.M.B. Selhlstedt-Persson, High-temperature drying of Scots pine. A comparison between HT- and LT-drying, Holtz als Roh- und Werkstoff 53 (1995) 95–99.
[4] H. Holmgren, Influence of grain angle on Brinell hardness of Scots pine (*Pinus sylvestris* L.), Holtz als Roh- und Werkstoff 58 (2000) 91–95.
[5] J.B. Boutelje, Träfakta, 2nd ed., Trätek, Stockholm, 1989, pp. 27–28.
[6] A.L. Antti, Heating and drying wood using microwave power, Doctoral Thesis, Luleå University of Technology, Division of Wood Physics, Skellefteå, 1999, p. 35.
[7] J.M. Dinwoodie, Timber: Its Nature and Behaviour, 2nd ed., E & FN Spon, London, 2000, pp. 159–177.

IV

Available online at www.sciencedirect.com
SCIENCE DIRECT®
Measurement 38 (2005) 15–20
Measurement
www.elsevier.com/locate/measurement

Microwave penetration in wood using imaging sensor

L. Hansson [a,*], N. Lundgren [b], A.L. Antti [a], O. Hagman [b]

[a] Luleå University of Technology, Division of Wood Physics, Skellefteå Campus, SE-93187 Skellefteå, Sweden
[b] Luleå University of Technology, Division of Wood Technology, Skellefteå Campus, SE-93187 Skellefteå, Sweden

Received 10 May 2004; received in revised form 14 March 2005; accepted 16 March 2005
Available online 22 June 2005

Abstract

It is possible to determine properties of wood using microwave scanning techniques. The purpose of this study was to verify the measured values from a microwave imaging sensor. Attenuation and phase shift of an electromagnetic wave transmitted through birch wood were measured and compared with theoretical calculated values. A test piece with varying thickness was measured with a scanner based on a microwave sensor (Satimo 9.375 GHz) at different temperatures and moisture contents. The density distribution of the test piece was determined by computer tomography scanning. The result showed good correspondence between measured and theoretical values. The proportion of noise was higher at low moisture content due to lower attenuation. There is more noise in attenuation measurement than in measurement of phase shift. A reason for this could be that wood is an inhomogeneous material in which reflections and scattering affect attenuation more than phase shift. The microwave scanner has to be calibrated to a known dielectric to quantify the error in the measurement.

Keywords: Microwave scanning; Wood; Dielectric properties; Modulated scattering technique

1. Introduction

It is known that the dielectric properties of wood are affected by density, moisture content (mc), temperature and frequency [1]. For many applications, such as drying, sorting and strength grading, it is necessary to detect mc or density distribution in wood. These parameters can be detected by nondestructive testing using microwaves. This technique has been investigated by Portala [2] among others. The scanner used in the present work is based on the same microwave sensor (Satimo 9.375 GHz) as in Portala's study [2] where several types of sensors for measurements on wood were investigated. The sensor uses modulated scattering technique [3] with 128 fixed probes. The frequency corresponds to a wavelength of 32 mm in vacuum and gives an acceptable ratio between resolution and

* Corresponding author.
E-mail address: lars.hansson@tt.luth.se (L. Hansson).

0263-2241/$ - see front matter © 2005 Elsevier Ltd. All rights reserved.
doi:10.1016/j.measurement.2005.03.007

penetration. A similar technique has been used by James et al. [4]. The main difference in his method is frequency and probe construction. Johansson [5] has shown that simultaneous prediction of moisture content and density is possible using a scanner system based on the sensor from Satimo where scanner data was used as input for calibration of a multivariate model. These models have to be compensated for variations in temperature and thickness of the wood. Johanssons [5] study does not compare the multivariate model with a physical model.

The present study was carried out in order to examine how measurements from the microwave sensor vary at different mc, thickness and temperatures for birch wood. This provides a more detailed study of the sensor in comparison to Portala's [2]. The experimental scanner data was compared to theoretical values of phase shift and attenuation of the signal.

2. Theory

Electromagnetic waves have an electric field strength ($\boldsymbol{E}$) and a magnetic field strength ($\boldsymbol{H}$) that oscillate perpendicular to each other. When the wave is moving in the z-direction it can be described mathematically with the harmonic wave equation as:

$$\boldsymbol{E}(x,y,z,t) = \boldsymbol{E}_0 \cdot \mathrm{e}^{-\mathrm{j}\cdot\omega\cdot t-\gamma\cdot z}, \tag{1}$$

$$\boldsymbol{H}(x,y,z,t) = \boldsymbol{H}_0 \cdot \mathrm{e}^{-\mathrm{j}\cdot\omega\cdot t-\gamma\cdot z}, \tag{2}$$

where $\boldsymbol{E}_0$ and $\boldsymbol{H}_0$ are the amplitudes of the electric field and the magnetic field strength. They are transverse to the z-direction and move through space with a complex distribution factor:

$$\gamma = \mathrm{j}\cdot\omega\cdot\sqrt{\varepsilon\cdot\mu} = \alpha + \mathrm{j}\cdot\beta, \tag{3}$$

where ω is angular frequency and μ is the complex permeability, which is equal to the permeability μ_0 of the free space, since wood is not a magnetic material. Furthermore, α is the attenuation factor and β is the phase factor of the wave. ε is the relative complex permittivity defined as:

$$\varepsilon = \varepsilon_0\cdot(\varepsilon' - \mathrm{j}\cdot\varepsilon''), \tag{4}$$

where ε_0 is the absolute permittivity for vacuum, ε' is the relative permittivity and ε'' is the relative loss factor. The absolute permittivity and the relative loss factor have been thoroughly investigated by Torgovnikov [1]. These investigations have shown that the absolute permittivity and the relative loss factor of wood depend on moisture content (mc), density, material temperature, direction of electric field relative to the fibre direction and wave frequency.

If the real and imaginary parts of Eq. (3) are equated, the expression for the attenuation factor and phase factor will be:

$$\alpha = \omega\cdot\sqrt{\varepsilon_0\cdot\mu_0}\cdot\left(\frac{\varepsilon'}{2}\cdot\left(\sqrt{1+\left(\frac{\varepsilon''}{\varepsilon'}\right)^2}-1\right)\right)^{1/2}, \tag{5}$$

$$\beta = \omega\cdot\sqrt{\varepsilon_0\cdot\mu_0}\cdot\left(\frac{\varepsilon'}{2}\cdot\left(\sqrt{1+\left(\frac{\varepsilon''}{\varepsilon'}\right)^2}+1\right)\right)^{1/2}. \tag{6}$$

Insertion of Eq. (3) into wave Eq. (1) shows that the wave amplitude is attenuated exponentially with the factor $\mathrm{e}^{-\alpha\cdot z}$ as the wave penetrates the dielectric wood material (Fig. 1).

If the electric field strength decreases from $\boldsymbol{E}(0)$ to $\boldsymbol{E}(z)$, over the length Δz of wood (Fig. 1), the attenuation expressed in decibel is defined as:

$$\log\left(\frac{\boldsymbol{E}(0)}{\boldsymbol{E}(z)}\right) = \log(\mathrm{e})\cdot\alpha\cdot\Delta z\ [\mathrm{dB}], \tag{7}$$

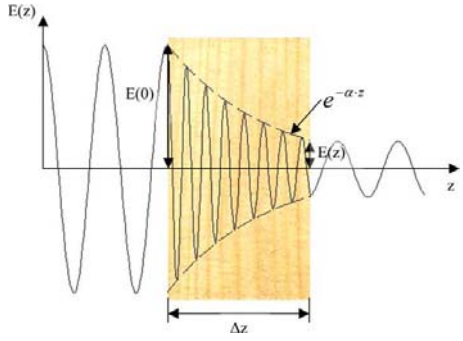

Fig. 1. An electromagnetic wave transmitted into wood.

and the phase shift ϕ over a length Δz as it penetrates wood instead of empty space is defined as:

$$\phi = \beta \cdot \Delta z \text{ [rad]}. \quad (8)$$

3. Material and methods

The study was based on one piece of birch wood with dimensions as shown in Fig. 2. The thickness increases linearly from 0 to 31 mm over a length of 248 mm. This will give a theoretical maximum attenuation of about 12 dB at 25% mc, which is within the dynamic range for the scanner system, which is stated to be about 40 dB. Measurements were excluded within 24 mm from the wood edges to reduce boundary effects on the field. The region of interest is inside the dotted line in Fig. 2.

The values of measured attenuation and phase shift over a width of 64 mm were compared with theoretical values calculated from Eqs. (7) and (8). For each moisture level the object was held at equilibrium mc in a climate chamber until the calculated target weight was reached. Initially the object was dried to 5% mc. By placing the piece in the climate chamber, the mc could be raised to a maximum of 21%. An intermediate measurement was taken at 13% mc. At each of these three levels, the object was scanned at room temperature using both the microwave and Computer Tomograph (CT) scanner. Then the object was dried to zero mc and scanned. Finally, the mc was raised once more to 21% and then the object was kept in a refrigerator for 48 h. Then a microwave scan was done with the object frozen to −20 °C.

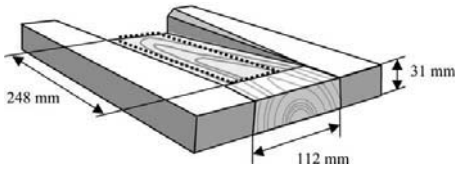

Fig. 2. Test object with birch pieces glued to the edges.

4. CT scanner

A CT scanner (Siemens Somatom AR.T.) was used to measure the density distribution in the test object. A scan was taken at every 8 mm with a 5 mm-wide X-ray beam. The 3D images from the CT scanner were transformed to 2D images with a pixel size of 8 mm × 8 mm.

5. Microwave scanner

Fig. 3 shows a schematic drawing on the main part of the microwave scanning system. The sensor (Satimo 9.375 GHz) is based on modulated scattering technique, MST, which makes it possible to measure the field at many points without a moving probe or microwave multiplexer [3]. The wood is illuminated by a quasi plane wave generated by a slotted waveguide that acts as a transmitting antenna. The transmitted wave is locally perturbed in the retina by a low frequency signal applied sequentially to 128 dual-polarised nonlinear dipoles loaded by PIN diodes. This will cause a modulation of the radio frequency (RF) signal that is proportional to the electromagnetic field. The modulated signal is collected by another slotted waveguide. The signal that reaches the RF receiver consists of a carrier wave modulated at the diode switching frequency. Down-conversion of the RF signal is done in a homodyne receiver that produces the real and imaginary parts of the electromagnetic field at the position of the dipoles. The

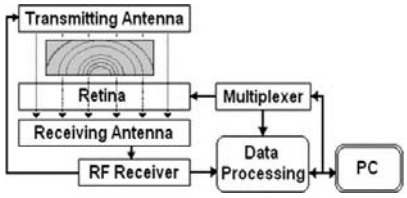

Fig. 3. Sensor system for the microwave scanner. The microwave signal is modulated by a low frequency signal at 128 probes in the retina. The electromagnetic field at each probe is then extracted from the signal.

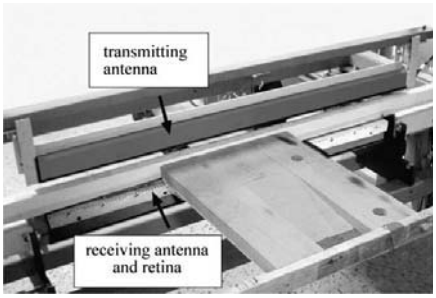

Fig. 4. Conveyer for the microwave scanner with antennas.

antennas are mounted on opposite sides of a conveyer shown in Fig. 4.

The conveyer position is controlled by programmable logic connected to the PC [5]. The distance between dipoles in the retina is 8 mm, which corresponds to one quarter of a wavelength. Since there are 128 dipoles, the resulting image covers a width of one meter. By setting the conveyer to stop for scanning every 8 mm, the same resolution is attained in both directions. From the collected data two images are extracted. One image describes the phase shift of the electromagnetic wave, and the other image describes the attenuation of the signal in dB after passing through the wood. There is a difference in level between sensors and also a small variation between measurements. These errors were minimized by setting the level in air to zero at every measurement.

6. Results and discussion

Fig. 5 shows the distribution of experimental and theoretical values for attenuation over the test object at 0% mc. The theoretical values are calculated with Eq. (7) using empirical values from Torgovnikov [1] and the density distribution obtained from CT scanning. Here the noise is about half of the maximum attenuation.

The measured surface has the same shape at 21% mc in Fig. 6, and the noise level is the same. The maximum attenuation has increased, which gives a better signal to noise ratio.

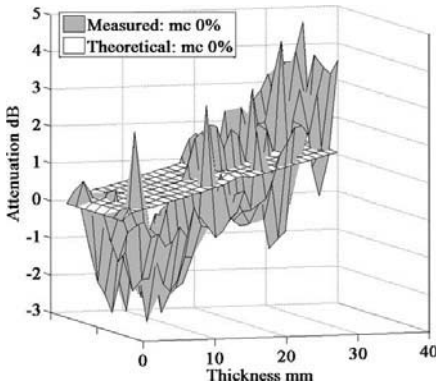

Fig. 5. Distribution of attenuation over a width of 64 mm in birch at 0% mc as thickness increases from 0 to 31 mm.

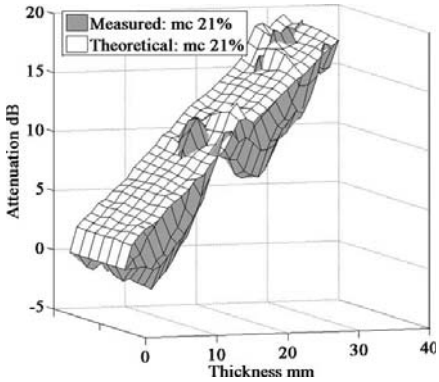

Fig. 6. Distribution of attenuation over a width of 64 mm in birch at 21% mc as thickness increases from 0 to 31 mm.

Figs. 7 and 8 show the corresponding distribution of phase shift at 0 and 21% mc where theoretical values have been calculated with Eq. (8) using empirical values from Torgovnikov [1] and the density distribution obtained from CT scanning.

Variations from the plane in Figs. 5–8 correspond to density variations as shown in Fig. 9. Different annual ring patterns or small regions with high density may cause reflections at bound-

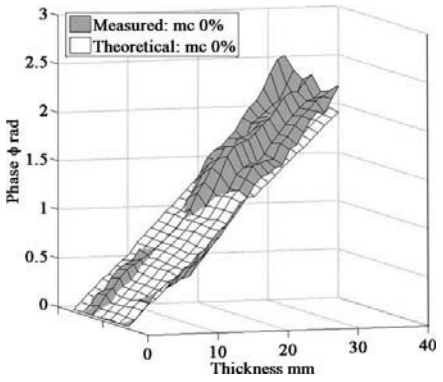

Fig. 7. Distribution of phase shift over a width of 64 mm in birch at 0% mc as thickness increases from 0 to 31 mm.

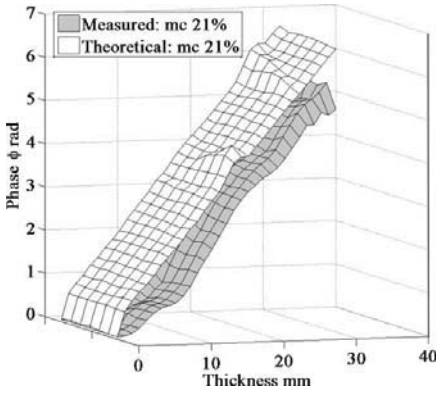

Fig. 8. Distribution of phase shift over a width of 64 mm in birch at 21% mc as thickness increases from 0 to 31 mm.

aries because of different dielectric properties. This will give deviations in attenuation from theoretical values, since theoretical values do not include effects from reflections. Attenuation is more affected by multiple reflections and mismatch losses than is the phase shift [6], and hence the deviations from theoretical values are smaller in phase shift than for attenuation. Another factor which may influence attenuation and phase shift is the variation of grain angle.

Fig. 10 shows the average over the area inside the dotted line in Fig. 2 of theoretical and measured values of attenuation versus thickness at mc 13% at room temperature and frozen at mc 21%. The water molecules in the frozen wood will not oscillate with the field, and the influence of water is decreased. This means that the attenuation in

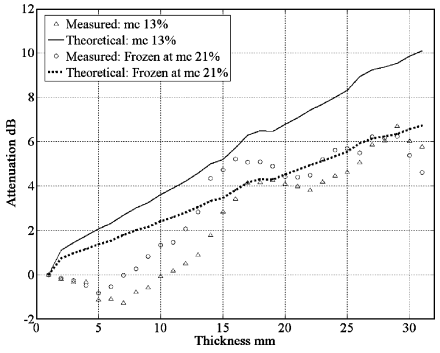

Fig. 10. Average values of attenuation versus thickness for microwaves at 9.375 GHz in birch wood. Measured and theoretical values.

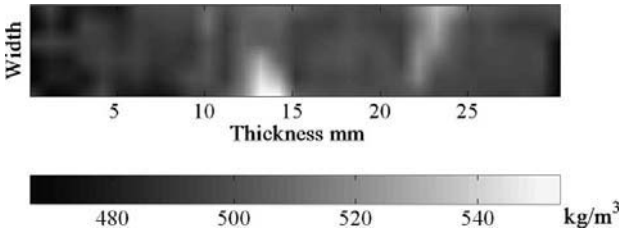

Fig. 9. Density distribution over the measured region. Two small regions have about 10% higher density.

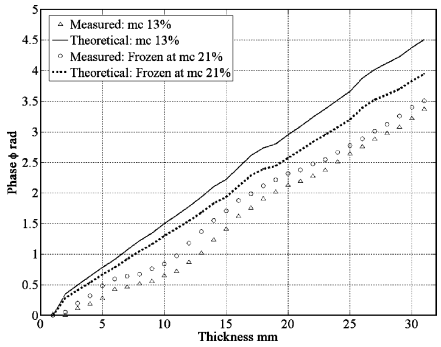

Fig. 11. Average values of phase shift versus thickness for microwaves at 9.375 GHz in birch wood. Measured and theoretical values.

frozen birch with mc 21% is almost the same as in room temperature with mc 13%. The same goes for phase shift in Fig. 11.

The influence of thickness on measured values is lower than on theoretical values, which may be caused by systematic errors in the microwave scanner. There could be gradients in the moisture distribution that cause deviations from theoretical values at some moisture levels. Another possible error is that theoretical values do not involve effects from reflections and scattering. These errors increase in dry wood.

7. Conclusions

- Good correspondence in measured and theoretical values of phase shift.
- The microwave scanner has to be calibrated with a known dielectric to quantify the error in the measurement.
- Reflections and scattering create more noise in attenuation measurement than in measurement of phase shift.
- The proportion of noise is higher at lower moisture content due to lower attenuation.

References

[1] G.I. Torgovnikov, Dielectric Properties of Wood and Wood-Based Materials, Springer, Berlin, 1993.
[2] Jean-F. Portala, Characterisation Du Bois Par Intercorrelation de Measures Multisensorielles. These, Institut National Polytechnique de Lorraine, 1992.
[3] J.C. Bolomey, F.E. Gardiol, Engineering Applications of the Modulated Scatterer Technique, Artech House Inc., 2001, ISBN 1-58053-147-4.
[4] W.L. James, You-Hsin Yen, R.J. King, A microwave method for measuring moisture content, density and grain angle of wood. USDA Forest Products Laboratory, Research Note FPL-0250, 1985.
[5] J. Johansson, Property Predictions of Wood Using Microwaves. Licentiate Thesis, Luleå University of Technology. LIC 2001, 35, 2001.
[6] E. Nyfors, P. Vainikainen, Industrial Microwave Sensors, Artech House, Norwood MA, 1989, pp. 207–212.

V

J Wood Sci (2006)
DOI 10.1007/s10086-005-0794-8

ORIGINAL ARTICLE

Lars Hansson · Nils Lundgren · Anna-Lena Antti
Olle Hagman

Finite element modeling (FEM) simulation of interactions between wood and microwaves

Received: April 4, 2005 / Accepted: November 11, 2005

Abstract The aim of this study was to use finite element modeling (FEM) as a tool to analyze microwave scattering in wood and to verify the model by measurements with a microwave scanner. A medical computed tomography scanner was used to measure distribution of density and moisture content in a piece of Scots pine (*Pinus sylvestris*). Dielectric properties were calculated from measured values for cross sections from the piece and used in the model. Images describing the distribution of the electric field and phase shift were obtained from the FEM simulation. The model was verified by measurements with a scanner based on a microwave sensor. The results show that simulated values correspond well to measured values. Furthermore, discontinuities in the material caused scattering in both the measured and the simulated values. The greater the discontinuity in the material, the greater was the need for computational power in the simulation.

Key words Microwave scanning · Wood · Dielectric properties · Modulated scattering technique · Finite element modeling

Introduction

Microwave scanning is a fast and nondestructive method of measuring internal properties, such as density and moisture content (MC) of wood. This method has previously been studied, for example, by Johansson et al.[1] The aim of the present study was to use finite element modeling (FEM) as a tool to analyze microwave scattering in wood and to verify the model by measurements with a microwave scanner. Values of phase shift and attenuation from the measurements were compared with the FEM model.

By transforming the Maxwell equations into second-order partial differential equations (PDEs) it is possible to solve electromagnetic wave propagation problems. Because wood is an inhomogeneous and anisotropic dielectric material, the wave scatters in different directions as it propagates. Moisture and heat flow during microwave drying of wood have been modeled by Antti,[2] Perre and Turner,[3] and Zhao and Turner.[4] No previous models have been made of electromagnetic wave propagation inside wood because of difficulties in ascertaining the internal structure and because of the need of computational power. In the present analysis, the internal structure of density and moisture content in wood was determined by computed tomography (CT) scanning, as described by Lindgren.[5] From these density and moisture content values, the distribution of dielectric properties was determined. The finite element modeling electromagnetic module in FEMLAB[6] version 3.1 software was used to solve PDEs that describe the wave propagation.

Theory

The dielectric properties of wood depend on moisture content, density, frequency, grain angle, and temperature. The real and imaginary part of the dielectric permittivity, ε' and ε'', perpendicular to the grain versus moisture content and density are shown in Figs. 1 and 2. The free water in the cell cavities, when above the fiber saturation point (FSP), seems to affect permittivity values somewhat differently from water that is bound in the cell walls. Parallel to the grain, the values are 1.1–2 times higher.[7]

Simulation models were constructed with the finite element method as described by, among others, Jin[8] using FEMLAB[6] 3.1. The models describe how a transverse electric (TE) wave propagates through a piece of wood surrounded by air. The variations in the material require a three-dimensional model to obtain a correct solution. How-

L. Hansson · A.-L. Antti
Division of Wood Physics, Luleå University of Technology, Skellefteå Campus, Skellefteå SE-93187, Sweden

N. Lundgren (✉) · O. Hagman
Division of Wood Technology, Luleå University of Technology, Skellefteå Campus, Skellefteå SE-93187, Sweden
Tel. +46-910-58-5707; Fax +46-910-58-5399
e-mail: nils.lundgren@ltu.se

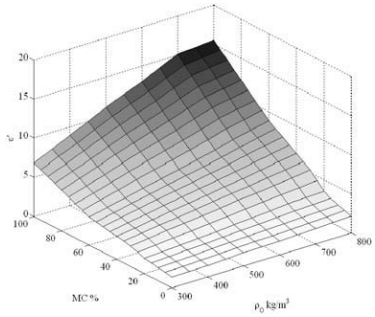

Fig. 1. The relative permittivity ε' at 10 GHz and room temperature, perpendicular to the grain versus moisture content and density[7]

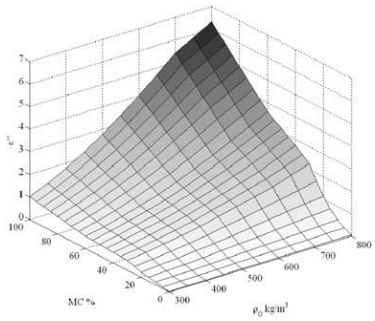

Fig. 2. The relative loss factor ε'' at 10 GHz and room temperature, perpendicular to the grain versus moisture content and density[7]

ever, insufficient computational power made it necessary to restrict the simulation to a two-dimensional model. Variations of dielectric properties in the z direction were neglected, which may increase the errors in the final solution. In the model domain, the z component of the $\boldsymbol{E}$ field is solved by the following equation:

$$\nabla \times \left(\frac{1}{\mu_r} \nabla \times \boldsymbol{E}_z \right) - \left(\varepsilon^* - j \cdot \frac{\sigma}{\omega} \cdot \varepsilon_0 \right) \cdot k_0^2 \cdot \boldsymbol{E}_z = 0, \tag{1}$$

where μ_r is the relative permeability, which is equal to the permeability μ_0 of the free space in the total model domain, because wood is not a magnetic material. Furthermore, ω is the angular frequency, σ is the conductivity, and k_0 is the wave number in free space. In this case σ is close to zero. ε^* is the dielectric permittivity defined as:

$$\varepsilon^* = (\varepsilon' - j \cdot \varepsilon''), \tag{2}$$

where ε' is the relative permittivity and ε'' is the relative loss factor. Tables from Torgovnikov[7] that describe ε^* at varying moisture content, density, and temperature are included in the model and values for ε' and ε'' are interpolated for each grid point and time step by the solver. The model uses a low-reflectance boundary condition on the transmitting and receiving antennas, with electric field $\boldsymbol{E}_z = 1$ on the transmitting antenna and with a source field of zero on the receiving antenna. The low-reflectance boundary to free space is defined as:

$$\boldsymbol{e}_z \cdot (\boldsymbol{n} \times \boldsymbol{H}) + \boldsymbol{E}_z = 2 \cdot \boldsymbol{E}_{0z}, \tag{3}$$

where $\boldsymbol{H}$ is the magnetic field and $\boldsymbol{E}_{0z} = \boldsymbol{E}_z$ is the electric field.

Because the incoming wave to the domain is propagated parallel to the vertical boundaries and the magnetic field is perpendicular to these boundaries, a perfect magnetic conductor (PMC) boundary condition is used. PMC is defined as:

$$(\boldsymbol{n} \times \boldsymbol{H}) = 0, \tag{4}$$

where $\boldsymbol{n}$ is a unit vector normal to the boundary.

Fig. 3. The piece of Scots pine that was used in the study

Material and methods

The material chosen for the study was one piece of Scots pine (*Pinus sylvestris*) shown in Fig. 3 with dimensions 40 × 150 × 320 mm. Close to the center of the piece was a cone-shaped knot with a diameter varying from 18 to 25 mm.

A CT scanner (Siemens Somatom) was used to measure the density in the cross sections. The geometric shape, dielectric properties, and moisture distribution in the green condition for each cross section were calculated from the measured density.

Density data from CT scanning was used to calculate variations in the dielectric properties of the wood and of the moisture distribution in the green condition. The difference between CT images in green and dry conditions was calculated and the resulting image was assumed to describe the moisture distribution in the cross section. Cross sections of the piece, as shown in Fig. 4, were scanned with microwaves and CT both parallel and perpendicular to the grain in green and dry conditions.

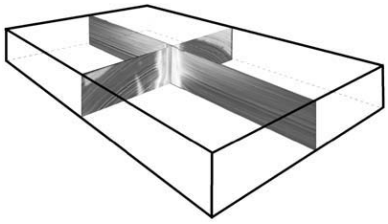

Fig. 4. Two cross sections from the object were scanned. One section was parallel to the grain and the other section was perpendicular to the grain. Regions with low density are darker in the computed tomography (CT) images

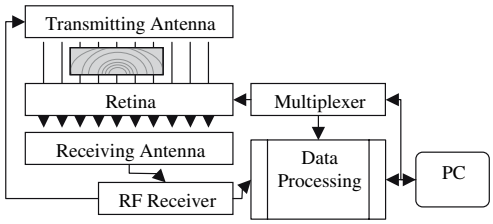

Fig. 6. Sensor system for the microwave scanner. The microwave signal is modulated by a low-frequency signal at 128 probes in the retina. The electromagnetic field at each probe is then extracted from the signal. *RF*, radio frequency; *PC*, personal computer

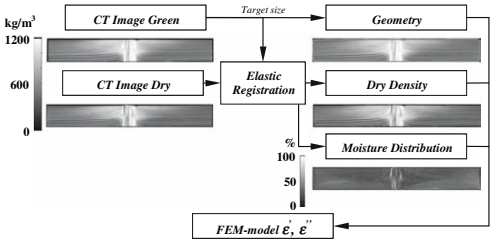

Fig. 5. Brief description of the working procedure in the generation of finite element models

Before the moisture content was calculated from the CT images, it was necessary to compensate the image of dry wood for shrinkage and deformation. Transformation of the CT image of dry wood to the shape of green wood was done by using elastic registration as described by Sorzano et al.[9] Figure 5 shows how the FEM model was generated using density images in green and dry conditions when the electric field (E-field) was oriented perpendicular to the grain (Fig. 4). The same procedure was used when the E-field was parallel to the grain, but the values for ε^* were multiplied with a moisture-dependent factor.[7] Within the knot, the E-field was perpendicular to the grain in both models.

A microwave scanning system described by Johansson[10] that measures attenuation and phase shift of the transmitted electromagnetic field every 8 mm was used for the measurements. Figure 6 shows a schematic drawing on the main part of the system. The wood is illuminated by a quasiplane wave generated by a slotted waveguide that acts as a transmitting antenna where the electrical field is perpendicular to the sensor (9.375 GHz).[11] The wave is locally perturbed at dipoles in the retina by a low frequency signal. This will cause a modulation of the radio frequency (RF) signal that is proportional to the electromagnetic field at the dipoles. This technique, known as modulated scattering technique (MST), has been described by Bolomey and Gardiol[12] among others. The measured values of attenuation and phase shift in the microwave signal after passing through the wood were compared with finite element simulations performed in two dimensions.

Results

The results show that simulated values correspond well to measured values. Figures 7–10 show attenuation and phase angle in the simulated and measured field after transmittance through dry wood. The measured values were obtained by repeated measurements with increasing antenna distance. Figures 11 and 12 show the attenuation when the E-field is oriented perpendicular and parallel to the grain. A clear pattern from the knot in the phase shift for dry wood is shown in Figs. 13 and 14. The phase shift perpendicular to the grain for green wood in Fig. 15 also shows a pattern caused by the knot. The knot is not visible in simulated or measured data for green wood parallel to the grain (Fig. 16).

Discussion

The phase shift is periodic and can only be measured and simulated in the interval $(-\pi, \pi)$. The vectors were unwrapped by changing absolute jumps greater than π to their 2π complement. This only works when the phase shift between adjacent points is less than 2π. The measurements that deviated from the model were attenuation in green wood with the E-field perpendicular to the grain and phase shift in dry wood with the E-field parallel to the grain. The first case can be explained by variations in the z direction. The moisture content was higher on both sides of the scanned cross section. In the second case, the result is very sensitive to changes in the correction factor for permittivity when the E-field is parallel to the grain.

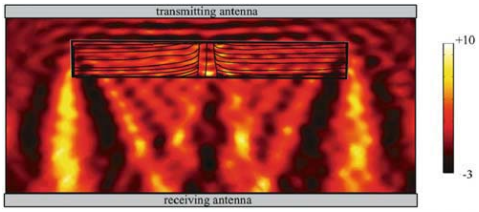

Fig. 7. Simulated attenuation of the electric field (E-field) in dB

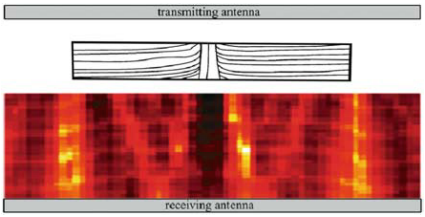

Fig. 8. Measured attenuation of the transmitted E-field

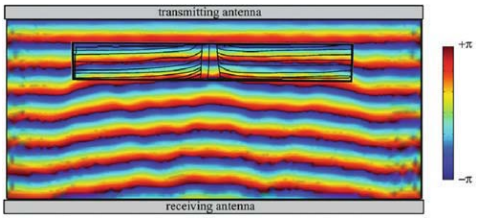

Fig. 9. Simulated phase angle of the E-field in radians

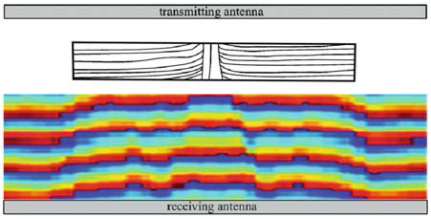

Fig. 10. Measured phase angle of the transmitted E-field

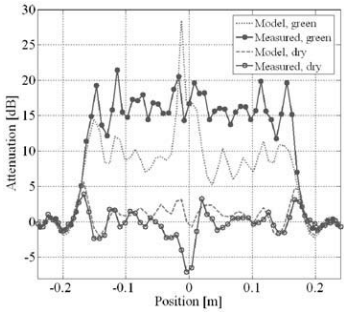

Fig. 11. Simulated and measured attenuation of electromagnetic (EM) wave with the E-field oriented perpendicular to the grain after transmittance through green and dry wood

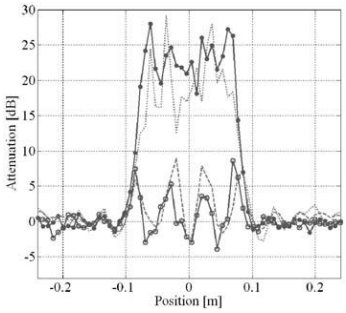

Fig. 12. Simulated and measured attenuation of EM wave with the E-field oriented parallel to the grain after transmittance through green and dry wood

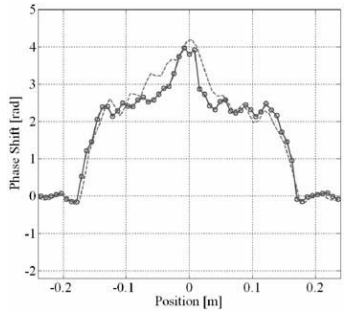

Fig. 13. Simulated and measured phase shift of EM wave with the E-field oriented perpendicular to the grain after transmittance through dry wood

Conclusions

The model corresponds well to the measured values, which show that the FEM simulation could be a useful tool for analyzing microwave scattering in wood. Because wood is an inhomogeneous material, there are discontinuities in density and moisture content in the wood pieces that result in a huge scattering in the measured and simulated values. The greater the discontinuities, the greater is the need for computational power in the simulation. Variations in the z direction give errors if the models are restricted to the xy

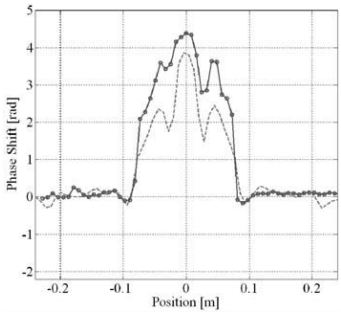

Fig. 14. Simulated and measured phase shift of EM wave with the E-field oriented parallel to the grain after transmittance through dry wood

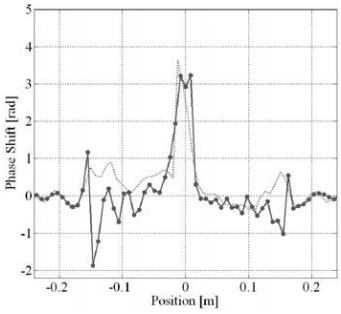

Fig. 15. Simulated and measured phase shift of EM wave with the E-field oriented perpendicular to the grain after transmittance through green wood

plane. The model for dry wood is sensitive to changes in the correction factor for permittivity.

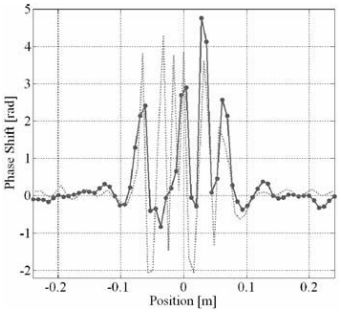

Fig. 16. Simulated and measured phase shift of EM wave with the E-field oriented parallel to the grain after transmittance through green wood

References

1. Johansson J, Hagman O, Fjellner BA (2003) Predicting moisture content and density distribution of Scots pine by microwave scanning of sawn timber. J Wood Sci 49:312–316
2. Antti L (1999) Heating and drying wood using microwave power. Doctoral Thesis, Luleå University of Technology
3. Perre P, Turner IW (1997) Microwave drying of softwood in an oversized waveguide: theory and experiment. AIChE J 43:2579–2595
4. Zhao H, Turner IW (2000) Use of a coupled computational model for studying the microwave heating of wood. Appl Math Model 24:183–197
5. Lindgren O (1992) Medical CT-scanners for non-destructive wood density and moisture content measurements. Doctoral Thesis, Luleå University of Technology
6. Comsol AB (2005) Comsol home page. http://www.comsol.se. Cited 31 Oct 2005
7. Torgovnikov GI (1993) Dielectric properties of wood and wood-based materials. Springer, Berlin Heidelberg New York
8. Jin J (2002) The finite element method in electromagnetics. Wiley, New York
9. Sorzano COS, Thévenaz P, Unser M (2005) Elastic registration of biological images using vector-spline regularization. IEEE Trans Biomed Eng 52:652–663
10. Johansson J (2001) Property predictions of wood using microwaves. Licentiate Thesis, Luleå University of Technology
11. Satimo France (2005) Satimo home page. http://www.satimo.com. Cited 31 Oct 2005
12. Bolomey JC, Gardiol FE (2001) Engineering applications of the modulated scatterer technique. Artech House, Boston

VI

FEM Simulation Of Interactions Between Microwaves And Wood During Thawing

N. Lundgren, L. Hansson, O. Hagman, A.L. Antti

Luleå University of Technology, Division of Wood Science and Technology, Skellefteå Campus, SE-93187 Skellefteå, Sweden

Abstract. Dipole polarization of water molecules is an important factor when microwaves interact with moist wood. Hence there will be a considerable change in dielectric properties when the wood changes from frozen to nonfrozen condition. The aim of this study was to develop a model that simulates measurements with a microwave scanner based on a sensor working at 9.4 GHz. Two-dimensional finite element modelling (FEM) was implemented to analyze interactions between microwaves and green wood during thawing of frozen wood at room temperature. A medical computed tomography scanner was used to measure the internal structure of density in a piece of wood in green and dry condition. From these density images the distribution of dry weight moisture content was calculated for a cross section of the piece and used in the model. Images describing the distribution of the electric field and phase shift at different temperatures where obtained from the FEM simulation. The results show that simulated values correspond well to measured values. This confirms that the model presented in this study is a useful tool to describe the interaction between microwaves and wood during microwave scanning at varying conditions.

Keywords: microwave scanning, wood, dielectric properties, finite element modelling, thawing, phase transition.

PACS: 41.20.Jb

INTRODUCTION

The dielectric properties of dry wood and water can be used to determine the distribution of moisture or density in sawn lumber, as has been described by Hansson et al. [1], among others. It has also been proposed that microwaves should be used to measure grain angle in wood [2]. Depending on geographical location and the properties being measured, it might be necessary to consider temperature dependence. Especially at temperatures around 0°C, there is a steep change in the way water molecules will interact with the electromagnetic field, and the influence of moisture content is small for measurements on frozen wood. Hansson et al. [3] have simulated the interaction between wood and microwaves at a constant temperature by finite element modelling (FEM). The heating of wood in an industrial microwave applicator has also been modelled [4]. A microwave system for scanning of sawn lumber has been developed at Luleå University of Technology. The aim with the present study

was to simulate the response from the microwave sensor when measurements are made on a piece of wood during thawing at room temperature. The model includes heat conduction in wood and the temperature dependence of dielectric properties.

MATERIALS AND METHODS

The study was based on one piece of frozen green birch wood, with dimensions 21 x 17.5 x 30.5 cm. The object was frozen to a temperature of about –15°C. After that, the frozen test piece was allowed to thaw out at room temperature. The test piece was microwave scanned every half hour in the centre in axial direction during thawing until almost the whole object had reached room temperature. The microwave scanning system described by Johansson [5], measures attenuation and phase shift of the transmitted electromagnetic field every eight millimetres. The wood is illuminated by a quasiplane wave generated by a slotted waveguide that acts as a transmitting antenna. The sensor [6] (9.375 GHz) is based on modulated scattering technique (MST) as described by Bolomey and Gardiol [7]. The internal temperature during thawing was measured continuously using a fibre-optic sensor (ASEA 1110) placed in centre of the object. After each microwave measurement, the sample was removed from the microwave scanner, and the heat distribution at the surface was captured using an infrared (IR) camera (AGEMA 550). A CT scanner (Siemens Somatom AR.T.) was used to measure green and dry density of the wood specimen.

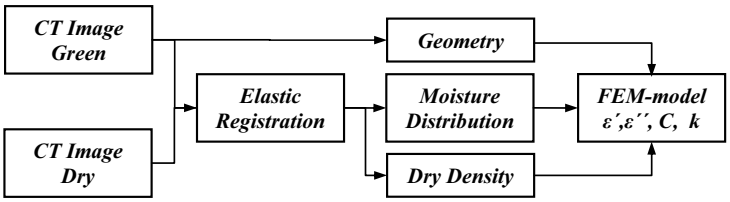

FIGURE 1. Description of the working procedure for generating the FEM model. Dielectric properties (ε', ε''), thermal heat conductivity (k) and specific heat capacity (C) were calculated as functions of temperature, dry density and dry weight moisture distribution in the model.

A schematic description of how the model was generated is shown in figure 1. Transformation of the CT image of dry wood to the shape of green wood was done using elastic registration as described by Sorzano et al [8]. Dry weight moisture distribution was calculated as the difference between these images. The thawing process was then simulated in a two-dimensional section by FEM using the software FEMLAB [9] version 3.1, where the dry weight moisture distribution and the transformed dry wood density images were used as input to estimate values for thermal heat conductivity, specific heat capacity and the dielectric properties for the object. The dielectric properties were calculated from empirical data given by Torgovnikov [10].

ELECTROMAGNETIC WAVE PROPAGATION IN WOOD

When a plane electromagnetic wave is exposed in y-direction through a dielectric material such as wood, the wave can be described as:

$$\mathbf{E}(x,y,z,t) = \mathbf{E}_0 \cdot e^{-j\cdot\omega\cdot t-\gamma\cdot y} \ , \tag{1}$$

$$\mathbf{H}(x,y,z,t) = \mathbf{H}_0 \cdot e^{-j\cdot\omega\cdot t-\gamma\cdot y} , \tag{2}$$

where $\mathbf{E}_0$ and $\mathbf{H}_0$ are the amplitudes of the electric and the magnetic field and γ is the complex distribution factor:

$$\gamma = j\cdot\omega\cdot\sqrt{\varepsilon\cdot\mu} = \alpha + j\cdot\beta , \tag{3}$$

where ω is angular frequency and μ is the complex permeability. Since wood is not a magnetic material, the complex permeability is equal to the permeability μ_0 of the free space. Furthermore, ε is the relative complex permittivity defined as:

$$\varepsilon = \varepsilon_0 \cdot (\varepsilon' - j\cdot\varepsilon'') , \tag{4}$$

where ε_0 is the absolute permittivity for vacuum, ε' is the relative permittivity and ε'' is the relative loss factor. These factors for wood are dependent on the dry weight moisture content, density, frequency, temperature and grain angle. They have been thoroughly investigated by Torgovnikov [10]. If the electric field is parallel to the grain, the dielectric values are about 1.1–2 times higher. If the real and imaginary parts of equation 3 are equated, the expression for the attenuation factor α and the phase factor β of the wave will be:

$$\alpha = \omega\cdot\sqrt{\varepsilon_0\cdot\mu_0}\cdot\left(\frac{\varepsilon'}{2}\cdot\left(\sqrt{1+\left(\frac{\varepsilon''}{\varepsilon'}\right)^2}-1\right)\right)^{1/2} , \tag{5}$$

$$\beta = \omega\cdot\sqrt{\varepsilon_0\cdot\mu_0}\cdot\left(\frac{\varepsilon'}{2}\cdot\left(\sqrt{1+\left(\frac{\varepsilon''}{\varepsilon'}\right)^2}+1\right)\right)^{1/2} , \tag{6}$$

Insertion of equation 3 into equation 1 shows that the amplitude is attenuated exponentially with a factor $e^{-\alpha\cdot y}$ as the wave propagates. If the magnitude of the electric field decreases from $\mathbf{E}(0)$ to $\mathbf{E}(y)$, the attenuation per metre is defined as:

$$\frac{20\cdot\log\left(\dfrac{\mathbf{E}(0)}{\mathbf{E}(y)}\right)}{y} = 20\cdot\log(e)\cdot\alpha \quad [\text{dB/m}], \tag{7}$$

The phase shift per metre is defined as:

$$\frac{\phi}{y} = \beta \quad \text{[rad/m]}. \tag{8}$$

The attenuation and phase shift per metre versus dry weight moisture content and density when the electric field is perpendicular to the grain are shown in figures 2 and 3. The free water in the cell cavities above the fibre saturation point affects attenuation and phase shift values somewhat differently than water that is bound in the cell walls.

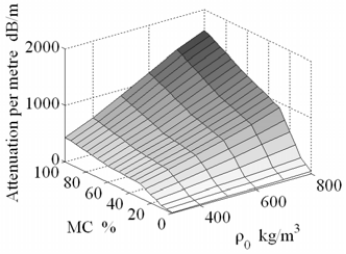

FIGURE 2. Attenuation per metre as a function of dry wood density and dry weight moisture content at room temperature.

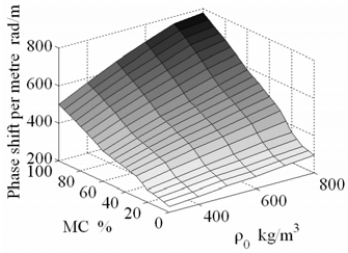

FIGURE 3. Phase shift per metre as a function of dry wood density and dry weight moisture content at room temperature.

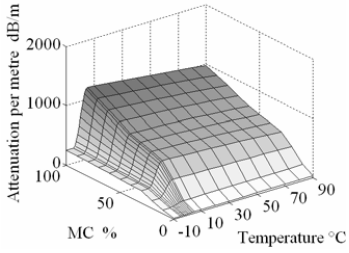

FIGURE 4. Attenuation per metre as a function of temperature and dry weight moisture content at a dry density of 600 kg/m^3.

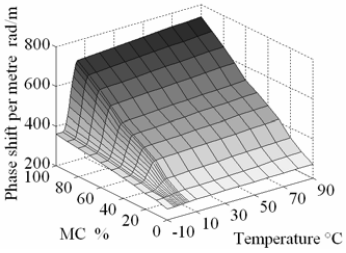

FIGURE 5. Phase shift per metre as a function of temperature and dry weight moisture content at a dry density of 600 kg/m^3.

The attenuation and phase shift per metre versus dry weight moisture content and temperature, when the electric field is perpendicular to the grain, are shown in figures 4 and 5. There is a step transition for the attenuation and for the phase shift when the temperature is zero. To emulate these steps, a smoothed Heaviside function with continuous first derivative [9] is used in the model in order to improve numerical reliability and convergence. The model uses a low-reflectance boundary condition on the transmitting and receiving antennas, with an electric field E_z = 1 on the transmitting antenna and with a source field of zero on the receiving antenna. The low-reflectance boundary [11] to free space used in Femlab's electromagnetic module is defined as:

$$\mathbf{e}_z \cdot (\boldsymbol{n} \times \boldsymbol{H}) + E_z = 2 \cdot E_{0z}, \tag{9}$$

where $\mathbf{e}_z$ is a unit vector, $\boldsymbol{H}$ is the magnetic field, $\boldsymbol{n}$ is the normal to the boundary and $E_{0z} = E_z$ is the electric field at the boundary. Since the incoming wave to the domain is propagated parallel to the vertical boundaries, and the magnetic field is perpendicular to these boundaries, a perfect magnetic conductor (PMC) boundary condition is used. PMC is defined as:

$$(\boldsymbol{n} \times \boldsymbol{H}) = 0, \tag{10}$$

where $\boldsymbol{n}$ is a unit vector perpendicular to the boundary.

HEAT TRANSFER IN WOOD

The temperature variation in a given region over time can be described mathematically with a partial differential equation. This heat equation describes the heat transfer by conduction and convection. In this model, heat transfer by convection is ignored and the heat equation has the form:

$$\rho \cdot C \cdot \frac{\partial T}{\partial t} - \nabla \cdot (k \cdot \nabla T) - Q = 0, \tag{11}$$

where T is the temperature, ρ is the density, t is time, C is the specific heat capacity for constant volume or constant pressure, k is the thermal conductivity and Q is heat-source or sink. In this case, the heat term is zero, because the microwave energy is ignored. In the region of the model, the density of wood,

$$\rho = \rho_0 \cdot \frac{1+u}{1+s_u}, \tag{12}$$

is a function of given dry weight moisture content u, the dry density ρ_0 and also the volumetric swelling or shrinking coefficient, s_u [12]. This coefficient has approximately linear behaviour below the fibre saturation point:

$$s_u = \frac{s_{\max}}{u_{fsp}} \cdot u \tag{13}$$

whereas above the fibre saturation point it is constant:

$$s_u = s_{\max}, \tag{14}$$

where u_{fsp} is the dry weight moisture content at the fibre saturation point at room temperature, and $s_{\max}$ is the maximum volumetric swelling or shrinking coefficient for birch [13]. The specific heat capacity for wood [12] is temperature and dry weight

moisture content dependent, as shown in figure 6. The thermal conductivity of wood [14] is temperature and dry weight moisture content dependent, but also density dependent (figure 7). Furthermore, thermal conductivity in the longitudinal direction is, in the dry weight moisture content range from about 0.06 to 0.15, approximately 2.25 to 2.75 times the conductivity across the grain [12].

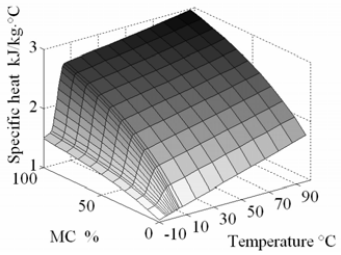

FIGURE 6. Specific heat as a function of temperature and dry weight moisture content.

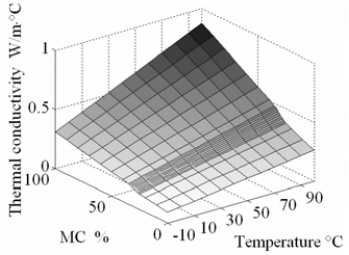

FIGURE 7. Thermal conductivity as a function of temperature and dry weight moisture content at dry density 600 kg/m^3.

Figures 6 and 7 show step transition for specific heat and thermal conductivity respectively when the temperature is zero and the dry weight moisture content has reached the fibre saturation point. These steps were emulated with a smoothed Heaviside function in the same way as the dielectric properties. The model uses a prescribed temperature boundary condition on the transmitting, receiving antennas and on the free space boundary, with a room temperature of T = 20°C. The generalized boundary heat flux condition between the air and the wood surface is defined as:

$$\mathbf{n} \cdot (k \cdot \nabla T) = q_0 + h \cdot (T_{\inf} - T) + C_{const} \cdot (T_{amb}^4 - T^4), \qquad (15)$$

where q_0 represent the heat flux due to evaporation from the surface and is ignored. The second term on the right hand side in equation (15) is the convective heat flux with the surrounding environment, where h is the heat transfer coefficient and T_{inf} is the ambient bulk temperature calculated as the mean value of the prescribed temperature and surface temperature. In general, the geometry and the ambient flow condition are used to determine the value of the heat transfer coefficient. Here, simplified equations are used for the free convection on the wood. The last term in equation (15) is the radiation heat flux with the surrounding environment, where T_{amb} is the surrounding environment temperature; i.e., the prescribed temperature. C_{const} is a product of the surface emissivity and the Stefan-Boltzmann constant.

RESULTS AND DISCUSSION

Figures 8 and 9 show the measured and simulated surface temperature. Energy loss due to evaporation is not included in the simulated model. The mass loss during thawing was 21.3 g. Hence there are some differences in the values.

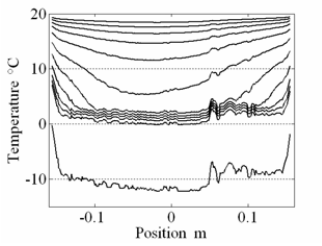

FIGURE 8. Measured surface temperature every 30 min during thawing.

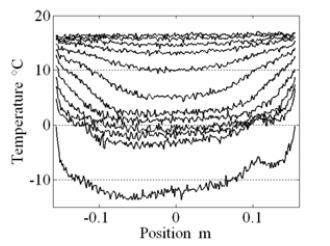

FIGURE 9. Simulated surface temperature every 30 min during thawing.

At low temperatures, the surface temperature is higher on the right hand side in both figures. This is due to lower moisture content in the right side of the wood, as can be seen in figure 10.

Figure 10. Moisture content distribution in the cross section.

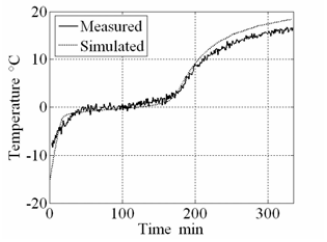

FIGURE 11. Measured and simulated core temperature.

Figure 11 shows measured and simulated core temperature. There is a small deviation in the end of the thawing process that also originates from evaporation that is not included in the model. Figures 12–15 show that the simulated values correspond well to measured values during thawing, both for attenuation and phase shift.

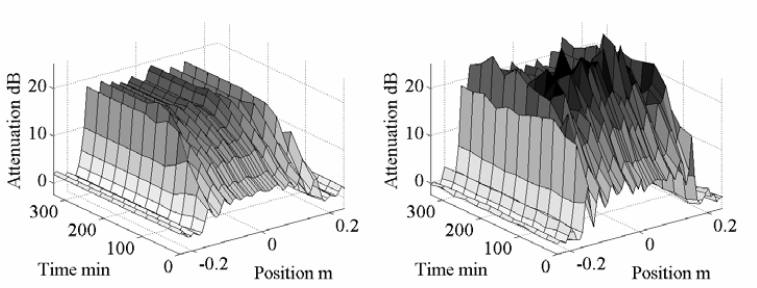

FIGURES 12 - 13. Simulated (left) and measured (right) attenuation.

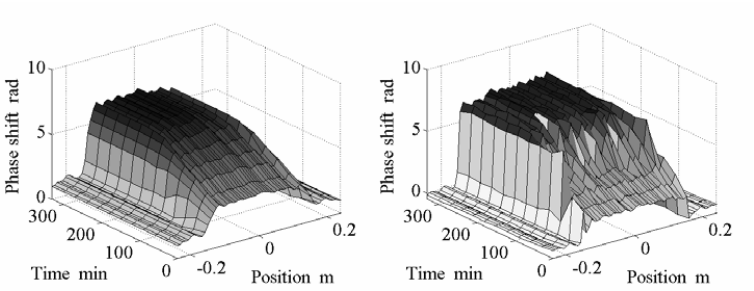

FIGURES 14 - 15. Simulated (left) and measured (right) phase shift.

The agreement in simulated and measured values implies that the FEM model provides a reliable description of the scanner system and that the tabulated values for dielectric and thermal properties on which the model is based are correct.

CONCLUSIONS

The simulated attenuation and phase shift corresponds well to measured values. The model can be used to develop and verify algorithms for scanning of frozen or non-frozen lumber. No reliable predictions of wood properties can be made at temperatures around the freezing point. The response from different types of wood or from knots can easily be simulated by changing the dielectric properties in the model.

REFERENCES

1. L. Hansson, N. Lundgren, A. L. Antti and O. Hagman, *Microwave Penetration in Wood Using Imaging Sensor*, Journal of International Measurement Confederation 38 pp15–20 (2005).
2. J. Shen, G. Schajer and R. Parker, *Theory and Practice in Measuring Wood Grain Angle Using Microwaves*, IEEE Transactions on Instrumentation and Measurement 43(6) pp 803–809 (1994).
3. L. Hansson, N. Lundgren, A. L. Antti and O. Hagman, *FEM Simulation of Interactions Between Wood and Microwaves*, Accepted for publication in Journal of Wood Science (November 2005).
4. L. Hansson, N. Lundgren, A. L. Antti and O. Hagman, *FEM Simulation of Heating Wood In an Industrial Microwave Applicator,* Proceedings from 10th International Conference on Microwave and High Frequency Heating pp 415–418 (2005).
5. J. Johansson, *Property Predictions of Wood Using Microwaves*, Licentiate Thesis Luleå University of Technology, LIC-2001:35 (2001).
6. Satimo France. 22 Avenue de la Baltique Z.A. Courtaboeuf 91953 France. Home page: www.satimo.com.
7. J. C. Bolomey and F. E. Gardiol, *Engineering Applications of the Modulated Scatterer Technique*, Artech House Inc. ISBN: 1-58053-147-4, 2001.
8. C. O. S. Sorzano, P. Thévenaz and M. Unser, *Elastic Registration of Biological Images Using Vector-Spline Regularization*, IEEE Transactions on Biomedical Engineering: 2005. Vol. 52:652–663.
9. Comsol AB. Tegnérgatan 23 SE-11140 Stockholm. Home page: www.comsol.se
10. G. I. Torgovnikov, *Dielectric Properties of Wood and Wood-Based Materials*, Berlin: Springer, 1993.
11. Anonymous, *FEMLAB3 Electromagnetic Module Users Guide*, January 2004
12. F. F. P. Kollman and W.A. Côté, *Principle of Wood Science and Technology (Vol. 1. Solid wood)*, New York: Springer, 1984.
13. J. B. Boutelje, *Träfakta 2nd ed*. Stockholm: Trätek, 1989.
14. J. D. MacLean, *Thermal conductivity of wood*, Heating, Piping and Air Conditioning Vol. 13:380–391 (1941).

VII

FEM SIMULATION OF HEATING WOOD IN AN INDUSTRIAL MICROWAVE APPLICATOR

Lars Hansson, Nils Lundgren, Lena Antti, Olle Hagman
Luleå University of Technology, Division of Wood Technology, SE-931 87 Skellefteå, Sweden, www.ltu.se

ABSTRACT
The aim with this study was to use two-dimensional finite element modelling to investigate microwave heating of a heterogeneous material such as wood. Dielectric properties of wood depend on moisture content, density, frequency, grain angle and temperature. A CT scanner (medical computer tomography) was used to detect density and, with that, moisture content in birch wood. Dielectric properties were calculated within a wood cross section and used in the model. Heat distribution in wood was simulated and verified by measuring temperatures at specific locations in the wood during the process. A specially designed industrial microwave drier equipped with 1 kW magnetrons, 2.45 GHz, was used in the tests. The results show that finite element modelling is a powerful tool in estimation of heat distribution when microwave heating is applied to a well-described porous material such as wood.
KEYWORDS: Wood, FEM, Phase transition, Heating, CT-scanning

INTRODUCTION

Wood is a complex material composed of cellulose, lignin hemicelluloses and minor amounts of extractives. The variation in characteristics and volume of these components as well as differences in cellular structure makes the wood heavy or light, stiff or flexible and hard or soft. These properties are relatively constant in the same kind of wood. A living tree generally has a moisture content exceeding 30%, which means that the cell walls are fully saturated. The higher the moisture content is, the more water will be filled in the cell cavities. The use of microwave heating for drying of wood has been investigated and developed, among others, by Perré and Turner [1] and by Antti [2]. Uneven distribution of the field and material properties will lead to uneven distribution of the heat energy, which also has been studied by Zielonka and Dolowy [3]. When wood is placed in an electric field, the field will be influenced by wood properties such as temperature, density, moisture content, and fibre direction. Finite element modelling (FEM) has been used by Hansson et al. [4] to visualize the interior field when wood is exposed to microwaves. For simulation models of microwave heating it is also necessary to take into account temperature dependence. Especially for frozen wood there is a large change in dielectric properties during the phase transition from ice to water (Hagman et al. [5]). The dielectric and thermal properties of moisture within wood depend on whether the water is bound in the cell walls or free in the cavities. The relative dielectric constant and the loss factor values for the model are based on the literature such as, for instance, Torgovnikov [6]. The heat conductivity of wood depends on density, moisture content and direction of the heat flow with respect to the grain (MacLean [7]). The specific heat of wood is low as compared to other materials. It depends on moisture content and temperature of the wood (Kollman & Côté [8]). The purpose of the present study was to generate an FEM model for microwave heating of wood based on the internal structure and the external field distribution.

MATERIAL AND METHODS

Three pieces of birch wood with the dimensions 55 x 100 x 440 mm where heated in a microwave drier (Hansson and Antti [9]) as shown in Fig. 1. The drier is equipped with a 1 kW magnetron working at 2.45 GHz.

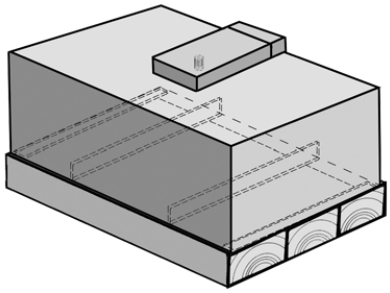

Fig. 1: Microwave drier used for heating of green birch wood from frozen to 100 C.

The internal temperature during the heating process was measured continuously using a fibre-optic sensor (ASEA 1110) placed at the maximum of the electric field. Every five minutes the samples were removed from the applicator for about 30 seconds, and the heat distribution at the surface was captured using an IR camera (AGEMA 550).

A CT scanner (Siemens Somatom AR.T.) was used to measure green and dry density of the wood specimen. Transformation of the CT image of dry wood to the shape of green wood was done using elastic registration as described by Sorzano et al. [10] Moisture distribution was calculated as the difference between these images. From density and moisture content it was possible to estimate values for heat conduction, heat capacity and the dielectric properties. The heating process was then simulated in a two-dimensional section by the use of finite element modelling (FEM) using the software FEMLAB [11] version 3.1. A schematic description of the procedure is shown in Fig. 2.

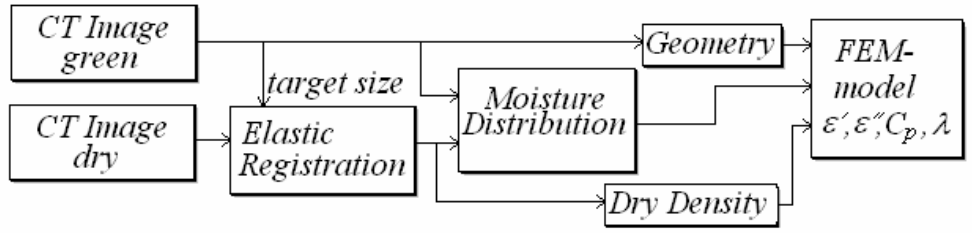

Fig. 2: Description of the working procedure for generation of the FEM models. Dielectric properties (ε′, ε′′), heat conduction (λ) and heat capacity (C_p) were calculated as functions of temperature, dry density and moisture distribution in the model.

At the phase transition from ice to water there is a step function both in dielectric (Fig. 3 and 4) and in thermal properties. Convergence problems due to this step are avoided by using a smoothed Heaviside function. The latent heat that is consumed when ice transforms into liquid water also has to be taken into account. The specific heat around the transition temperature is calculated by multiplying the latent heat with a normalized Gaussian pulse. A fine spatial grid is required for the whole cross section since the phase transition will move during thawing.

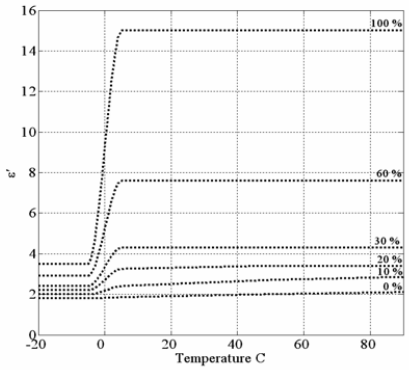

Fig. 3: Relative dielectric constant for wood as a function of temperature with different moisture contents at a density of 600 kg/m^3.

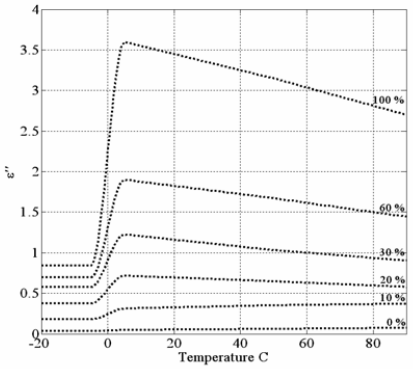

Fig. 4: Relative loss factor for wood as a function of temperature with different moisture contents at a density of 600 kg/m^3.

RESULTS

The simulated core temperature describes the heating process of wood from frozen to 100°C, but also the phase transition at 0°C and 100°C. At the end of the heating process there is a difference between the simulated and the measured core temperature. This difference is probably caused by the water movement in the wood piece, which is not included in the model. The weight of the pieces decreases about 0.1 kilogram during the heating process. Measured and simulated core temperatures are shown in Fig. 5.

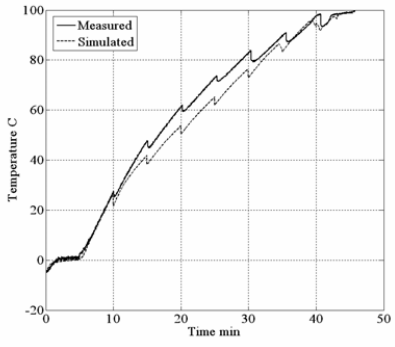

Fig. 5: The measured and the simulated core temperature.

The measured surface temperature at different moments is displayed in Fig. 6. Furthermore, the simulated surface temperature at the same point in time is displayed in Fig. 7. A comparison of the figures shows a difference between the simulated and the measured surface temperature. This difference is due to the fact that the model only approximately handles evaporation, which has a large influence on the surface temperature. The wood pieces used in this model had an average moisture content of about 0.43. Also the fact that the model is only made in 2D causes differences between the measured results and the simulated results. As wood is an inhomogeneous material, there can be discontinuities in density and moisture content in the wood pieces. This causes microwave scattering in all directions, which in turn affects the heating process.

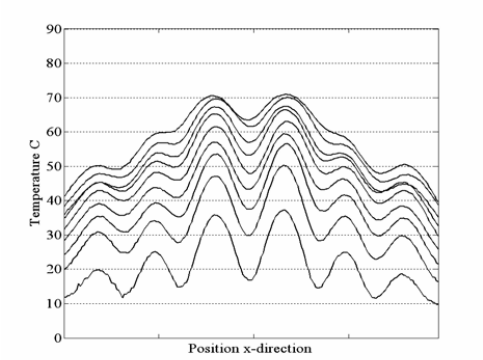

Fig. 6: Measured surface temperature every 5 min during the heating.

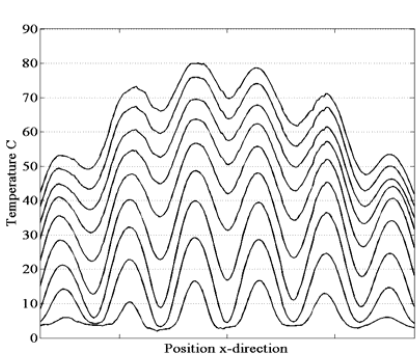

Fig. 7: Simulated surface temperature every 5 min during the heating.

CONCLUSIONS

The model accuracy and adequacy have been verified by a comparison using experimental measurement. The results show that FEM is a powerful tool in estimation of heat distribution when microwave heating is applied to wood. The model predicts the core temperature well. There is a difference between the model and the measurement regarding the surface temperature since the model does not handle all physical processes adequately, e.g., evaporation.

REFERENCES

[1] Perré, P. and Turner, I. (1997). Microwave drying of softwood in an oversized waveguide: Theory and experiment. AIChE Journal 43(10) pp 2579–2578.

[2] Antti, A.L. (1999) Heating and drying wood using microwave power (Doctoral thesis, 1999:35). Skellefteå: Luleå University of Technology, Division of wood physics.

[3] Zielonka, P. and Dolowy, K. (1998). Microwave drying of spruce: moisture content, temperature, and heat energy distribution. Forest Products Journal 48(6) pp 77–80.

[4] Hansson, L., Lundgren, N., Antti L. and Hagman O. (2005) FEM simulation of interactions between wood and microwaves. Submitted to Journal of Wood Science (March 2005)

[5] Hagman, O., Lundgren, N. and Johansson, J. (2004) Calibration for Frozen/Non-Frozen Conditions When Predicting Moisture Content and Density Distribution of Wood by Microwave Scanning of Sawn Timber. Forest Products Society 58th Annual meeting, Grand Rapids, June 27–30 2004.

[6] Torgovnikov, G.I. 1993. Dielectric Properties of Wood and Wood-Based Materials. Springer, Berlin.

[7] MacLean, J.D. 1941. Thermal conductivity of wood. Heating, Piping and Air Conditioning. Vol.13:380–391.

[8] Kollman, F.F.P. and Côté, W.A. 1984. Principle of Wood Science and Technology (Vol. 1. Solid wood). Springer. New York.

[9] Hansson, L. and Antti L. (2003) Design and performance of an industrial microwave drier for on-line drying of wood components. The 8th International IUFRO Wood Drying Conference. 24–29 August, Brasov, Romania, pp 156–158.

[10] Sorzano, C.O.S., Thévenaz, P. and Unser, M. (2005) Elastic Registration of Biological Images Using Vector-Spline Regularization. IEEE Transactions on Biomedical Engineering. In press.

[11] Comsol AB. Tegnérgatan 23 SE-11140 Stockholm. Home page: www.comsol.se

VIII

MODELLING HEATING AND DRYING OF WOOD

Lars Hansson, Lena Antti

Luleå University of Technology, Division of Wood Technology,

SE-931 87 Skellefteå, Sweden, www.ltu.se

ABSTRACT

A finite element model was developed to describe and explain microwave drying of wood. Dielectric and thermal properties are of great importance, since they are continuously affected during the process by moisture content, density, grain direction, temperature and more. Computer tomography was used to detect wood density and moisture content. Heat distribution was verified by fibre-optic temperature sensors. The tests were performed in a designed microwave drier based on 1 kW generators, 2.45 GHz. The results show that finite element modelling is a powerful tool to simulate heat and mass transfer in wood, providing the material is well described.

KEYWORDS: Scots Pine, FEM, Phase transition, CT scanning, Heat and Mass transfer

INTRODUCTION

Wood is a complex porous material composed of cellulose, lignin hemicelluloses and, in soft wood, minor amounts of extractives. A living tree generally has a dry-weight moisture content (mc) considerably exceeding 0.3, which is approximately the fibre saturation point and means that the cell walls are fully saturated. The higher the mc, the more water will be filled in the cell lumina. Before using wood for construction, carpentry, etc., the material needs to be dried. The most common drying method nowadays is conventional air-circulation drying, which is based on heat conduction, from the surface of the wood towards the interior. Furthermore, the moisture moves towards the surface by mass flow in liquid and vapour phases. This mass flow is divided into three different phases: capillary, transition and diffusion phase [1]. Microwave drying, in contrast to conventional drying, is based on the principle that heat is absorbed throughout the moist load. The use of microwave heating technology for wood drying has been investigated and developed, among others, by Antti [2] and Perré and Turner [3]. When wood is placed in an electromagnetic field, the field will interact with wood properties, since the dielectric properties of wood are dependent on temperature, dry density, mc, and fibre direction. Uneven distribution of the field and the interaction with material properties will lead to uneven distribution of the heat energy, which phenomenon also has been studied by Antti [4] as well as by Zielonka and Dolowy [5]. The dielectric loss, i.e., microwave absorption, provides a volumetrically distributed heat source. The heat conductivity of wood depends on oven dry density, mc and direction of heat flow with respect to the grain direction [6]. The specific heat of wood is low compared to other materials and depends on mc and temperature [7]. A one-dimensional multiphase porous media model has been developed by Ni et al. [8] in which the model predicts the moisture movement in biomaterial during intensive microwave heating. Constant et al. [9] have presented a model of simultaneous heat and mass transfer during drying of porous isotropic light concrete in which the numerical results agree with the experimental observations in terms of the drying kinetics and transfer mechanisms. Furthermore, a 3-D version of a comprehensive heat and mass transfer computational model for simulating the high-temperature convective drying of anisotropic softwood, wherein the high temperature induces an overpressure in the longitudinal direction of the board, has been presented by Perré et al. [10]. The building up of internal pressure gradients is a distinguishing characteristic for microwave applications. Furthermore, this pressure build up causes internal moisture

movement. None of the previous models for heating and drying wood take the internal structure into consideration. Finite element modelling (FEM) has been used by Hansson et al. [11] in order to simulate in 2D the heating of birch wood from frozen state up to the boiling point for water at atmospheric pressure. As the distributions of the dry density and the mc are not uniform in a wood board, Hansson et al., as well as Lundgren et al. [11, 12, 13], used CT scanning (medical computer tomography) to detect these distributions.

The purpose of the present study was to generate a 2-D FEM model for microwave heating and drying of wood in a specially designed microwave applicator for industrial use. The internal structure, i.e., density, was determined by CT scanning before and after drying and in addition when the wood piece was totally dried to zero mc in an oven. This information provides the opportunity to determine the initial and the final mc. The received initial mc values as well as the oven dry density values were used in the model to simulate the final mc and were verified by the measured final mc.

MATERIAL AND METHODS

The study was based on one specimen of Scots pine wood, with a dimension of 440 x 175 x 50 mm and with an initial average mc of 0.17. In order to avoid predried butt ends on the board, the test piece was cut from the middle of a longer board, and a specimen was also taken for determination of initial average mc using the oven-dry-weight method. Internal temperatures during the drying process were measured continuously using four-channel fibre-optic equipment (NEOPTIX, ReFlex). The sensors were placed 10, 21, 28 and 40.5 cm from one butt end (figure 2). The selection of these positions is based on the electromagnetic field distribution within the microwave applicator—positions where hot spots appear were chosen.. A CT scanner (Siemens Somatom AR.T.) was used to measure the density before and after microwave drying. After microwave drying, the specimen was cooled for one hour in room temperature before CT scanning, since high temperature affects the density values. In order to be able to distinguish between wood and water, the CT images before and after microwave drying needed to be compared to images of the totally dried wood. To reach zero mc, the sample was for that reason further dried at 103˚C in an ordinary oven until the weight loss ended and then CT-scanned.

Since wood shrinks, it was necessary to transform the dried wood CT images to the shape of the initial wood sample images. Elastic registration according to Sorzano et al. [14] was used. From these transformed images, with correction for shrinkage, determination of the mc distribution was made for the initial and for the microwave-treated state.

THE MICROWAVE EQUIPMENT

A microwave applicator designed and patented by Microtrans AB [15], was used in this work. The applicator according to its inventor makes use of an evanescent main power-transferring mode, which is complemented by a second mode. The effect of the cooperation of the two modes is that the field pattern extends over a significant distance below the applicator opening, such that a load placed below the applicator opening is heated according to the field pattern arising from the combined modes [15].

The waveguides guiding the microwaves into the microwave applicator (cavity, see figure 1) are simple rectangular tubes dimensioned for the current frequency 2.45 GHz. The standard magnetron generating the microwaves has an output power of 1 kW. The power to the magnetron is supplied by an efficient power source that has been developed by Dipolar AB [16]. With this power supply, the output power can be continuously varied.

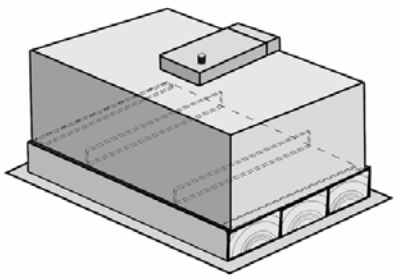

Figure 1. Microwave applicator used for heating and drying Scots pine.

Inside the cavity, the waves reflect against the walls. Furthermore, the waves interfere with each other and thereby distribute the electric field in determined patterns in the cavity space. The field distribution depends on the design of the cavity, i.e., its dimensions, and to some extent on the dielectric property of the load, its position in the cavity and its size. However, the influence from the load is small and here assumed to be negligible.

Since a model in three dimensions needs very powerful and time consuming computations, the model is made in only two dimensions (figure 2).

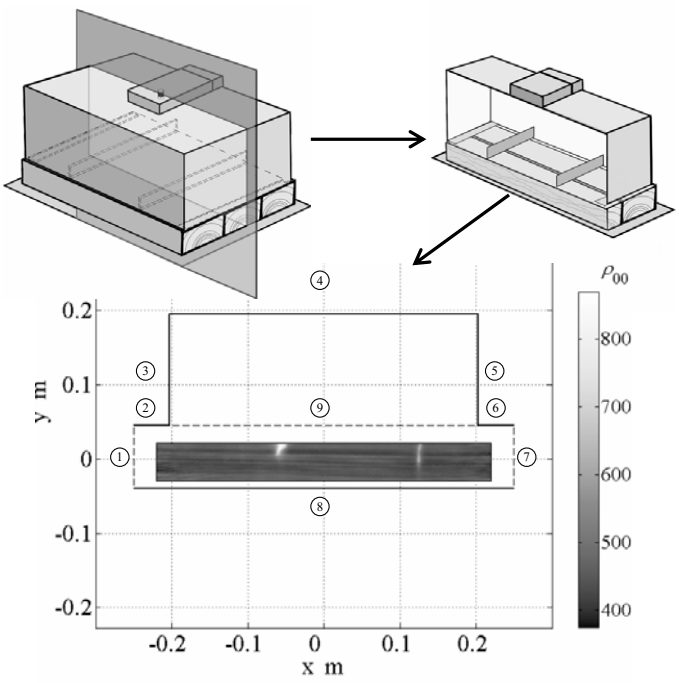

Figure 2. The schedule shows the modelled 2-D cross-section part of the microwave applicator and the wood modelled in 2-D.

Furthermore, the heating and drying process was simulated in a two-dimensional section by FEM using the software COMSOL version 3.3a [17], wherein the mc distribution and the transformed dry wood density images were used as inputs when estimating variables of the thermal heat conductivity, specific heat capacity, dielectric properties and the porosity of the object.

MICROWAVES IN WOOD

If wood is placed in an electromagnetic field such as a microwave field, the electric part of the field and the wood will affect each other, since wood is a biological dielectric material with a complex structure. A dielectric material is a substance that is a poor conductor or nonconductor of electric current; instead, an electrical polarization occurs. This means that the positive charges move into the same directional orientation as the electric field and the negative charges in the opposite direction. When wood is exposed to a microwave field, parts of the field are transmitted, parts are absorbed and parts are reflected. The absorbed electromagnetic field generates resistive heat or energy loss to the wood and is defined as:

$$Q = \frac{1}{2}\mathrm{Re}\left[(\sigma - j \cdot \omega \cdot \varepsilon)\mathbf{E} \cdot \mathbf{E}^*\right], \tag{1}$$

where σ is the conductivity, $\mathbf{E}$ is the electric field intensity, $\mathbf{E}^*$ is the conjugate of the electric field intensity, ω denotes the angular frequency and ε is the relative complex permittivity defined as:

$$\varepsilon = \varepsilon_0\left(\varepsilon' - j \cdot \varepsilon''\right), \tag{2}$$

where ε_0 is the absolute permittivity for vacuum, ε' is the relative permittivity and ε'' is the relative dielectric loss factor. Relative permittivity indicates how much slower the electromagnetic wave propagates within the wood, compared to propagation in vacuum. Investigations by Torgovnikov [18] have shown that the dielectric properties, as the relative permittivity and the relative dielectric loss factor of wood, depend on the mc, the dry density, the wood temperature and the direction of electric field relative to the fibre direction. This means that the dielectric properties of wood will change during heating and drying.

In the model, the electric field was modelled only in the rectangular domain where the wood piece was placed (figure 2). An electric field was transmitted into this domain from boundary 9 (figure 2). All boundaries, apart from the open edge boundaries 1 and 7, in this rectangular domain are stainless steel boundaries. These boundaries are interfaces between air and a perfect conductor. The boundary condition is defined as:

$$E_z = 0\,. \tag{3}$$

At the open edges, the boundary condition is a perfect magnetic conductor, defined as:

$$\mathbf{n} \times \mathbf{H} = \mathbf{0}\,, \tag{4}$$

where **H** is the magnetic field and **n** is the normal vector to the surface.

HEAT TRANSFER WITHIN WOOD

When wood absorbs microwave energy over time, the temperature difference causes the heat to be conducted throughout the volume of the wood. This heat transfer is dependent on the thermal conductivity of the material. Thermal conductivity in wood is mc-, dry density-, temperature- and fibre direction-dependent [6, 7, 19]. Furthermore, the conductivity in longitudinal or grain direction is significantly higher than across the grain [7]. In a given region within the wood, the temperature variation over time can be physically described by the transient energy-balance equation:

$$\rho_{u,u} C_{tot} \frac{\partial T}{\partial t} + \nabla \cdot \left(-k_w \nabla T\right) = Q\,, \tag{5}$$

where the heat transfer by convection inside the wood is ignored and T is the temperature, $\rho_{u,u}$ is the wood density at mc u, t is time, C_{tot} is the specific heat capacity for wood including water, k_w is the thermal conductivity of wood and Q is the external heat source, i.e., the microwave energy.

The specific heat capacity of wood is influenced by the mc, the dry density and the temperature [6, 20] and is defined as:

$$C_{tot} = \frac{u\left(c_{H_2O} + \left(c_{vap} - c_{H_2O}\right)\delta + \theta \Delta L_v\right) + c_w}{u+1}, \tag{6}$$

where u is the mc, c_{H_2O} is the specific heat capacity of water in liquid form, c_{vap} is the specific heat of water in vapour form, c_w is the specific heat capacity of wood and ΔL_v is the latent heat of evaporation. Both the specific heat capacity of water and of wood are temperature dependent, and the latent heat of evaporation is assumed to not being temperature dependent. Furthermore, δ is a smoothed Heaviside function which switches from 0 to 1 when the temperature exceeds 100˚C, which means that the specific heat for water changes from liquid to vapour. To take into account the latent heat of evaporation during the phase shift from liquid to vapour form, a normalized pulse around this temperature transition was used, where the integral of $\theta(T)$ must be equal unity to satisfy the following:

$$\int_{-\infty}^{\infty} \rho\theta(T)\Delta L_v dT = \rho\Delta L_v, \tag{7}$$

such that the pulse width denotes the range between the liquidus and solidus temperatures [17].

HEAT TRANSFER IN THE AIR SURROUNDING THE WOOD

When the wood has a different temperature from that of the surrounding fluid, i.e., the air, a transfer of thermal energy occurs. This transfer occurs by conduction, convection, radiation or a combination of these. A combination of conduction and the transfer of thermal energy by movement of hot air to cooler areas in the air medium give convection. In this model, cooler air is flowing around the wood piece. This flow can be forced, natural, or a combination of these. The natural convection is caused by the change in air density. Hence, the density of air is temperature dependent; the higher the temperature, the lower the air density. The forced convection occurs when a fan creates unnaturally induced convection air flow. In the model, nonisothermal flow was used to describe the air flow around the wood piece, since there are small density variations in the air caused by temperature differences. The nonisothermal flow is defined as:

$$\begin{aligned} \rho_{air}\frac{\partial \mathbf{u}_{air}}{\partial t} + \rho_{air}(\mathbf{u}_{air}\cdot\nabla)\mathbf{u}_{air} = \\ \nabla\cdot\left[-p_{air}\mathbf{I} + \eta\left(\nabla\cdot\mathbf{u}_{air} + (\nabla\cdot\mathbf{u}_{air})^T\right)\right] - (2\eta/3 - \kappa)(\nabla\cdot\mathbf{u}_{air})\mathbf{I} \end{aligned}, \tag{8}$$

$$\frac{\partial \rho_{air}}{\partial t} + \nabla \cdot \left(\rho_{air} \mathbf{u}_{air} \right) = 0 \,, \tag{9}$$

where η_{air} is the dynamic viscosity, κ is the dilatational viscosity, ρ_{air} is the air density and p_{air} is the pressure of the air [17]. The pressure and density variables are temperature dependent. $\mathbf{u}_{\text{air}}$ is the surrounding air fluid velocity around the wood piece.

The initial air fluid velocity and its pressure are set to zero and atmospheric pressure, respectively. The open ended sides 1 and 2 (figure 2) have normal flow or pressure conditions in which the pressure has a constant value equal to atmospheric pressure. All surfaces, apart from the wood surface, have a no-slip condition, which means that that condition is fullfilled when the fluid velocity is zero at the surfaces in all directions.

The transient energy-balance equation for the air around the wood piece is defined as:

$$\rho_{air} C_{air} \frac{\partial T}{\partial t} + \nabla \cdot \left(- k_{air} \nabla T + \rho_{air} C_{air} T \mathbf{u}_{air} \right) = 0 \,, \tag{10}$$

where ρ_{air} is the density of air and C_{air} is the heat capacity for air.

The initial temperatures of wood and air are 13˚C and 17˚C respectively in the model (figure 2). These temperatures were chosen to agree with the measured ones. The stainless steel borders 2–6 and 8 in figure 2 have a constant temperature of 17˚C for the same reason. The convective border condition at the open ended sides 1 and 7 is defined as:

$$\mathbf{n} \cdot \left(- k_{air} \nabla T \right) = 0 \,. \tag{11}$$

HEAT TRANSFER BETWEEN WOOD AND THE SURROUNDINGS

When evaporation takes place at the surface of the wood piece, this physical process will make the surface temperature lower than the interior temperature. To determine this evaporation, or mass transport, the transient mass-balance equation can be used for the surrounding vapour around the wood piece:

$$\frac{\partial c_{ext}}{\partial t} + \nabla \cdot \left(- D_{H_2O} \nabla c_{ext} + c_{ext} \mathbf{u}_{air} \right) = 0 , \tag{12}$$

where c_{ext} is the external water concentration and D_{H_2O} is the diffusion coefficient for water vapour. In order to describe the temperature dependency on saturated water vapour pressure, the Clausius-Clapeyron equation was used and is defined as:

$$\frac{d \ln p}{dT} = \frac{\Delta L_v}{RT^2} , \tag{13}$$

where R is the molar gas constant. This equation allows calculation of the vapour pressure at another temperature than the reference temperature if the vapour pressure is known at certain temperatures, i.e., a reference temperature and pressure, and the heat of vaporization is assumed not being temperature dependent. With this equation, the water concentration in the gas phase at the interface between the wood and air could be estimated as:

$$c_{surf} = \frac{M_{H_2O} \cdot p_{ref}}{R \cdot T} \cdot e^{\left(- \frac{\Delta L_v \cdot M_{H_2O}}{R} \left(\frac{1}{T} - \frac{1}{T_{ref}} \right) \right)} , \tag{14}$$

where M_{H_2O} is the molar mass of water, p_{ref} reference saturation pressure, T_{ref} is the reference temperature. Obtaining equation 13, the heat of vaporization is assumed to be constant, i.e., not temperature dependent, and the reference point is zero degrees Celsius. The boundary heat source, due to the latent heat of evaporation at the interface between the wood and air, is defined as:

$$q_{vap} = \Delta L_v \nabla \cdot \left(- D_{H_2O} \nabla c_{ext} + c_{ext} \mathbf{u}_{air} \right). \tag{15}$$

The heat transfer due to the thermal radiation is defined as:

$$q_{rad} = \varepsilon_w \sigma \left(T_{amb}^4 - T^4 \right) , \tag{16}$$

where ε_w is the wood emissivity and has a value of 0.9 [21], σ is the Stefan-Boltzmann constant and T_{amb} is the ambient temperature, here 290 K. The amount of heat radiation into

or out from the wood piece is a function of several components, such as surface reflectivity, emissivity, surface area, temperature and the geometric orientation of the thermally surrounding objects in relation to the wood piece. The surface reflectivity and emissivity of the wood piece and the surrounding objects are here a function of their condition and composition. However, in this simulation model, the wood is approximated to be a small object in a large enclosure**,** allowing the simple relation of equation 16 to be used [21].

The expressions for the heat transfer due to the thermal radiation and latent heat of evaporation together with the amount of heat transfer through the wood boundary give:

$$\mathbf{n} \cdot \left(-k_w \nabla T_w - \left(k_{air} \nabla T_{air} - \rho_{air} C_{air} T_{air} \mathbf{u}_{air} \right) \right) = q_{vap} + q_{rad} \tag{17}$$

where **n** is the normal vector to the wood surface. In the model (figure 2), the open-ended sides 1 and 7 have a convective flux border condition, which is defined as:

$$\mathbf{n} \cdot \left(D_{H_2O} \nabla c_{ext} \right) = 0 \,. \tag{18}$$

Furthermore, all stainless steel borders have an insulation or symmetry border condition, which is defined as:

$$\mathbf{n} \cdot \left(D_{H_2O} \nabla c_{ext} + c_{ext} \mathbf{u}_{air} \right) = 0 \,. \tag{19}$$

FLOW WITHIN THE WOOD

Wood is a hygroscopic and porous material, and this means that it contains both free water and bound water. The porosity or the void volume, [7], of such a porous material as wood describes the fraction of void space in the wood, and at a mc above fsp is defined as:

$$\phi = 1 - \rho_{00} \left(1 - \beta_{\max} \right) \left(\frac{1}{\rho_w} + \frac{u_b}{\rho_b} + \frac{u_f}{\rho_{H_2O}} \right), \tag{20}$$

where ρ_{00} is the dry density, $\beta_{\max}$ is the maximum shrinkage coefficient [7], u_b and u_f is the amount of bound respectively free water in the wood matrix, ρ_{H_2O} is the density of the free water, ρ_w is the compact density of wood and ρ_b is the bound water density. The compact density is the density of wood substance of a completely solid wood specimen, i.e., the compact density without pores, and it has a value of approximately 1500 kg/m^3. The density of bound water in the wood matrix is the density of compressed absorbed water, and is dependent on the amount of hygroscopic water, [7]. The porosity at mc below fsp is defined as:

$$\phi = 1 - \frac{\rho_{00}\left(1-\beta_{\max}\right)}{\left(1-\frac{\beta_{\max}}{u_{usp}}\left(u_{usp}-u\right)\right)}\left(\frac{1}{\rho_w}+\frac{u_b}{\rho_b}\right), \tag{21}$$

where u_{usp} is the mc at the fsp and depends on the temperature. Furthermore, it has a maximal value of approximately 0.3 at a temperature of 20 ˚C. If the temperature increases, the fsp will decrease [22].

The time rate of change of the vapour gas density in the porous media at a fixed point in space can be described with a combination of the continuity equation and Darcy's law as:

$$\frac{\partial \phi \rho_g}{\partial t} + \left(\nabla \rho_g \cdot \mathbf{u}_{\text{int}}\right) = F\,, \tag{22}$$

where ϕ is the porosity of the material, F is the vapour source and $\mathbf{u}_{\text{int}}$ is Darcy's equation defined as:

$$\mathbf{u}_{\text{int}} = -\frac{\kappa_g}{\eta_g}\left(\nabla p_g - \rho_g \mathbf{g}\right), \tag{23}$$

where κ_g is the permeability, η_g is the dynamic viscosity and $\mathbf{g}$ is the acceleration of gravity at sea level. However, in the present model, the last part in Darcy's equation is negligible, since it has no significant influence on the model. The velocity $\mathbf{u}_{\text{int}}$, which is defined as the volume

rate of flow through a unit cross-sectional area of the solid plus fluid, is averaged over a small region of space.

Permeability is the ability of wood to transmit fluid, as gas in this model, under the influence of a pressure gradient. The permeability value depends on the size of cell lumina and the interconnected pit openings. Hence a wood piece with closed cell structure would have zero permeability. Siau, [22], has presented a theory of the transport processes in wood. However, the permeability in this model is assumed to be constant, and the value is estimated by iteration. So the modelled final mc is equal to the measured one. Furthermore, the permeability is assumed to be a thousand times greater in the axial direction, i.e., in the x-direction of the model, than in the transverse direction (figure 2).

The vapour source is bound water in the wood cell walls, which starts to evaporate when the internal temperature increases during heating. The largest internal evaporation from the wood structure occurs when the water shifts phase from liquid to vapour form, i.e., when the temperature exceeds 100˚C. As the evaporation below 100˚C is ignored, the vapour source term is defined as:

$$F = \delta \frac{Q}{\Delta L_v} \frac{u}{(1+u)}. \tag{24}$$

The interface between wood and air has a pressure condition that has a constant value of atmospheric pressure.

The transport of water within the wood was described by a nonconservative convection-diffusion equation as:

$$\frac{\partial \phi c_{\text{int}}}{\partial t} + \nabla \cdot \left(-\phi \cdot D_w \cdot \nabla c_{\text{int}} \right) = \mathbf{u}_{\text{int}} \cdot \nabla c_{\text{int}}, \tag{25}$$

where c_{int} is the internal water concentration and D_w is the wood moisture diffusion coefficient. In this model, the wood moisture diffusion coefficient was negligible, since it is assumed to have minor influence on the drying rate during microwave drying. This assumption was made based on the fact that drying using microwave energy enables drying

of pine and spruce 20–30 times faster than conventional drying, [23], and the conventional drying rate is controlled by the diffusion coefficient.

The boundary condition between the wood and the air has a flux condition that is defined as:

$$\mathbf{n} \cdot \left(\phi D_w \nabla c_{\text{int}} - \mathbf{u}_{\text{int}} c_{\text{int}} \right) = \left(\mathbf{n} \cdot \nabla \cdot \left(- D_{H_2O} \nabla c_{ext} + c_{ext} \mathbf{u}_{ext} \right) \right). \tag{26}$$

THE SIMULATION SCHEDULE

In order to get as fine finite element resolution in the wood domain as possible, and in order to save computational power, the simulation started with the heating part. Furthermore, the moisture flow was based on the temperatures and the vapour flux at the wood surfaces from the heating simulation. The finite element resolution on the wood domain is about four times larger than the CT image. The CT image pixel size is about 0.88 mm^2.

RESULTS AND DISCUSSION

Figure 3 shows the measured core temperatures and the share of maximum input power during the heating and drying, and figure 4 shows the simulated results. According to the results, the simulated values agree very well with the measured ones. The control schedule for the maximum input power is chosen to keep the temperature below 110°C. This temperature limit is based on earlier experiences where fast heating above this limit causes too high internal vapour pressure, which causes internal cracks. The same control schedule from the tests was used in the simulation model.

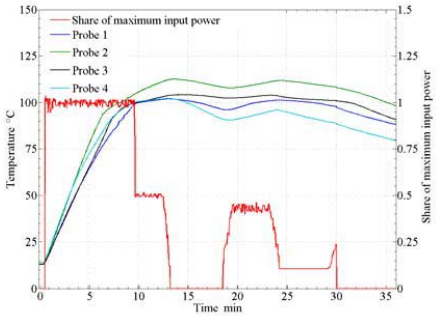

Figure 3. Measured core temperatures and share of maximum input power.

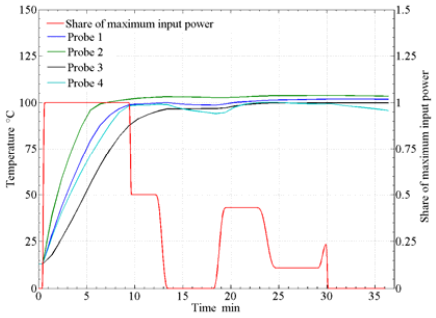

Figure 4. Simulated core temperatures and share of maximum input power.

The largest deviation between measured and simulated temperatures is found at the phase-shift point of water when the temperatures increase above 100°C. The reason is found in a rather coarse physical assumption in the model: no vaporization occurs during the heating phase up to 100°C; i.e., the mc is constant at its initial value.

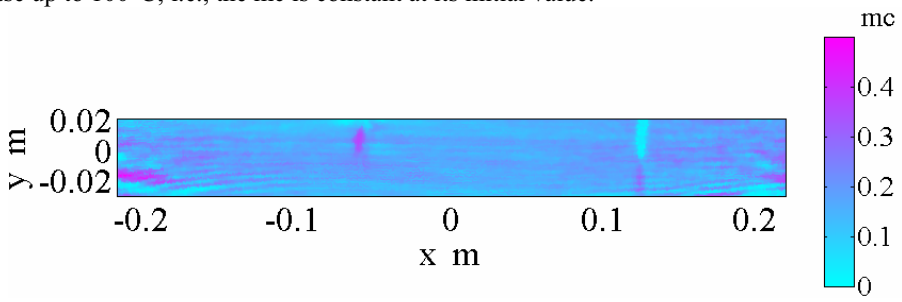

Figure 5. Initial mc distribution in Scots pine along the fibre direction, x, and across the thickness, y. The mean mc value is 0.17.

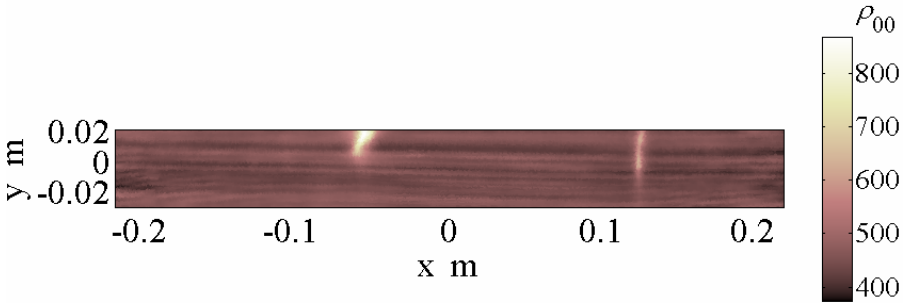

Figure 6. Dry density distribution, with a mean value of 451 kg/m^3 for the same intersection as in figure5.

In figure 5, the internal initial mc distribution is shown. Small accumulations with higher mc appear on the butt ends. There is also an accumulation spot at the left hand side from the centre. This spot is a region where a knot is situated, which is visible also in the dry density distribution in figure 6. Furthermore, the drier spot at the right hand side from the centre is a knot as well (figures 5 and 6). However, this knot was not possible to observe on the surface of the wood piece.

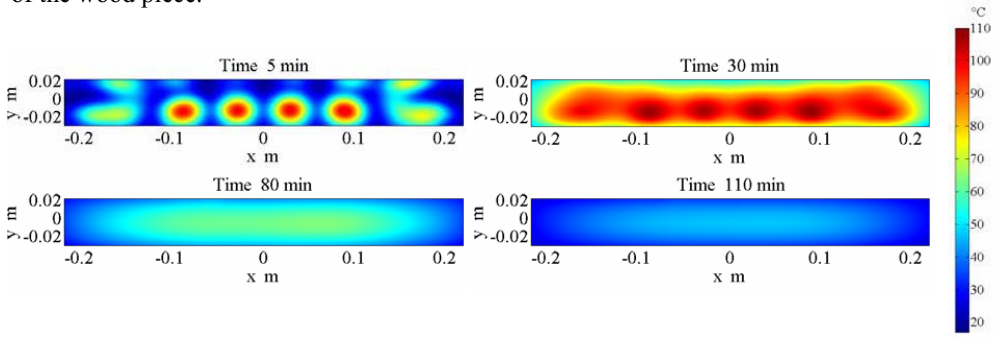

Figure 7. Internal temperature distribution within the wood at 5, 30, 80 and 110 minutes of heating.

Figure 7 shows the internal temperature distribution within the wood at 5, 30, 80 and 110 minutes of heating.

This figure also shows how the thermal energy has been transferred from the hotter spots throughout the wood during the heating. The boundary is cooler because of the heat transfer between air and wood that is caused by the water evaporation, the convection, the conduction and the radiation.

When comparing the measured mc distribution, which originates from CT images, with the simulated mc distribution (figure 8 and 9) similarities are apparent. The positions of the drier spots are very much the same in both figures. There is also an accumulation of vapour in the ends in the simulated mc distrubution, as as there is in the measured sample.

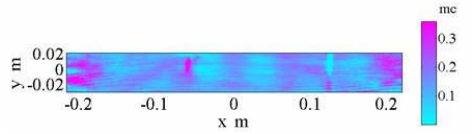

Figure 8. Measured mc distribution, with a mean value of 0.15 for the intersection.

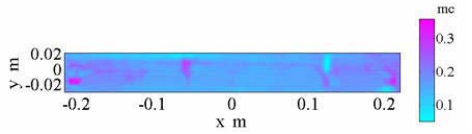

Figure 9. Simulated mc distribution, with a mean value of 0.16 for the intersection.

However, the drier spots are not lighter in the simulated result. It may depend on the difficulty of determining the proper permeability value. In the model, the permeability value was estimated to $0.5 \cdot 10^{-18}$

Compared to the measured mc distrubution, the positions of the two middle spots in the simulated mc distrubution are located lower down. Again, this result could be an effect of the assumption of no vapourization during the heating phase.

CONCLUSION

The conclusions of this modelling and verifying work can be summarized as follows:

- A 2-D FEM heat and mass transfer model where the material is well described can be used for simulation of the process—the correspondence between the model and the experiment is convincing.
- Simulated core temperature values agree with measured ones.
- Simulated moisture content distribution agrees with the measured mc distribution.
- The phase change from liquid to vapour needs refined modelling.

REFERENCES

[1] Wiberg, P. *X-ray CT-scanning of Wood During Drying*; Ph.D. Thesis. Vol. 10. Luleå University of Technology, Division of Wood Physics. 2001.

[2] Antti, A.L. Microwave drying of hardwood: simultaneous measurements of pressure, temperature, and weight reduction. Forest Products Journal 1992, 42, 49–54.

[3] Perré, P.; Turner, I. Microwave drying of softwood in an oversized waveguide: Theory and experiment. AIChE Journal 1997, 43 (10), 2579–2578.

[4] Antti, A.L. Microwave drying of hardwood: Moisture measurement by computer tomograph. In *Proceedings of the 3rd International Conference on wood drying*, Vienna, Austria, August 18–21, 1992.

[5] Zielonka, P.; Dolowy, K. Microwave drying of spruce: moisture content, temperature, and heat energy distribution. Forest Products Journal 1998, 48 (6), 77–80.

[6] MacLean, J.D. Thermal Conductivity of Wood. Heating, Piping and Air Conditioning 1941, 13 (6), 380–391.

[7] Kollman F.F.P.; Côté W.A. *Principles of Wood Science and Technology* Vol. 1. Solid wood; Springer-Verlag; New York, 1984.

[8] Ni, H.; Datta, A.K.; Torrance, K.E. Moisture transport in intensive microwave heating of biomaterials: a multiphase porous media model. International Journal of Heat and Mass Transfer 1999, 42, 1501–1512.

[9] Constant, T.; Moyne, C.; Perré P. Drying with Internal Heat Generation: Theoretical Aspect and Application to Microwave heating. A.I.Ch.E. Journal 1996, 42 (2), 359368.

[10] Perré, P.; Turner, T. A 3-D version of TranPore: a comprehensive heat and mass transfer computational model for simulating the drying of porous media. International Journal of Heat and Mass Transfer 1999, 42, 4501–4521.

[11] Hansson L.; Lundgren N.; Antti A.L.; Hagman, O. FEM Simulation of Heating Wood In an Industrial Microwave Applicator. In *Proceedings from 10th International Conference on Microwave and High Frequency Heating*, Modena, Italy; September 12–15, 2005; 415–418.

[12] Hansson L.; Lundgren N.; Antti A.L.; Hagman, O. Finite element modeling (FEM) simulation of interactions between wood and microwaves. Journal of Wood Science 2005, 52 (5), 406–410.

[13] Lundgren N.; Hansson L.; Antti A.L.; Hagman, O. FEM Simulation Of Interactions Between Microwaves And Wood During Thawing. In *Proceedings from 2nd Conference on Mathematical Modelling of Wave Phenomena*, Växjo, Sweden, August 14–19, 2005; 260–267.

[14] Sorzano, C.O.S.; Thévenaz, P.; Unser, M.; Elastic Registration of Biological Images Using Vector-Spline Regularization. IEEE Transactions on Biomedical Engineering 2005, 52, 652–663.

[15] Risman, Per O. 2005. Microwave heating applicator. Patent WO/2005/022956 A1.

[16] Dipolar AB. Gymnasievägen 16, SE-931 57 Skellefteå, Sweden. Home page: www.dipolar.se.

[17] Comsol AB. Tegnérgatan 23, SE-11140 Stockholm, Sweden. Home page: www.comsol.se

[18] Torgovnikov, G.I. *Dielectric Properties of Wood and Wood-Based Materials*; Springer-Verlag; New York, 1993.

[19] Steinhagen, H.P. *Thermal Conductive Properties of Wood, Green or dry, from -40 to 100 ˚C: A literature review*. USDA Forest Service General Technical Report FPL-9, Forest Products Laboratory, Madison, WI., 1977.

[20] Kanter, K.R. The Thermal Properties of Wood. Derev. Prom. 1957, 6 (7), 17–18.

[21] Holman, J.P. *Heat Transfer*, 8th edition; McGraw-Hill; New York, 1997.

[22] Siau, J.F. Wood: Influence of moisture on physical properties. Virginia Polytechnic Inst. and State Univ.; Blacksburg, Virginia, 1995

[23] Antti A.L. *Heating and drying wood using microwave power*. Doctoral Thesis; Luleå University of Technology, 1999.